FINITE DEFLECTION DYNAMIC RESPONSE OF AXIALLY RESTRAINED BEAMS

By

ROBERT BRIAN SCHUBAK

B.A.Sc., University of British Columbia, 1984

A THESIS SUBMITTED IN PARTIAL FULFILLMENT OF

THE REQUIREMENTS FOR THE DEGREE OF

MASTER OF APPLIED SCIENCE

in

THE FACULTY OF GRADUATE STUDIES

(Department of Civil Engineering)

We accept this thesis as conforming

to the required standard

The University of British Columbia

August 1986

© Robert Brian Schubak, 1986

In presenting this thesis in partial fulfilment of the requirements for an advanced degree at the University of British Columbia, I agree that the Library shall make it freely available for reference and study. I further agree that permission for extensive copying of this thesis for scholarly purposes may be granted by the head of my department or by his or her representatives. It is understood that copying or publication of this thesis for financial gain shall not be allowed without my written permission.

Department of Civil Engineering

The University of British Columbia
1956 Main Mall
Vancouver, Canada
V6T 1Y3

Date August 1986.

Abstract

The deformation response of symmetrically supported, axially restrained beams subjected to uniformly distributed pulse loads is studied herein, leading to the development of an analytical procedure to predict the character and magnitude of such response. The procedure is valid for beams of any singly symmetric or doubly symmetric cross-section, and is based upon the assumption that the beam material can be approximated as behaving in a rigid-perfectly plastic manner. The governing equations of motion are derived from variational statements consisting of the principle of virtual work and d'Alembert's principle, and include the effects of finite geometry changes.

From the static analysis of axially restrained beams it is found that the yield curve of a beam section may be replaced by a linear approximation thereof to obtain a good estimate of the beam's load capacity. Incorporating the linear yield curve approximation in a dynamic analysis of an axially restrained beam results in the uncoupling of the response into two distinct phases — an initial small deflection phase in which the beam retains bending resistance and deforms as a mechanism formed by plastic hinges, and a subsequent large deflection phase in which the beam has no bending resistance and deforms as a plastic string. The results of such an analysis for a rectangular beam subjected to a rectangular load pulse compare well with the results of a previous solution which used the true quadratic yield curve.

The linear yield curve approximation further results in linear differential equations of motion, and the response to load pulses of general load-time history may be solved in closed form. Blast-type pulses of varying shape are found to induce significantly different permanent deflections in a beam than a rectangular pulse. On the other hand, the effect of finite rise time of the pulse's load intensity is found to be small if the the rise time is less than about twenty to thirty percent of the pulse duration.

A procedure developed by C.K. Youngdahl is used to obtain rough estimates of the permanent deformation response by converting a pulse of triangular shape to an "effective" rectangular pulse. These estimates compare well with results obtained by the complete analysis of a triangular pulse developed herein. The use of Youngdahl's procedure combined with the analysis of a rectangular pulse developed herein can provide a quick, simple solution to the permanent deformation of a dynamically loaded beam which is amenable to hand computation.

Contents

Abstract ii
Figures v
Tables vii
Notation viii
Acknowledgements x

1 Introduction 1

1.1 Background 1
1.2 Purpose and Scope of This Study 3

2 Response of Doubly Symmetric Beams 4

2.1 Statement of the Problem 4
2.2 Assumptions 4
2.3 Static Analysis 7
2.4 Differential Equations of Motion 24
2.5 General Blast-Type Pulses 31
2.6 Rectangular Pulses 34
2.7 Triangular Pulses 55

3 General Pulses 66

3.1 Statement of the Problem 66
3.2 Response to an Arbitrary Pulse 67
3.3 Triangular Pulse with Finite Rise Time 75

4 Eliminating the Effect of Pulse Shape 92

4.1 Simplifying the Analysis 92
4.2 Equivalent Rectangular Pulses 92
4.3 Youngdahl's Correlation Parameters 97

5 Response of Singly Symmetric Beams 102

5.1 Statement of the Problem 102
5.2 Static Analysis 102
5.3 Response to Blast-Type Pulses 106

6 Conclusion **116**
6.1 Summary of Results 116
6.2 Limitations of the Theory 117

References **120**

Figures

2.1 Symmetrically supported beams subjected to uniformly distributed pulse loading 5

2.2 Blast-type pulses 5

2.3 Rigid-perfectly plastic material and section behaviour 7

2.4 Deflection modes for approximate static analysis 9

2.5 Uniformly loaded beam just after collapse 10

2.6 The yield curve and the associated plastic deformation vector 12

2.7 Free body diagram of a beam segment during static plastic string response 14

2.8 Gürkök and Hopkins' "exact" deflection modes for symmetrically supported beams 15

2.9 Static load capacity of pinned rectangular beams 17

2.10 Static load capacity of clamped rectangular beams 18

2.11 Yield curves of doubly symmetric sections 19

2.12 Yield curve and plastic deformation vector of an open-web section . . 20

2.13 Static load capacity of pinned beams 22

2.14 Static load capacity of clamped beams 23

2.15 Displaced bending response configuration of a beam subjected to medium loading 25

2.16 Half-beam load, shear and moment diagrams 27

2.17 Initial displaced configuration of a beam subjected to high intensity loading 28

2.18 Rectangular load pulse 34

2.19 Final midspan displacement vs. impulse of a pinned beam subjected to medium intensity rectangular load pulses 46

2.20 Final midspan displacement vs. impulse of a pinned beam subjected to medium intensity rectangular load pulses 47

2.21 Final midspan displacement vs. impulse of a pinned beam subjected to high intensity rectangular load pulses 48

2.22 Comparison of results of the present study with those of Vaziri for the case of a pinned beam subjected to medium intensity rectangular load pulses 52

2.23 Comparison of results of the present study with those of Vaziri for the case of a pinned beam subjected to high intensity rectangular load pulses 53

2.24 Pinned wide flange beam subjected to a rectangular pressure pulse . . . 54

2.25 Comparison of results between rigid-plastic analysis and elastic-plastic F.E.M. analysis for wide flange beam example 54

2.26 Triangular load pulse 55

2.27 Final midspan displacement vs. impulse of a pinned beam subjected to medium intensity triangular load pulses 63

2.28 Final midspan displacement vs. impulse of a pinned beam subjected to high intensity triangular load pulses 64

3.1 Load pulse of general load-time history 67

3.2 Displaced configuration of a beam subjected to a rising high intensity load 69

3.3 Free body diagram of a pinned beam's rigid end segment 70

3.4 Triangular load pulse with finite rise time 76

3.5 Final midspan displacement vs. impulse of a pinned beam subjected to medium intensity triangular load pulses with varying rise times 90

3.6 Final midspan displacement vs. impulse of a pinned beam subjected to high intensity triangular load pulses with varying rise times 91

4.1 Final midspan displacement of a pinned beam subjected to a medium intensity triangular load pulse as computed using Youngdahl's correlation parameters 100

4.2 Final midspan displacement of a pinned beam subjected to a high intensity triangular load pulse as computed using Youngdahl's correlation parameters 101

5.1 Singly symmetric beam subjected to a uniformly distributed pulse load . 103

5.2 Pinned T-beam example 104

5.3 True and approximate linear yield curves for the T-beam 107

5.4 Static load capacity of the T-beam 108

5.5 Typical singly symmetric beam sections and their associated yield curves . 110

5.6 Free body diagram of a curved plastic beam segment 114

Tables

2.1 Final midspan displacement of a pinned beam subjected to a medium load ($\bar{p} \leq 3$) rectangular pulse 44

2.2 Final midspan displacement of a pinned beam subjected to a high load ($\bar{p} > 3$) rectangular pulse 45

2.3 Final midspan displacement of a clamped beam subjected to a medium load ($\bar{p} \leq 3$) rectangular pulse 49

2.4 Final midspan displacement of a clamped beam subjected to a high load ($\bar{p} > 3$) rectangular pulse 50

Notation

A, B	coefficients of the homogeneous solution of an initial value problem
I	nominal impulse defined by Equation (2.5.1)
I^*	true impulse defined by Equation (4.3.1)
M	bending moment in a fully plastic section
M_o	ultimate moment capacity of the beam
N	axial load
N_o	axial load capacity of the beam
S	area swept by the deforming beam mechanism
W_{ext}	external work done by the loads
W_{int}	internal work dissipated in plastic deformation
$g(x)$	time at which the plastic segment boundary reaches a section at x
h	depth of a rectangular beam
l	length of the half-beam
m	mass per unit length of the beam
$\overline{m}$	dimensionless moment M/M_o
$\overline{n}$	dimensionless axial load N/N_o
p	static load per unit length
$p(t)$	dynamic load per unit length
p_o	static load capacity of the beam
p_m	maximum intensity of the load pulse
$\overline{p}$	p_m/p_o
t	time
t_o	time at which the beam begins to deform—$p(t_o) = p_o$
t_1	time at which the plastic segment begins to extend outward from midspan
t_2	time at which the the travelling hinges join at midspan
t_f	time at which the beam reaches its permanent deformed position
t_m	time at which the load intensity is maximum—$p(t_m) = p_m$
t_p	pulse duration
t_s	time at which string response begins

$w(x,t)$ transverse displacement of the beam at x

$w_o(t)$ midspan displacement

w_{o_f} final midspan displacement

$w_{o_p}(t)$ particular solution of an initial value problem

x coordinate along the beam axis measured from midspan

$x_o(t)$ location of the plastic segment boundary or plastic hinge

Δ extension of the beam

β non-dimensional impulse parameter defined by Equation (2.6.4)

ε longitudinal strain in a fully plastic section

ς t_m/t_p—ratio of pulse time rise to pulse duration

θ rotation of the midspan hinge

λ measure of the symmetry of the beam section as defined in Figure 5.5

ξ coordinate along the beam axis measured from the supports

ξ_o location of the plastic segment boundary or plastic hinge

σ_o uniaxial yield stress of the beam material

τ dummy time integration variable

ψ curvature in a fully plastic section

$\dot{(\,)}$ $\partial(\,)/\partial t$

$\delta(\,)$ virtual change of a quantity $(\,)$

Acknowledgements

The author would like to thank his supervisors, Dr. D.L. Anderson and Dr. M.D. Olson, for their valued time and advice during the preparation of this thesis. Beneficial discussion with fellow students, particularly Reza Vaziri and Bryan Folz, was also appreciated.

The continuing financial support of the Canadian Department of National Defence (through a contract with the Defence Research Establishment Suffield) is gratefully acknowledged.

Finally, the author is deeply indebted to his friends and family for their encouragement and support of his academic endeavours.

CHAPTER 1

INTRODUCTION

1.1 BACKGROUND

There exist a variety of situations in which a structure may be subjected to dynamic pulse loads of sufficient intensity to cause permanent deformations or damage to the structure. For example, pulse loads arise in vehicle collisions, in water wave impact on ships or offshore structures, and in the loading of structures by blast waves from internal or external explosions. In many of these cases the structural response will be inelastic, and much recent effort has been devoted to the analysis of such response. The review articles by Jones [1–4] † and Ari-Gur *et al* [5] are thorough surveys of these efforts in dynamic plastic analysis. As the review articles imply, dynamic plasticity is a very complex field of study which must include the effects of non-linear material behaviour and deformed structure geometry. As such, complete theoretical analyses of even the simplest structural elements are usually intractable, and resort has been made to numerical analysis. However, these numerical analyses are often expensive and time consuming and theoretical analyses, if only approximate, remain desirable as methods of preliminary (or even final) design and as reliable checks on the results of numerical analyses.

† Numbers in brackets identify References at the end of this study.

Considerable progress has been made in the theoretical analysis of symmetrically supported beams. This problem is simple enough to lend itself to hand methods of analysis, provided that it is further simplified by sweeping, often restrictive, assumptions regarding the beam's material behaviour and deformed geometry.

Some of the earliest studies in dynamic plastic beam response were those by Lee and Symonds [6] and Symonds [7] which dealt with beams with free ends acted upon by concentrated midspan pulse loads. These analyses were facilitated by the use of a rigid-plastic material idealization, the use of which is based on the assumption that elastic strains in the beam are much smaller than plastic strains and therefore can be neglected.

Symonds [8] later used the rigid-plastic idealization to obtain solutions for the response of simply supported and clamped beams subjected to uniformly distributed pulse loads. In order to retain simple deformation modes the pulses were restricted to be of the so-called "blast-type" — loads that rise instantaneously to a peak intensity and then decrease monotonically to zero — and the displacements were assumed to be very small so that linear bending theory was applicable.

Symonds and Mentel [9] then obtained solutions for rigid-plastic beams of rectangular cross-section, with ends restrained against in-plane displacements, subjected to uniformly distributed impulsive ‡ loads. The analysis included the effects of finite beam deflections and the axial loads that arise due to the deflections. It was found that, as deflections increased, the beam's resistance to loading progressed from an initial bending response to a final catenary or string response. The permanent deformations predicted by this analysis were much smaller than those predicted by the previous bending-only analysis, demonstrating the beneficial effect of axial restraints on the load capacity of a beam.

Following the pioneering work of Symonds, Vaziri [10] carried out an analysis of rigid-plastic, axially restrained, rectangular beams subjected to uniformly distributed

‡ An impulsive load is a pulse load of infinite intensity and zero duration which imparts an initial velocity to the structure.

pulse loads of finite duration and constant intensity. Vaziri found that the beam response was dependent upon both the pulse's peak load and its impulse (the area beneath the pulse's load-time curve). For pulse loads tending to be impulsive, Vaziri's solution gave results which compared favourably with the results of Symonds and Mentel.

As has been noted, the aforementioned solutions have been found through the use of several sweeping assumptions, not the least of which is the rigid-plastic material idealization. Further to these assumptions, failure of the beam due to tearing or shearing has not been considered. This apparent disregard for the possibility of beam failure may seem to be the result of a narrow perspective on the problem, but in reality the deformation response alone often provides sufficient information for analysis and design. As well, deformation response analyses have provided insights into the general structural response to pulse loads. These insights have led to rational procedures for improving the energy absorption capabilities of structures.

1.2 PURPOSE AND SCOPE OF THE PRESENT STUDY

Vaziri's solution [10] is significant in that it is applicable to situations involving loading durations in the dynamic range as well as in the impulsive and quasi-static ranges. However, the solution is only valid for beams of rectangular cross-section and for loads of constant intensity over the loading duration, *i.e.* "rectangular" pressure pulses. Practical situations more often involve non-rectangular sections such as I-beams and T-beams. Moreover, pressure loads due to air blasts are not accurately modelled by the rectangular shape and a solution for more general pulse shapes is desirable. The purpose of this study, then, is to develop a solution procedure similar to Vaziri's that will be applicable to the same basic problem of symmetrically supported beams with ends restrained against in-plane displacements, but which also takes into account more realistic loads and sections.

CHAPTER 2

RESPONSE OF DOUBLY SYMMETRIC BEAMS

2.1 STATEMENT OF THE PROBLEM

To begin, a beam of doubly symmetric cross-section with a mass per unit length of m will be considered. The beam is symmetrically supported with constraints against in-plane displacements at the ends and is subjected to a pressure pulse uniformly distributed along the length of the beam, as in Figure 2.1. The pressure pulse is for now restricted to be of the so-called "blast-type" loading. Symonds [8] described this to be a pulse whose load-time function $p(t)$ satisfies the inequality

$$\int_0^t p(\tau)\, d\tau \geq t\, p(t). \tag{2.1}$$

In physical terms, such a blast-type pulse consists of an instantaneous rise to the peak pressure p_m followed by a continuous monotonic decay to zero pressure. Some blast-type pulses are shown in Figure 2.2. The implications of this restriction will be discussed later.

2.2 ASSUMPTIONS

A complete solution of the deformation response which includes all of the phenomena demonstrated by the beam would be very difficult to obtain, if at all possible.

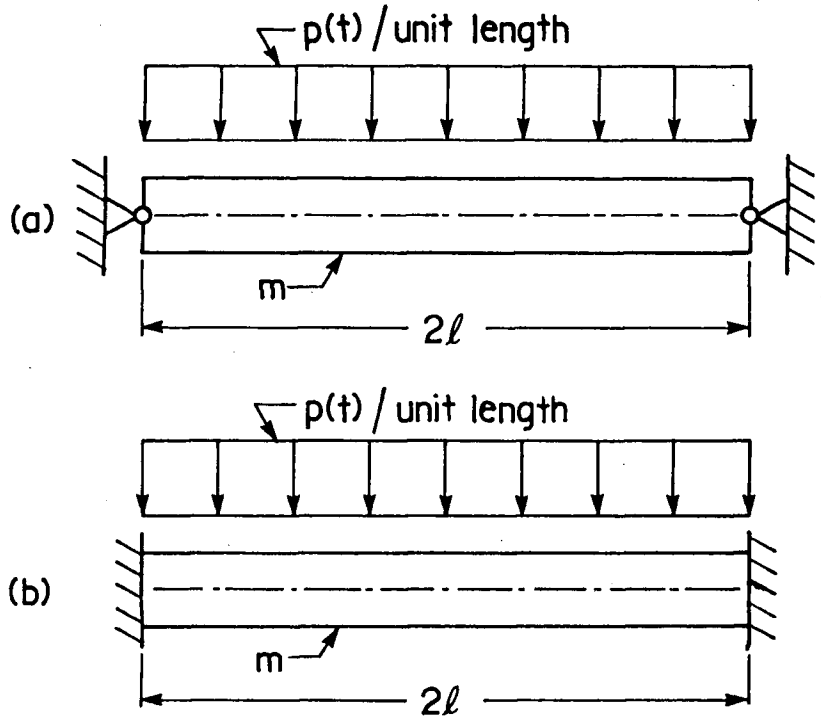

FIGURE 2.1 *Symmetrically supported beams subjected to uniformly distributed pulse loading. (a). Pinned beam. (b). Clamped beam.*

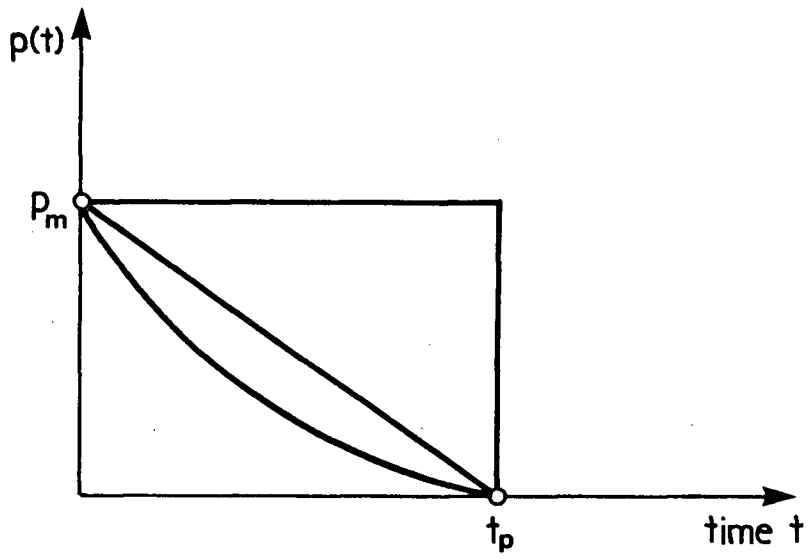

FIGURE 2.2 *Blast-type pulses.*

To obtain a relatively simple solution which lends itself to hand computation, the following assumptions regarding the beam's material and geometric properties have been made:

(i) The material of the beam is ductile and obeys a rigid-perfectly plastic type of stress-strain relation. It follows that the beam must also have rigid-perfectly plastic moment-curvature and axial load-extension relations as in Figure 2.3. This assumption is valid if the energy absorbed by the beam in plastic deformation is much larger than the strain energy absorbed in elastic deformation, and if the duration of the load t_p is much smaller than the fundamental period of elastic vibrations of the beam.

(ii) The effect of yield stress increasing with the rate of strain of the beam material is ignored.

(iii) The beam material is homogeneous and isotropic.

(iv) All effects due to shear such as shear deformations or failures and interaction with the moment and axial capacities of the beam are ignored.

(v) The effect of rotary inertia is negligible.

(vi) End constraints at the beam's support points provide for no transverse or axial displacements at the section's centroidal axis.

(vii) Beam deflections are finite but small compared to the beam span. The result is that the square of the slope of the deflection curve is small.

(viii) Extension of the beam, computed from consideration of transverse displacements, is distributed such that all plastic sections have equivalent ratios of axial extension to rotation. Together with assumptions (vi) and (vii), this requires the axial force to be constant over the entire length of the beam.

(ix) All of the relations of static plasticity remain valid for the dynamic problem.

(x) Longitudinal stress wave propagations through the beam are ignored.

(xi) Bernoulli-Euler beam theory is applicable.

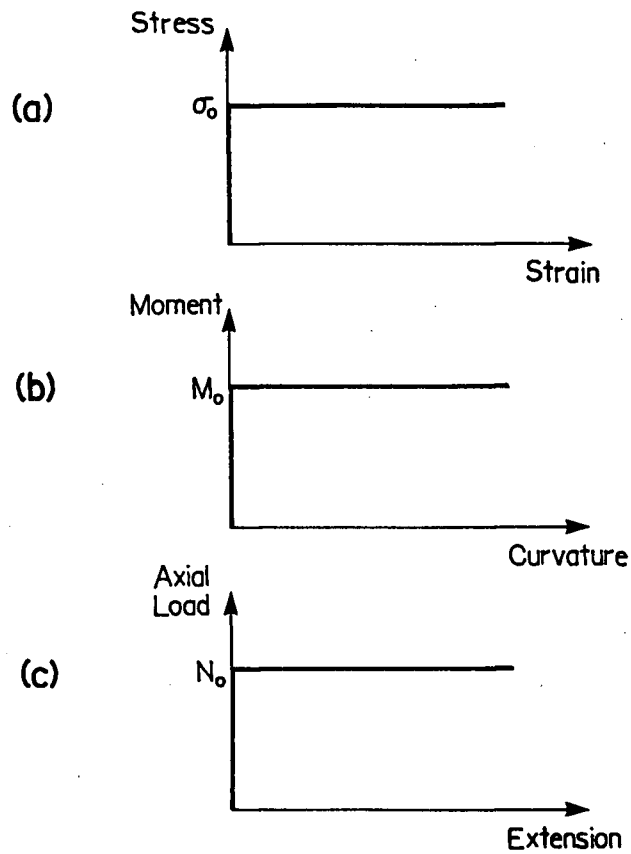

FIGURE 2.3 *Rigid-perfectly plastic material and section behaviour. (a). Stress-strain diagram. (b). Moment-curvature diagram for no axial load. (c). Axial load-extension diagram for no moment.*

These assumptions are essentially the same as those made by Symonds and Mentel (with the exception of assumption (x)) and Vaziri in their earlier studies of axially restrained beams.

2.3 STATIC ANALYSIS

As a preliminary step to the derivation of the differential equations of motion for the beam of Section 2.1, the concepts of limit analysis will be used to solve for the response of the beam to static loading. The assumptions of Section 2.2 shall hold for beams with pinned and clamped ends. Aside from being a convenient primer for the upcoming work in dynamic plasticity, this static analysis will provide important insights

into the load resistant behaviour of the rigid-plastic beam. These insights will in turn lead to a further simplifying assumption — a powerful assumption which will facilitate the analysis of non-rectangular beams subjected to pressure pulses of general load-time history.

2.3.1 APPROXIMATE LOAD CARRYING CAPACITY

Haythornwaite [11] found that beams with ends restrained against axial displacements exhibit different load resistance capacities than those without such restraints. Finite deflections imply a stretching of the beam, inducing tensile axial forces in the beam which help to resist the load. As the transverse deflection increases, so does the effect of the axial loads and the beam's load capacity.

In his analysis, Haythornwaite assumed that the beam deformed plastically according to the single midspan hinge mechanism of Figure 2.4(a) until the load level was such that the axial force had reached the section's capacity and the bending moment had reduced to zero. Beyond this load level the beam behaved as a plastic string with a funicular deflection curve, as in Figure 2.4(b). Haythornwaite performed his analysis on a rectangular beam with fully clamped ends. Vaziri, in his study, similarly analysed a rectangular beam with pinned ends. Their results will be reproduced here.

Consider the pinned beam of span $2l$, shown in Figure 2.1(a), subjected to a load per unit length p. For values of p below the beam's static collapse load p_o, no deformations will occur owing to the beam's rigid-plastic material behaviour. As the load is increased beyond p_o, however, a plastic hinge is formed at the midspan, and the beam begins to deform in the mechanism of Figure 2.4(a). The beam, now comprised of a central hinge and two rigid halves, is shown in its displaced configuration in Figure 2.5. Through its deformation, the beam has swept out an area S, and at the midspan hinge has been stretched by an amount Δ, rotated through an angle θ, and displaced transversely by an amount w_o.

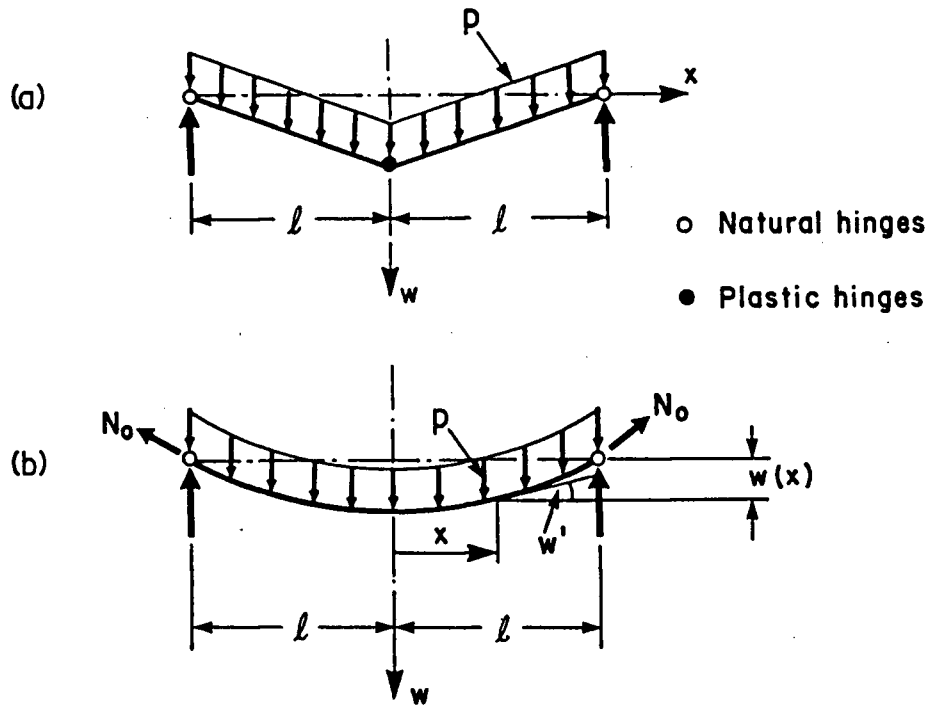

FIGURE 2.4 *Deflection modes for approximate static analysis. (a) Single midspan hinge mechanism. (b) Plastic string.*

Allowing the beam to undergo a further "virtual" displacement of δw_o, there will be a further hinge rotation of $\delta\theta$, a further stretching of $\delta\Delta$, and a further displaced area of δS. From the geometry of the beam,

$$\delta S = l\,\delta w_o = \tfrac{1}{2} l^2\,\delta\theta \tag{2.3.1}$$

and

$$\delta\Delta = \delta\left[2l\sec(\theta/2)\right] = l\sec(\theta/2)\tan(\theta/2)\,\delta\theta. \tag{2.3.2}$$

Assumption (vii) of Section 2.2 states that the square of the slope of the deflection curve is very small — *i.e.* that $\theta^2 \ll 1$. This leads to the small angle approximations $\sec\theta \approx 1$ and $\tan\theta \approx \theta$. Equation (2.3.2) can therefore be rewritten as

$$\delta\Delta = \tfrac{1}{2} l\theta\,\delta\theta = w_o\,\delta\theta. \tag{2.3.3}$$

The work dissipated in the plastic hinge through this virtual deformation is

$$\delta W_{int} = M\,\delta\theta + N\,\delta\Delta \tag{2.3.4}$$

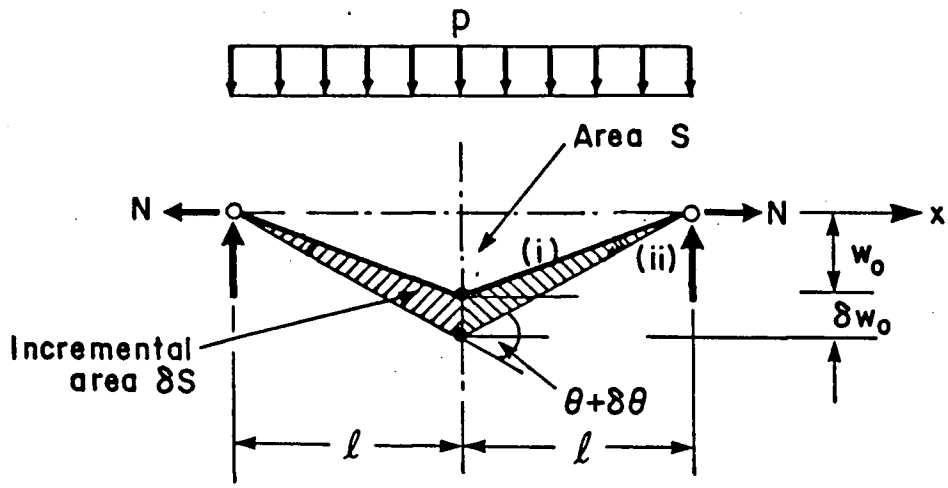

FIGURE 2.5 *Uniformly loaded beam just after collapse. (i) Deformed configuration. (ii) Virtually disturbed configuration.*

where M is the bending moment in the fully plastic section and N is the axial force, which as discussed in Section 2.2 is taken to be constant along the length of the beam. Inserting Equation (2.3.3) into Equation (2.3.4) gives the internal virtual work

$$\delta W_{int} = (M + N w_o)\,\delta\theta. \tag{2.3.5}$$

The work done by the uniformly distributed load in moving through the virtual displacement δw_o is

$$\delta W_{ext} = \delta\left(p\int_{-l}^{l} w(x)dx\right) = p\,\delta S, \tag{2.3.6}$$

where x is the distance measured along the beam from midspan. Inserting Equation (2.3.1) into Equation (2.3.6) gives the virtual external work

$$\delta W_{ext} = \tfrac{1}{2}pl^2\,\delta\theta. \tag{2.3.7}$$

By the theorem of virtual work, external and internal work must be equal so that

$$\delta W_{ext} = \delta W_{int}$$

$$\tfrac{1}{2}pl^2 = M + N w_o \tag{2.3.8}$$

where $\delta\theta$ can be disregarded as an arbitrary value. Defining M_o to be the plastic moment and N_o to be the axial load capacity of the beam section, and noting that $p_o = 2M_o/l^2$ for a pinned beam, Equation (2.3.8) can be rewritten as

$$\frac{p}{p_o} = \frac{M}{M_o} + \frac{Nw_o}{M_o}. \tag{2.3.9}$$

Further defining $\overline{m} = M/M_o$ and $\overline{n} = N/N_o$ yields the static load capacity in the form

$$\left(\frac{p}{p_o}\right)_{pinned} = \overline{m} + \left(\frac{N_o w_o}{M_o}\right)\overline{n}. \tag{2.3.10}$$

This analysis can be modified to accomodate clamped beams by noting that, for this case, $p_o = 4M_o/l^2$ and that plastic hinges are also formed at the supports so that the internal virtual work is now $\delta W_{int} = (2M + Nw_o)\delta\theta$. Again invoking the theorem of virtual work and taking the new value of p_o, the static load capacity of a clamped beam is found to be

$$\left(\frac{p}{p_o}\right)_{clamped} = \overline{m} + \frac{1}{2}\left(\frac{N_o w_o}{M_o}\right)\overline{n}. \tag{2.3.10a}$$

To this point, no consideration has been made of the beam's section geometry. To complete the solution, $\overline{m}$ and $\overline{n}$ must be known. This requires that the section's moment-axial load capacity interaction relation (or yield curve), and hence the section geometry, be defined.

For a beam of rectangular cross-section, the interaction relation is expressed by

$$\overline{m} = 1 - \overline{n}^2. \tag{2.3.11}$$

The flow rule of plasticity theory states that the plastic deformation vector with components $(N_o\delta\varepsilon, M_o\delta\psi)$, where ε is the longitudinal strain and ψ the curvature of the plastic section, is outwardly normal to the yield curve at the corresponding stress point $(\overline{n}, \overline{m})$ causing the deformations. Figure 2.6 shows this graphically. The flow rule may be equivalently stated as

$$\frac{M_o\delta\psi}{N_o\delta\varepsilon} \cdot \frac{d\overline{m}}{d\overline{n}} = -1. \tag{2.3.12}$$

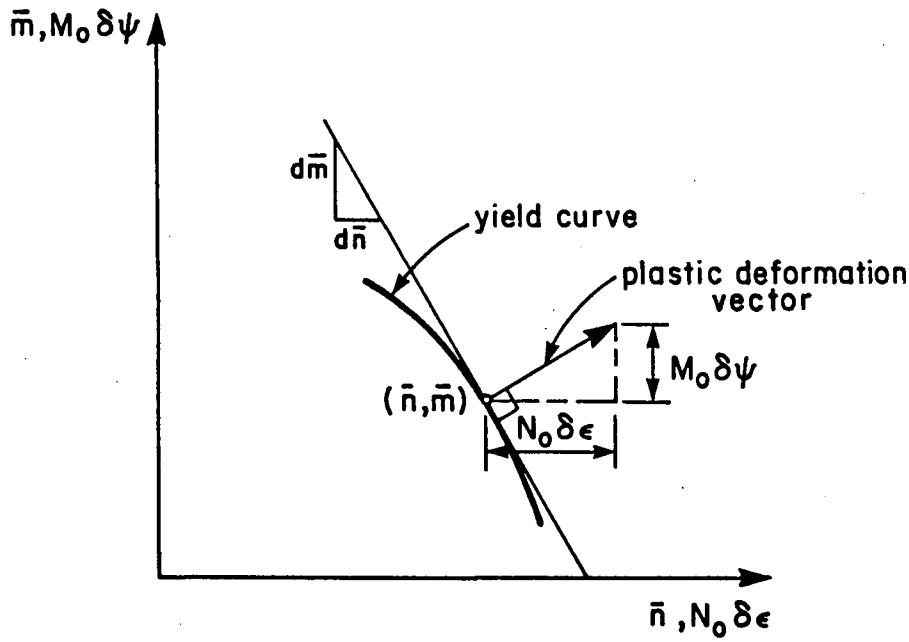

FIGURE 2.6 *The yield curve and the associated plastic deformation vector.*

With the plastic deformations concentrated at the midspan hinge it is seen that $\delta\varepsilon/\delta\psi = \delta\Delta/\delta\theta = w_o$ for the pinned beam. Differentiating Equation (2.3.11) with respect to $\overline{n}$, the flow rule for pinned rectangular beams becomes

$$\overline{n} = \frac{N_o w_o}{2M_o} \tag{2.3.13}$$

and substituting this back into the interaction relation gives

$$\overline{m} = 1 - \overline{n}^2 = 1 - \frac{1}{4}\left(\frac{N_o w_o}{M_o}\right)^2 . \tag{2.3.14}$$

Finally, combining Equations (2.3.10), (2.3.13) and (2.3.14), and noting that $M_o/N_o = h/4$ where h is the beam depth, the static load capacity of a pinned rectangular beam is found to be

$$\left(\frac{p}{p_o}\right)_{pinned} = 1 + 4\left(\frac{w_o}{h}\right)^2 \tag{2.3.15}$$

where $\overline{n} \leq 1$, or from Equation (2.3.13) $w_o \leq 2M_o/N_o = h/2$. Beyond this value of midspan displacement the pinned beam will behave as a plastic string.

Again the solution for clamped beams can be derived from the pinned beam solution by making a few changes. Because plastic hinges form at the supports, $\delta\varepsilon/\delta\psi$ is now equivalent to $\delta\Delta/2\delta\theta = w_o/2$ and the flow rule for clamped rectangular beams becomes

$$\overline{n} = \frac{N_o w_o}{4M_o} \tag{2.3.13a}$$

while substitution back into the interaction relation gives

$$\overline{m} = 1 - \frac{1}{16}\left(\frac{N_o w_o}{M_o}\right)^2. \tag{2.3.14a}$$

Combining Equations (2.3.10a), (2.3.13a) and (2.3.14a) gives the static load capacity of a clamped rectangular beam as

$$\left(\frac{p}{p_o}\right)_{damped} = 1 + \left(\frac{w_o}{h}\right)^2 \tag{2.3.15a}$$

where $\overline{n} \leq 1$, or from Equation (2.3.13a) $w_o \leq 4M_o/N_o = h$.

As the load p increases beyond the level at which $N = N_o$, the beam response to the load is that of a plastic string — the beam has no bending stiffness and resists the load through its axial strength only. Figure 2.7 shows a small segment of the beam of length dx. The entire length of the beam is plastic, and since $N = N_o$ is constant along the entire length, M must be zero everywhere. Therefore shear stresses do not exist in the beam.

Considering vertical equilibrium of the beam segment gives

$$p\,dx = N_o\frac{dw}{dx} - N_o\left(\frac{dw}{dx} + \frac{d^2w}{dx^2}dx\right)$$

$$p = -N_o\frac{d^2w}{dx^2}. \tag{2.3.16}$$

By integrating Equation (2.3.16) twice with respect to x, the deflection curve of the beam is found to be

$$w(x) = w_o - \frac{px^2}{2N_o}. \tag{2.3.17}$$

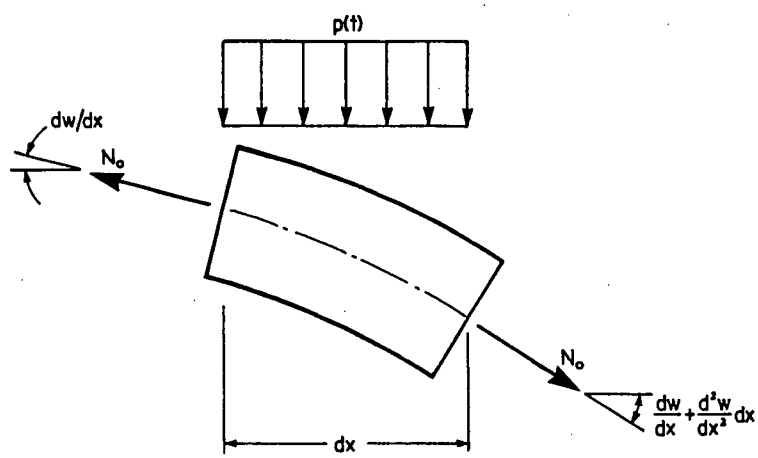

FIGURE 2.7 *Free body diagram of a beam segment during static plastic string response.*

At the ends $x = \pm l$ there can be no deflections so that $w(\pm l) = 0$ and the midspan displacement w_o must be

$$w_o = \frac{pl^2}{2N_o}. \tag{2.3.18}$$

Reorganizing Equation (2.3.18) and dividing by the static collapse load p_o, the static load capacities of pinned and clamped rectangular beams are found to be

$$\left(\frac{p}{p_o}\right)_{pinned} = 4\left(\frac{w_o}{h}\right) \tag{2.3.19}$$

and

$$\left(\frac{p}{p_o}\right)_{clamped} = 2\left(\frac{w_o}{h}\right) \tag{2.3.19a}$$

respectively, where $w_o \geq h/2$ for the pinned case and $w_o \geq h$ for the clamped case.

The preceeding analysis was based on the assumption that the beam deforms in a single midspan hinge mechanism until it reaches the plastic string state. This mechanism is strictly correct for zero deflection only — it is only an approximation for finite deflections. The assumed mechanism is kinematically admissible and equilibrium has been satisfied along the length of the beam. However, Equation (2.3.13) requires that the axial force N increase with deflection so that at some point the stress state $(\overline{n}, \overline{m})$ lies outside

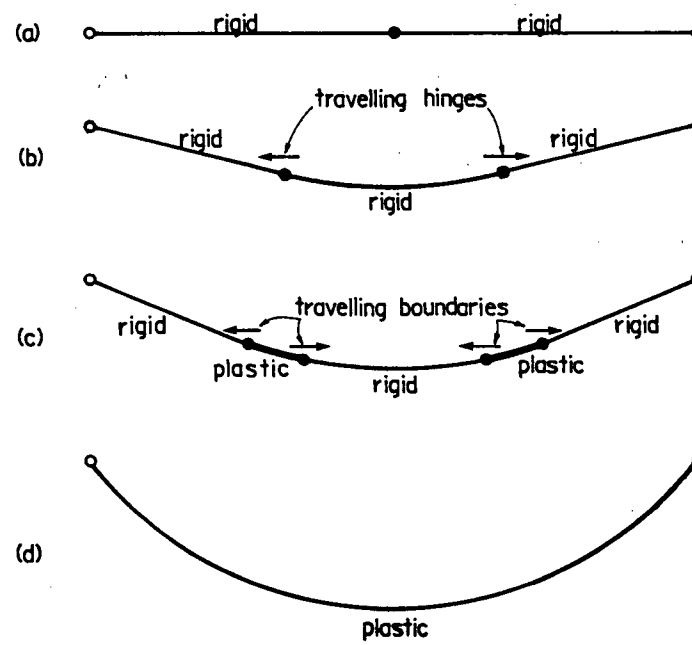

FIGURE 2.8 *Gürkök and Hopkins' "exact" deflection modes for symmetrically supported beams. (a) Zero deflection under p_o. (b–d) Increasing load.*

of the yield curve, violating the plasticity condition of the beam. In accordance with the kinematic theorem of limit analysis [12], the static load capacity of the beam as predicted by this analysis must exceed the actual capacity of the beam.

2.3.2 "EXACT" LOAD CARRYING CAPACITY

Gürkök and Hopkins [13] studied the static response of symmetrically supported rectangular beams with varying end contraints. Their study considers much more complicated deflection modes than does Haythornwaite's, with the single midspan hinge mechanism applying only to the undeformed beam. As deflection progresses under increasing load, the midspan hinge splits into two separate hinges which move outward to the supports. At some load level the hinges become plastic segments of finite length which extend further out to the supports and back inward to the midspan. Finally, at some higher load level the entire length of the beam is plastic and the beam responds as a plastic string. These deflection modes are shown in Figure 2.8.

The solution by Gürkök and Hopkins satisfies equilibrium, kinematic admissibility, and the yield condition along the entire length of the beam, and as such can be considered to be exact within the limitations of rigid-perfectly plastic material behaviour. This "exact" solution is plotted in Figures 2.9 and 2.10 for pinned and clamped beams respectively, along with the approximate solutions of Section 2.3.1. Comparison between the two solutions shows that the assumed mechanism of Haythornwaite is quite accurate in terms of the static load capacity of rectangular beams. This suggests that it would be reasonable to continue using the approximate single midspan hinge mechanism for the static analysis of beams subjected to uniformly distributed loads.

2.3.3 CAPACITY OF NON-RECTANGULAR BEAMS

It has been established that the approximate single midspan hinge mechanism of Section 2.3.1 provides good results for the static load capacity of beams subjected to uniformly distributed loads. Equations (2.3.10) and (2.3.10a) give the load capacity of pinned and clamped beams in terms of $\overline{m}$ and $\overline{n}$. To solve for $\overline{m}$ and $\overline{n}$, however, the interaction relation for the section must be known, and this relation differs for every section geometry. It follows that the load capacity differs for every section geometry, implying that a different static (and dynamic) analysis must be undertaken for every section to be analysed — an implication of formidable consequence.

Yield curves for doubly symmetric sections of varying geometry are given in Figure 2.11. Included are the yield curves for a rectangular section and for an open-web section comprised of two equal concentrated areas. These two sections may be seen to be the limiting cases of practical bending sections — the yield curves of all doubly symmetric I-beams and box-beams lie between the aforementioned pair. The solution for the static load capacity of the rectangular section was given in Section 2.3.1. The solution for the open-web section follows.

Consider the linear interaction relation of the open-web section, shown more closely in Figure 2.12. The flow rule requires that the plastic deformation vector be outwardly normal to the yield curve. At the stress states $(\overline{n}, \overline{m}) \equiv (0, 1)$ and $(\overline{n}, \overline{m}) \equiv (1, 0)$

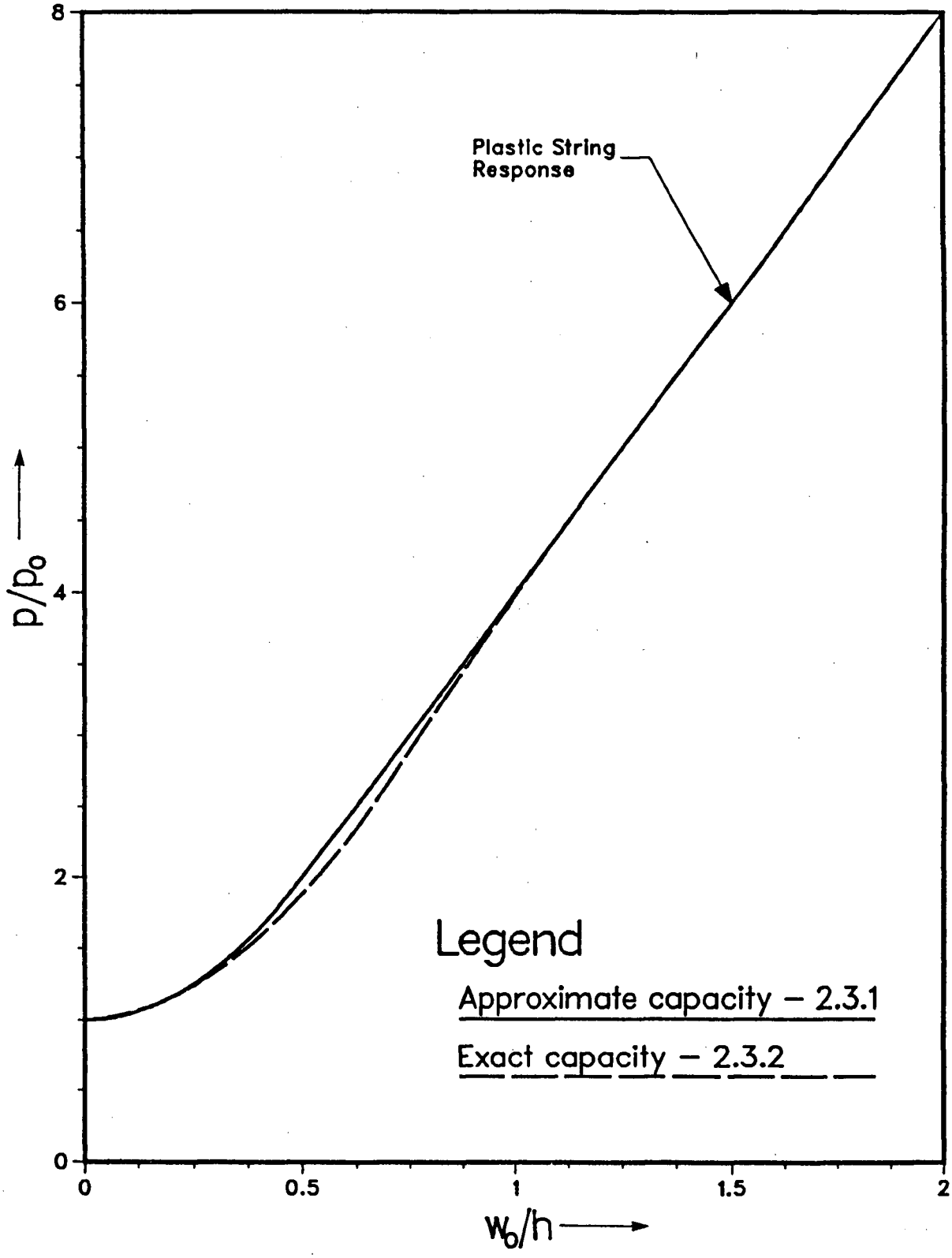

FIGURE 2.9 *Static load capacity of pinned rectangular beams.*

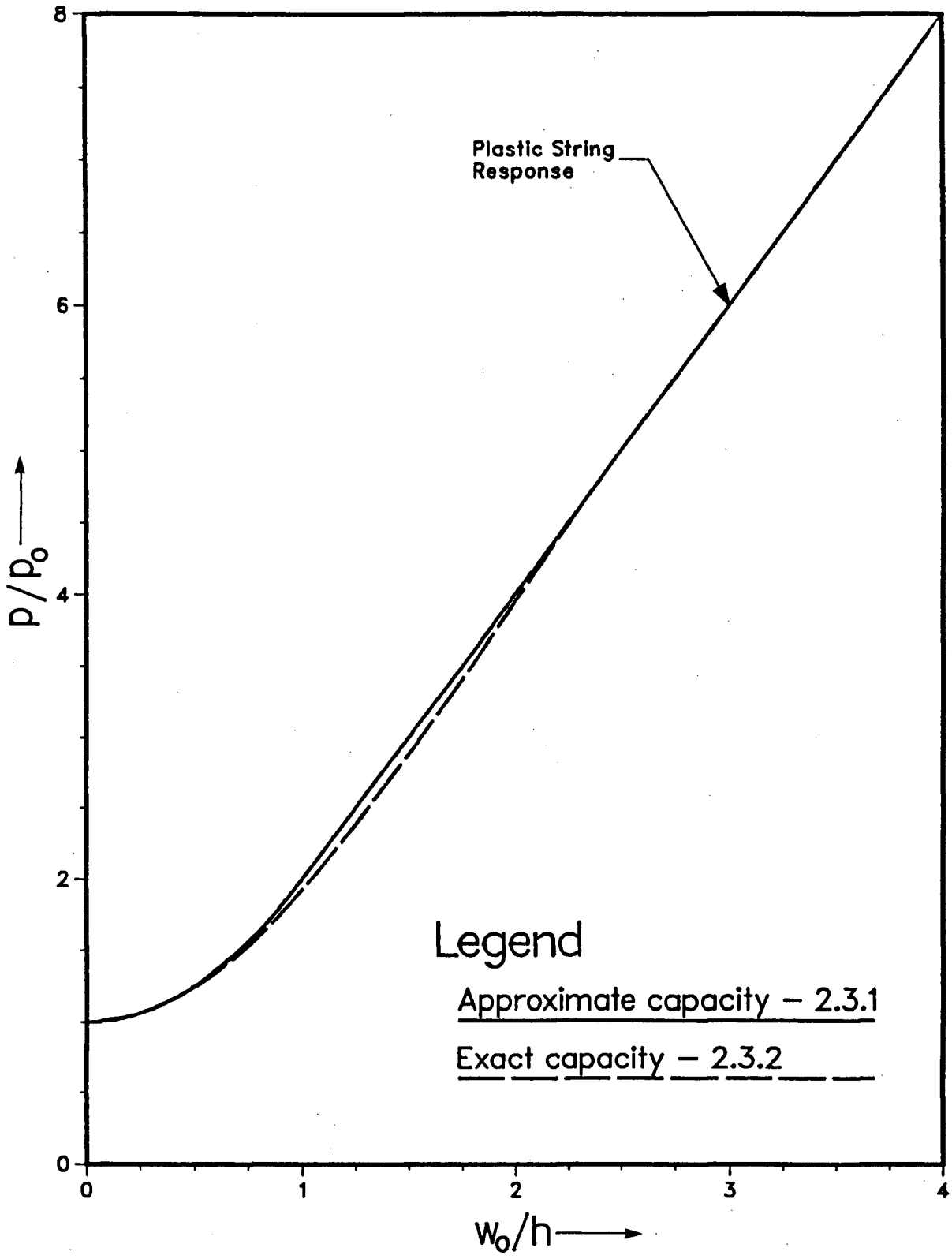

FIGURE 2.10 *Static load capacity of clamped rectangular beams.*

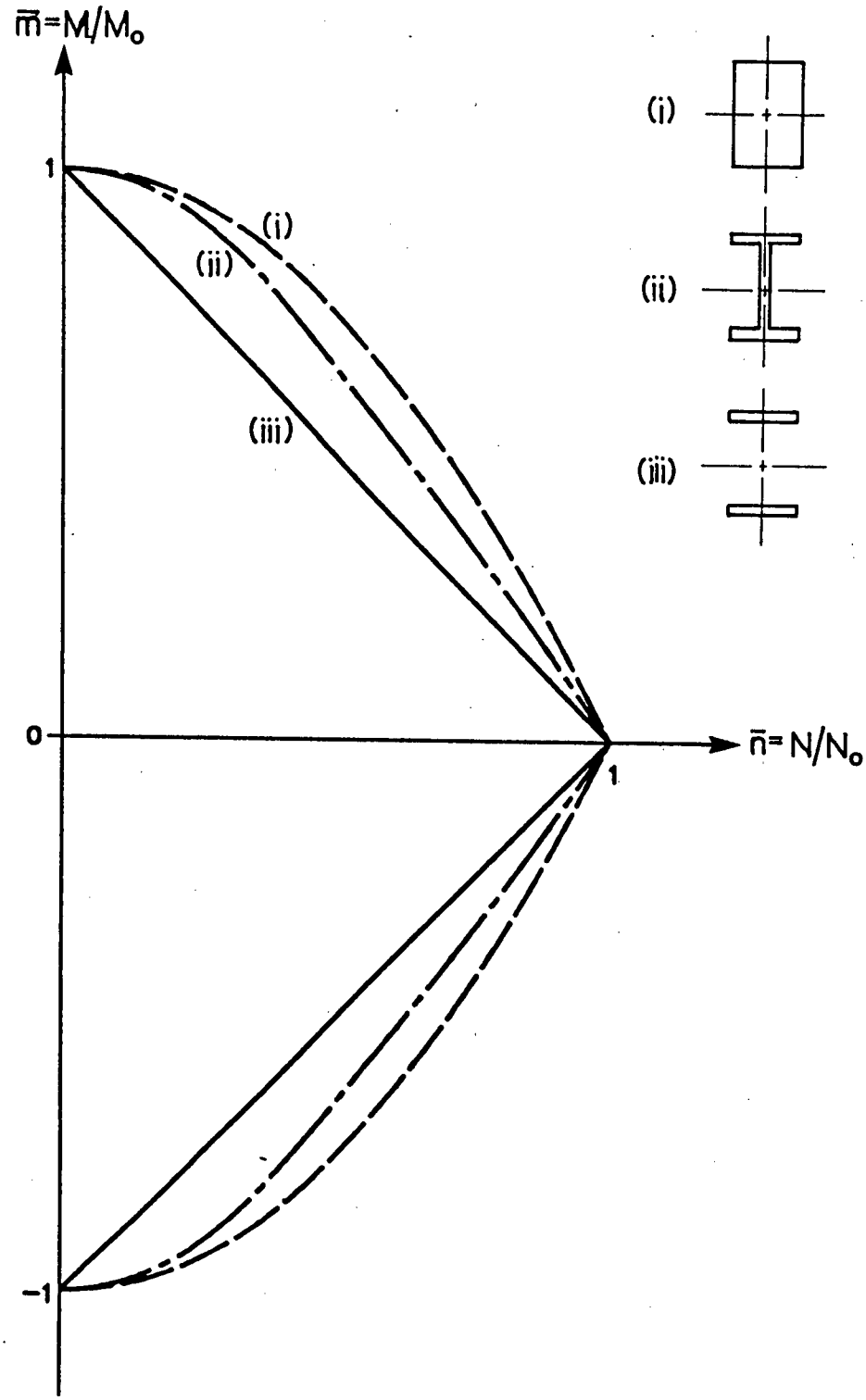

FIGURE 2.11 *Yield curves of doubly symmetric sections. (i) Rectangular section. (ii) I or box section. (iii) Open-web section.*

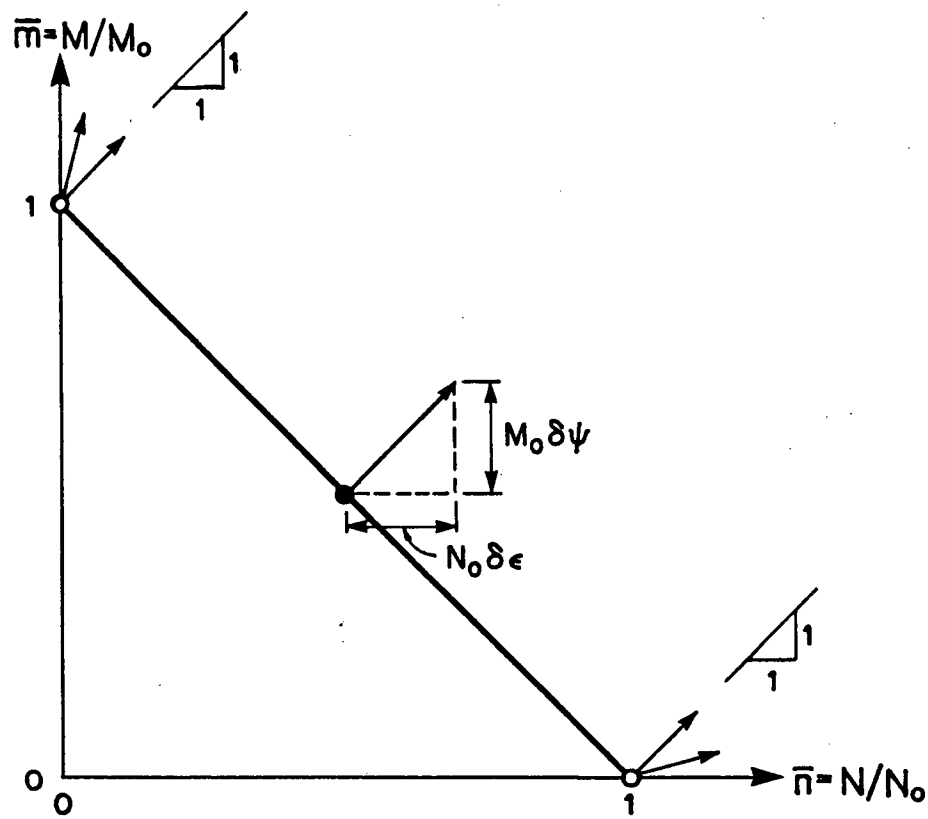

FIGURE 2.12 *Yield curve and plastic deformation of an open-web section.*

the slope of the yield curve is discontinuous, and the plastic deformation vector can take on an infinite number of values. At $(\overline{n}, \overline{m}) \equiv (0, 1)$ the plastic deformation vector can have any value such that

$$1 \leq \frac{M_o \delta\psi}{N_o \delta\varepsilon} \leq \infty. \tag{2.3.20}$$

By rearranging and noting that $\delta\varepsilon/\delta\psi = \delta\Delta/\delta\theta = w_o$ for a pinned beam and $\delta\varepsilon/\delta\psi = \delta\Delta/2\delta\theta = w_o/2$ for a clamped beam, it is found that the pure bending state exists for deflections

$$0 \leq w_o \leq M_o/N_o \tag{2.3.21}$$

for the pinned case and

$$0 \leq w_o \leq 2M_o/N_o \tag{2.3.21a}$$

for the clamped case. Putting $\overline{m} = 1$ and $\overline{n} = 0$ into Equation (2.3.10) or (2.3.10a) gives the static load capacity * as

$$p = p_o. \tag{2.3.22}$$

When $M_o\delta\psi/N_o\delta\varepsilon = 1$ the stress state "travels" instantaneously along the yield curve to $(\overline{n}, \overline{m}) \equiv (1, 0)$, and for all values of midspan deflection $w_o > M_o/N_o$ for pinned beams and $w_o > 2M_o/N_o$ for clamped beams the plastic string analysis of Section 2.3.1 applies. Rearranging Equation (2.3.18) gives

$$\frac{p}{p_o} = \frac{2N_o w_o}{p_o l^2}. \tag{2.3.23}$$

Recalling that $p_o = 2M_o/l^2$ for pinned beams and $p_o = 4M_o/l^2$ for clamped beams, the static load capacity for the plastic string response can be written as

$$\left(\frac{p}{p_o}\right)_{pinned} = \frac{N_o w_o}{M_o} \tag{2.3.24}$$

and

$$\left(\frac{p}{p_o}\right)_{clamped} = \frac{N_o w_o}{2M_o}. \tag{2.3.24a}$$

These results are plotted in Figures 2.13 and 2.14 along with the solutions for the rectangular section. The solutions for practical bending sections such as I-beams and box-beams will again lie between the previous two cases.

Using the linear interaction relation would underestimate the load capacity of practical bending sections, providing conservative estimates of the beam's deflection response. However, there is good agreement between the linear interaction solution and even the rectangular beam solution, suggesting that just such an estimate would be reasonable for all practical doubly symmetric sections. It will be shown that the linear interaction relation can also be used to great advantage in the dynamic analysis of doubly symmetric beams, making available solutions for non-rectangular sections subjected to pressure pulses of general load-time history.

* Note that since $\overline{n} = 0$, axial forces do not affect the analysis and the plasticity condition of the beam is not violated. The single midspan hinge mechanism is then seen to be correct for the case of linear $\overline{m}, \overline{n}$-interaction.

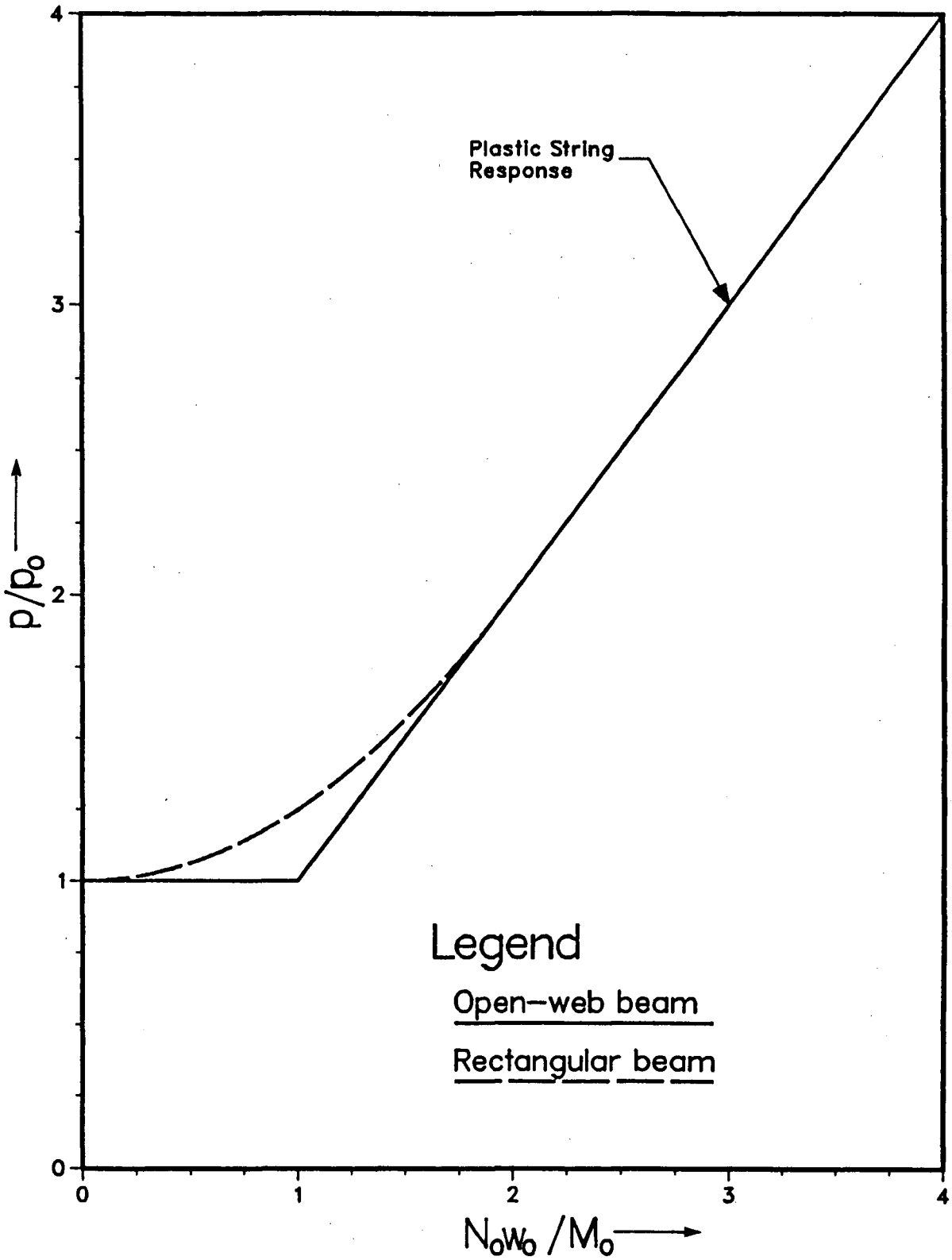

FIGURE 2.13 *Static load capacity of pinned beams.*

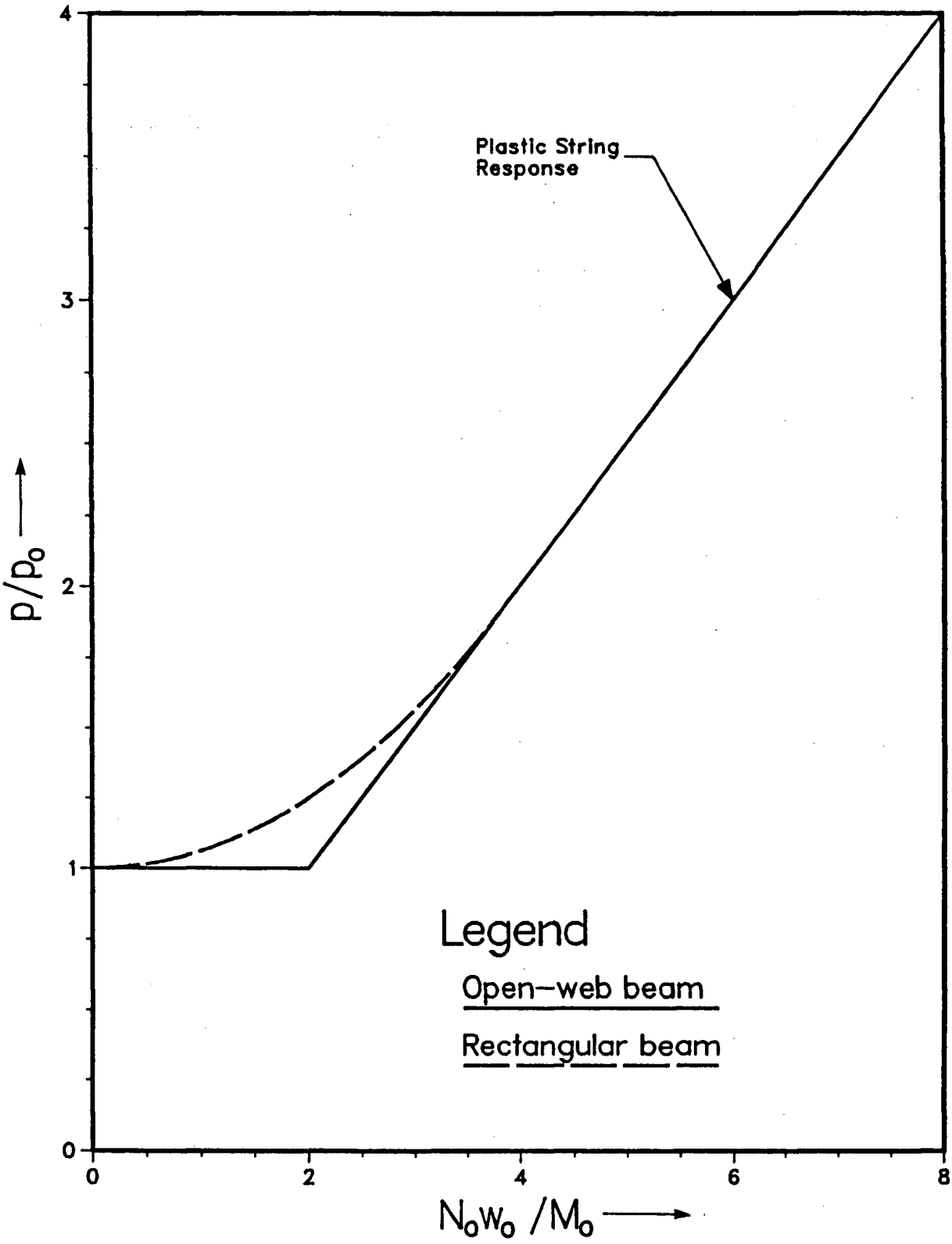

FIGURE 2.14 *Static load capacity of clamped beams.*

2.4 DIFFERENTIAL EQUATIONS OF MOTION

In Section 2.3 the basic concepts of plastic limit analysis were reviewed and applied to the static analyses of symmetrically supported beams subjected to uniformly distributed loads. These concepts and the resulting analytical procedures will now be applied to the dynamic analysis of the same beams subjected to uniformly distributed "blast-type" pressure pulses, by which means the differential equations of motion will be derived.

In deriving the differential equations of motion, the assumptions of Section 2.2 will be made. Furthermore, the yield curves of all doubly symmetric beam sections will be approximated by the linear interaction relation of Figure 2.12, as encouraged by the results of Section 2.3.3. The important effect of this last approximation, implied in Section 2.3.3, must now be explicitly stated so that it may be clearly understood and used to advantage. Linear $\overline{m}, \overline{n}$-interaction restricts the stress state of fully plastic sections to be $(\overline{n}, \overline{m}) \equiv (0, 1)$ or $(\overline{n}, \overline{m}) \equiv (1, 0)$ — the beam response to loading is uncoupled into phases of pure bending response for small displacements and pure string response for larger displacements. Linear bending-only solutions are easily obtained and, for the most part, already exist [8], and Vaziri has developed a simple approximation for string response [10]. A once formidable looking problem has been reduced to two relatively simple ones.

2.4.1 BENDING RESPONSE

For deflections $w_o \leq M_o/N_o$ for pinned beams and $w_o \leq 2M_o/N_o$ for clamped beams, the bending moment in fully plastic sections will be equal to the plastic moment M_o and the axial force N will be zero. Linear bending-only theory will apply and the axial constraints will have no effect on the beam response (for now).

Beam response to dynamic loading has been shown to be dependent upon the magnitude of the pressure pulse [8]. Pulses with a low peak pressure $p_m \leq p_o$ will not produce plastic hinging in the beam and, from the assumption of rigid-plastic material

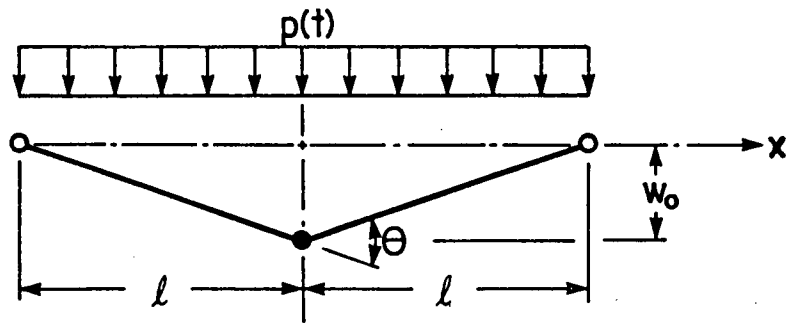

FIGURE 2.15 *Displaced bending response configuration of a beam subjected to medium loading.*

behaviour, no deformations will result. There are also distinguishable medium intensity and high intensity loadings which will now be discussed.

(a) Medium Load

For p_m somewhat exceeding p_o, deformation will proceed with a single hinge at midspan, as was the case for static loading. A pinned beam is shown in its displaced configuration in Figure 2.15. The displacement, velocity, and acceleration fields of the beam can be written as

$$\begin{aligned} w(x,t) &= w_o(1-|x|/l) \\ \dot{w}(x,t) &= \dot{w}_o(1-|x|/l) \\ \ddot{w}(x,t) &= \ddot{w}_o(1-|x|/l) \end{aligned} \qquad (2.4.1a,b,c)$$

where $w_o(t) = w(0,t)$ and $\dot{(\,)}$ denotes differentiation in time.

If the beam is allowed to undergo a further virtual midspan displacement of δw_o there will be a corresponding virtual hinge rotation $\delta\theta$ which is related to δw_o by

$$\delta w_o = \tfrac{1}{2} l\, \delta\theta. \qquad (2.4.2)$$

The work dissipated in the plastic hinge through the virtual deformation is

$$\delta W_{int} = M_o\, \delta\theta. \qquad (2.4.3)$$

The work done by the applied load $p(t)$ and the inertia load $-m\ddot{w}(x,t)$ is, by d'Alembert's Principle,

$$\delta W_{ext} = \int_{-l}^{l} \Big[p(t) - m\ddot{w}(x,t)\Big] \delta w(x,t)\, dx. \tag{2.4.4}$$

Inserting Equation (2.3.1) into Equation (2.4.4), and integrating with respect to x from $x = -l$ to $x = l$, the external virtual work becomes

$$\begin{aligned} \delta W_{ext} &= 2 \cdot \left[\tfrac{1}{2}p(t)l - \tfrac{1}{3}ml\ddot{w}_o\right] \delta w_o \\ &= \left[\tfrac{1}{2}p(t)l^2 - \tfrac{1}{3}ml^2\ddot{w}_o\right] \delta\theta. \end{aligned} \tag{2.4.5}$$

By the principle of virtual work, $\delta W_{ext} = \delta W_{int}$. Combining Equations (2.4.3) and (2.4.5) yields the differential equation of motion for a pinned beam

$$\ddot{w}_o + \frac{3M_o}{ml^2} = \frac{3p(t)}{2m}. \tag{2.4.6}$$

Making the substitution $p_o = 2M_o/l^2$ gives the differential equation of motion in its final form

$$\ddot{w}_o = \frac{3}{2m}\Big[p(t) - p_o\Big]. \tag{2.4.7}$$

In the case of a clamped beam, the internal virtual work δW_{int} is equal to $2M_o\delta\theta$ and $p_o = 4M_o/l^2$. It can be shown that the resulting differential equation of motion for a clamped beam is identical to that for a pinned beam.

Equation (2.4.7) is valid for the bending response phase of motion so long as the bending moments in the rigid halves of the beam are at all points less than the plastic moment M_o. Consider the diagrams for load, shear, and moment for the half-beam in Figure 2.16. If the midspan inertia load $m\ddot{w}_o$ is less than the applied pressure $p(t)$ the load, shear and moment diagrams are given by the solid curves in Figure 2.16, and the bending moment is always less than M_o. But if $m\ddot{w}_o > p(t)$, the diagrams are given by the dashed curves which indicate that the bending moment exceeds M_o, violating the plasticity condition. Equation (2.4.7) is therefore valid for $p(t) \geq m\ddot{w}_o = \frac{3}{2}[p(t) - p_o]$, which corresponds to $p(t) \leq 3p_o$. The same result can be found for clamped beams.

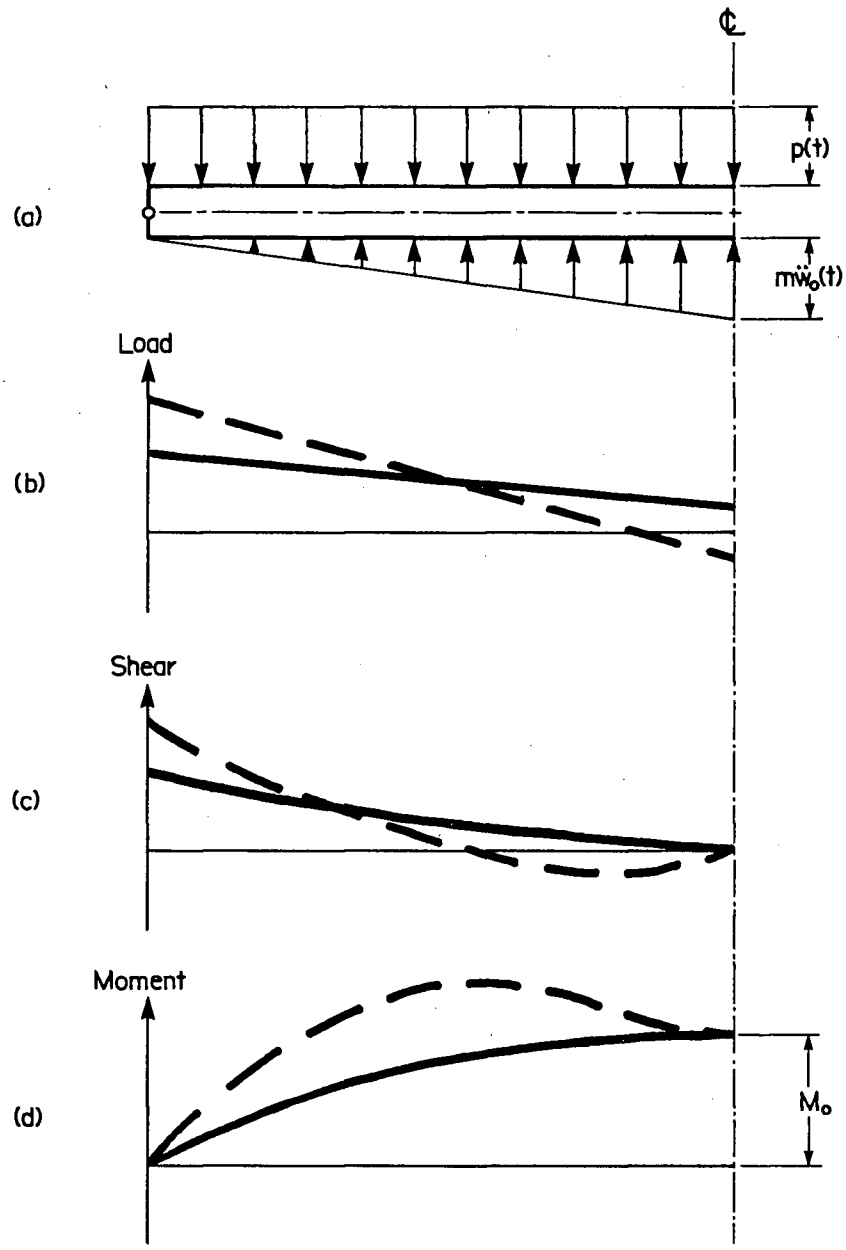

FIGURE 2.16 *(a) Loads on half-beam. (b) Load diagram. (c) Shear diagram. (d) Bending moment diagram.*

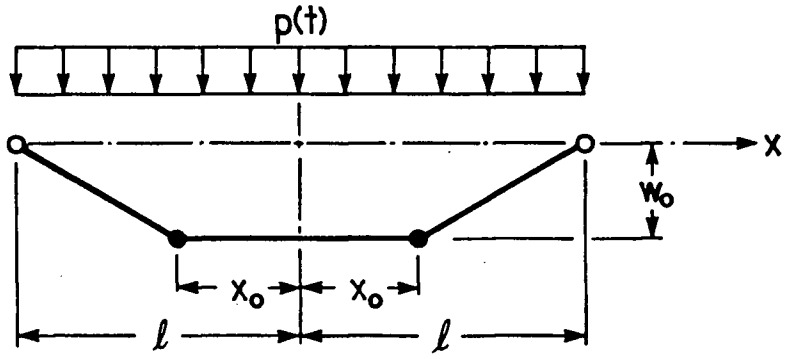

FIGURE 2.17 *Initial displaced configuration of a beam subjected to high intensity loading.*

(b) High Load

If the peak pressure p_m exceeds $3p_o$, the single midspan hinge mechanism will lead to a moment distribution which exceeds the plastic moment M_o. To satisfy the plasticity condition a flat central plastic zone bounded by two symmetrically located plastic hinges will immediately form. Figure 2.17 shows the beam at an instant after deformation has begun. A kinematically admissible velocity field for this deflection mode is

$$\dot{w}(x,t) = \begin{cases} \dot{w}_o(t), & \text{if } 0 \le x \le x_o \\ \dot{w}_o(t) \cdot \dfrac{l-x}{l-x_o}, & \text{if } x_o < x \le l \end{cases}$$

$$\ddot{w}(x,t) = \begin{cases} \ddot{w}_o(t), & \text{if } 0 \le x \le x_o \\ \left(\ddot{w}_o(t) + \dfrac{\dot{x}_o \dot{w}_o}{l-x_o}\right)\left(\dfrac{l-x}{l-x_o}\right), & \text{if } x_o < x \le l \end{cases} \tag{2.4.8a, b}$$

where $x_o(t)$ is the position of the hinges with respect to midspan.

On the flat central plastic zone $(0 \le x \le x_o)$ the bending moment is constant and equal to M_o. There can be no shear across the beam cross-section and therefore no force to resist the applied load $p(t)$ except the inertia load $-m\ddot{w}_o(t)$. Therefore,

$$\ddot{w}_o(t) = p(t)/m. \tag{2.4.9}$$

On the rigid end segments exists a similar situation to that for medium loads.

Taking Equation (2.4.6) and replacing l with $(l-x_o)$ and $\ddot{w}_o$ with $\ddot{w}_o+\dot{x}_o\dot{w}_o/(l-x_o)$ yields

$$\ddot{w}_o+\frac{\dot{x}_o\dot{w}_o}{l-x_o}+\frac{3M_o}{m(l-x_o)^2} = \frac{3p(t)}{2m}. \tag{2.4.10}$$

Combining this with Equation (2.4.9) and recalling that the static collapse load for a pinned beam is $p_o = 2M_o/l^2$ results in a differential equation for the hinge position x_o:

$$\frac{\dot{x}_o}{m(l-x_o)}\int_0^t p(\tau)\,d\tau+\frac{3p_ol^2}{2m(l-x_o)^2} = \frac{p(t)}{2m}. \tag{2.4.11}$$

Rearranging this to a form which will be seen to be more convenient, the differential equation of hinge motion becomes

$$-2(l-x_o)\dot{x}_o+\frac{p(t)(l-x_o)^2}{\int_0^t p(\tau)\,d\tau} = \frac{3p_ol^2}{\int_0^t p(\tau)\,d\tau}. \tag{2.4.12}$$

Equations (2.4.9) and (2.4.12) can be derived for the motion of clamped beams as well.

For blast-type pulses the hinges will be seen to move towards midspan as deflection progresses. As a hinge moves through a beam section, the moment in that section drops from M_o to a value just below M_o and no further rotation can occur in the section. Due to this rigid unloading, the segment of the beam through which the hinge has passed will be rigid but curved in shape. At some time t_2 the hinges will meet at midspan ‡ after which time the beam will continue to deform according to the single midspan hinge mode of part (a).

2.4.2 STRING RESPONSE

For deflections $w_o > M_o/N_o$ for pinned beams and $w_o > 2M_o/N_o$ for clamped beams, the beam has no bending stiffness and the axial force is equal to the section capacity N_o along the entire length of the beam. The beam therefore responds as a plastic string. The governing partial differential equation for the response can be obtained by recalling the equilibrium equation for static string response, *i.e.* Equation (2.3.16), and adding to

‡ The hinges will meet at midspan provided that the beam hasn't already deformed to the point where string response begins.

the applied load $p(t)$ the inertia load $-m\ddot{w}(x,t)$. In this way the differential equation of motion of the beam is found to be

$$m\frac{\partial^2 w}{\partial t^2} - N_o\frac{\partial^2 w}{\partial x^2} = p(t). \tag{2.4.13}$$

The deflection curve of the beam is complicated, but can be represented by a Fourier series of the form

$$w(\xi,t) = \sum_{n=1,3,5,\ldots}^{\infty} w_{o_n}(t)\sin\left(\frac{n\pi\xi}{2l}\right), \tag{2.4.14}$$

where ξ is the distance measured along the beam from one of the supports, *i.e.* $\xi = l - x$. Substituting Equation (2.4.14) back into Equation (2.4.13) and expressing the load $p(t)$ as a Fourier Series in ξ , the differential equation of motion becomes

$$\sum_{n=1,3,5,\ldots}^{\infty}\left\{\ddot{w}_{o_n} + \frac{N_o\pi^2 n^2}{4ml^2}w_{o_n}\right\}\sin\left(\frac{n\pi\xi}{2l}\right) = \frac{4p(t)}{\pi m}\sum_{n=1,3,5,\ldots}^{\infty}\frac{1}{n}\sin\left(\frac{n\pi\xi}{2l}\right). \tag{2.4.15}$$

The complete analysis is very difficult as the initial conditions of string response $w(x,t_s)$ and $\dot{w}(x,t_s)$, where t_s is the time when string response begins, can be complicated. However, Vaziri [10] showed that a good approximation to the solution can be found by considering only the first term (*i.e.* $n = 1$) of the Fourier series' in Equation (2.4.15). By doing this, the deflection curve of the beam becomes $w(x,t) = w_o(t)\sin(\pi\xi/2l)$ and a very simple differential equation of motion results:

$$\ddot{w}_o(t) + \frac{N_o\pi^2}{4ml^2}w_o(t) = \frac{4p(t)}{\pi m}. \tag{2.4.16}$$

For the above approximation to work, the kinetic energy of the beam at time $t = t_s$ must be conserved through the sudden change in the deformation mode. During the bending response phase the velocity profile of the beam is of triangular or trapezoidal shape, while during the string response phase the velocity profile is sinusoidal. Denoting the midspan velocity at an instant before $t = t_s$ as $\dot{w}_o(t_s^-)$ and at an instant after as $\dot{w}_o(t_s^+)$, equating the kinetic energy through the transition gives

$$\left[\dot{w}_o(t_s^+)\right]^2\int_0^{2l}\sin^2\left(\frac{\pi\xi}{2l}\right)d\xi = \int_{-l}^{l}\left[\dot{w}(x,t_s^-)\right]^2 dx$$

$$\dot{w}_o(t_s^+) = \sqrt{\frac{2}{l}\int_0^l\left[\dot{w}(x,t_s^-)\right]^2 dx}. \tag{2.4.17}$$

For $p_m \leq 3p_o$ or $t_s \geq t_2$, the velocity profile of the beam just before string response begins is

$$\dot{w}(x, t_s^-) = \dot{w}_o(t_s^-)(1 - x/l), \tag{2.4.18}$$

and for $t_s < t_2$ the velocity profile is

$$\dot{w}(x, t_s^-) = \begin{cases} \dot{w}_o(t_s^-), & \text{if } 0 \leq x \leq x_o \\ \dot{w}_o(t_s^-)\left(\dfrac{l - x}{l - x_o}\right), & \text{if } x_o < x \leq l. \end{cases} \tag{2.4.19}$$

Substituting these two velocity profiles into Equation (2.4.17) and integrating with respect to x from $x = 0$ to $x = l$ gives the initial velocity condition at time $t = t_s^+$ as

$$\dot{w}_o(t_s^+) = \begin{cases} \sqrt{2/3}\,\dot{w}_o(t_s^-), & \text{if } p_m \leq 3p_o \text{ or } t_s \geq t_2 \\ \sqrt{\frac{2}{3}[1 + 2x_o(t_s)/l]}\,\dot{w}_o(t_s^-), & \text{if } p_m \geq 3p_o \text{ and } t_s \leq t_2. \end{cases} \tag{2.4.20}$$

2.5 GENERAL BLAST-TYPE PULSES

The equations of motion as derived in Section 2.4 are valid when the load pulse applied to the beam is a blast-type pulse. Such a pulse consists of an instantaneous rise to the peak pressure (*i.e.* $p(0) = p_m$) followed by a continuous monotonic decay to zero pressure, as in Figure 2.2. The load pulse has duration t_p and the nominal impulse I is defined to be the area beneath the load-time relation for the pulse, *i.e.*

$$I = \int_0^{t_p} p(t)\,dt. \tag{2.5.1}$$

2.5.1 BENDING RESPONSE

(a) Medium Loads ($p_o < p_m \leq 3p_o$)

Equation (2.4.7) gives the midspan acceleration of the beam as

$$\ddot{w}_o(t) = \frac{3}{2m}\Big[p(t) - p_o\Big].$$

At the onset of the pulse load, the beam is at rest. The initial conditions are then $w_o(0) = 0$ and $\dot{w}_o(0) = 0$. Integrating Equation (2.4.7) and applying the zero initial conditions gives the deflection response of the beam as

$$\begin{aligned} w_o(t) &= \frac{3}{2m}\left[\int_0^t (t-\tau)p(\tau)\,d\tau - \frac{p_o t^2}{2}\right], \\ \dot{w}_o(t) &= \frac{3}{2m}\left[\int_0^t p(\tau)\,d\tau - p_o t\right]. \end{aligned} \tag{2.5.2a, b}$$

If t_f is the time at which the beam comes to rest, then $\dot{w}_o(t_f) = 0$ and

$$t_f = \int_0^{t_f} \frac{p(t)}{p_o}\,dt. \tag{2.5.3}$$

For Equation (2.5.3) to be true, the final midspan displacement $w_{o_f} = w_o(t_f)$ must be in the realm of bending response, *i.e.* $w_{o_f} \leq M_o/N_o$ for pinned beams and $w_{o_f} \leq 2M_o/N_o$ for clamped beams. If this is not the case, the time $t = t_s$ when $w_o(t_s) = M_o/N_o$ (or $2M_o/N_o$) must be determined, and used as an initial condition for a string response analysis.

(b) High Loads ($p_m > 3p_o$)

Equation (2.4.9) gives the midspan acceleration of the beam as $\ddot{w}_o(t) = p(t)/m$. With the initial conditions of $w_o(0) = 0$ and $\dot{w}_o(0) = 0$, integration in time gives the deflection response of the beam as

$$\begin{aligned} w_o(t) &= \int_0^t \frac{p(\tau)}{m}(t-\tau)\,d\tau, \\ \dot{w}_o(t) &= \int_0^t \frac{p(\tau)}{m}\,d\tau. \end{aligned} \tag{2.5.4a, b}$$

It is readily apparent that the beam cannot come to rest while the initial travelling hinge deflection mode is in effect.

The motion of the hinges is governed by Equation (2.4.12). Making the substitution $\xi_o = l - x_o$, Equation (2.4.12) reduces to

$$(\dot{\xi_o}^2) + \frac{p(t)}{\int_0^t p(\tau)d\tau}(\xi_o^2) = \frac{3p_o l^2}{\int_0^t p(\tau)d\tau}, \tag{2.5.5}$$

Examining Equation (2.5.5) at the time $t = 0$, it is found that $\xi_o^2(0) = 3p_o l^2/p_m$ so that the solution is

$$\xi_o^2 = \frac{3p_o l^2 t}{\int_0^t p(\tau)d\tau}, \tag{2.5.6}$$

and, hence,

$$x_o(t) = l\left(1 - \sqrt{\frac{3p_o t}{\int_o^t p(\tau)d\tau}}\right). \tag{2.5.7}$$

Unless the string response phase has already been reached, the hinges will meet at midspan at time $t = t_2$. Setting $x_o(t_2) = 0$ gives the result

$$t_2 = \frac{1}{3p_o}\int_0^{t_2} p(t)dt. \tag{2.5.8}$$

From time $t = t_2$ onwards, the beam will deform in the single midspan hinge mode and Equation (2.4.7) will again govern. Integrating with the initial conditions

$$w_o(t_2) = \int_0^{t_2} \frac{p(t)}{m}(t_2 - t)\,dt,$$

$$\dot{w}_o(t_2) = \int_0^{t_2} \frac{p(t)}{m}\,dt = \frac{3p_o t_2}{m},$$

the deflection response of the beam is found to be

$$\begin{aligned} w_o(t) &= \frac{3}{2m}\int_0^t (t-\tau)[p(\tau) - p_o]d\tau - \frac{1}{2m}\int_0^{t_2}(t_2 - t)[p(t) - 3p_o]dt, \\ \dot{w}_o(t) &= \frac{3}{2m}\left[\int_0^t p(\tau)d\tau - p_o t\right], \end{aligned} \tag{2.5.9a, b}$$

and the time at which the beam comes to rest is again given by Equation (2.5.3).

2.5.2 STRING RESPONSE

Combining the differential equation of motion for string response, Equation (2.4.16), with the appropriate initial conditions at time t_s, Equation (2.4.20), the deflection response of the beam is governed by the initial value problem

$$\ddot{w}_o + \frac{N_o\pi^2}{4ml^2}w_o = \frac{4p(t)}{\pi m},$$

$$w_o(t_s) = \begin{cases} M_o/N_o, & \text{for a pinned beam;} \\ 2M_o/N_o, & \text{for a clamped beam,} \end{cases}$$

$$\dot{w}_o(t_s^+) = \begin{cases} \sqrt{2/3}\,\dot{w}_o(t_s^-), & \text{if } p_m \le 3p_o \text{ or } t_s \ge t_2; \\ \sqrt{\frac{2}{3}[1 + 2x_o(t_s)/l]}\,\dot{w}_o(t_s^-), & \text{if } p_m \ge 3p_o \text{ and } t_s \le t_2. \end{cases}$$

The solution to this problem will be of the form

$$w_o(t) = A\cos\left[\frac{\pi}{2}\sqrt{\frac{p_o N_o}{mM_o}}(t - t_s)\right] + B\sin\left[\frac{\pi}{2}\sqrt{\frac{p_o N_o}{mM_o}}(t - t_s)\right] + w_{op}(t), \tag{2.5.10}$$

where A and B are constants to be determined by the initial conditions at time t_s, and $w_{op}(t)$ is the particular solution unique to the load function $p(t)$.

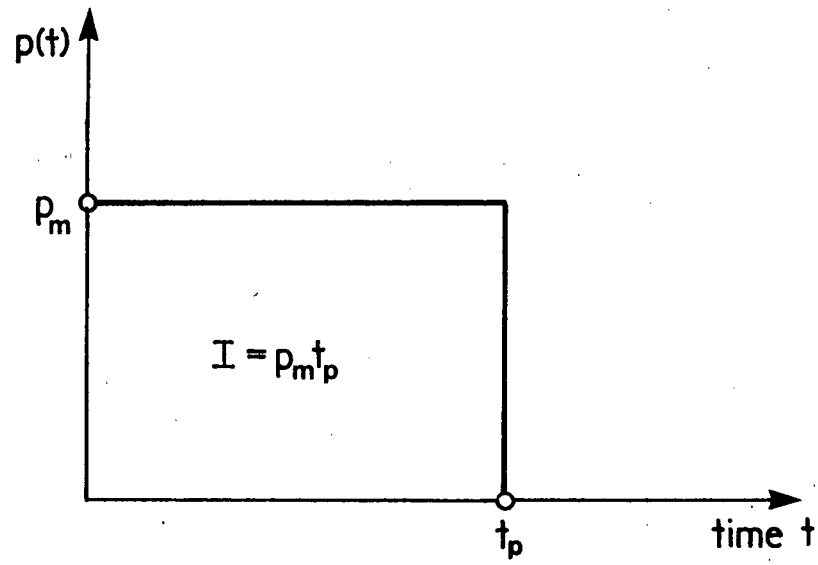

FIGURE 2.18 *Rectangular load pulse.*

2.6 RECTANGULAR PULSES

Consider the case of a *pinned* beam subjected to a pulse defined by

$$p(t) = \begin{cases} p_m, & \text{if } 0 \le t \le t_p, \\ 0, & \text{if } t > t_p, \end{cases} \tag{2.6.1}$$

and shown in Figure 2.18. This rectangular pulse is a special case of blast-type pulses. The nomimal impulse as defined by Equation (2.5.1) is

$$I = p_m t_p. \tag{2.6.2}$$

2.6.1 MEDIUM LOADS ($p_o < p_m \le 3p_o$)

(a) During The Load Pulse ($t \le t_p$)

The initial response of the beam will be according to Equations (2.5.2a,b) or

$$\begin{aligned} w_o(t) &= \frac{3p_o}{4m}(\overline{p} - 1)t^2, \\ \dot{w}_o(t) &= \frac{3p_o}{2m}(\overline{p} - 1)t, \end{aligned} \tag{2.6.3a, b}$$

where $\overline{p} = p_m/p_o$. Notice that, since $p(t) > p_o$ during the load pulse, the beam cannot come to rest during the loaded bending response phase. If we define a non-dimensional

impulse parameter β such that

$$\beta = \frac{I^2}{mp_oM_o/N_o}, \tag{2.6.4}$$

which, for the case of a rectangular pulse, is

$$\beta = \frac{p_o\bar{p}^2{t_p}^2}{mM_o/N_o}, \tag{2.6.5}$$

the beam response during the loaded bending response phase can be rewritten as

$$\begin{aligned} w_o(t) &= \frac{3M_o\beta(\bar{p}-1)}{4N_o\bar{p}^2}\left(\frac{t}{t_p}\right)^2, \\ \dot{w}_o(t) &= \frac{3M_o\beta(\bar{p}-1)}{2N_o\bar{p}^2t_p}\left(\frac{t}{t_p}\right). \end{aligned} \tag{2.6.6a, b}$$

The beam will begin to undergo string deformation during the load pulse if there exists a $t_s \leq t_p$ such that $w_o(t_s) = M_o/N_o$. From Equation (2.6.6),

$$t_s = \frac{2\bar{p}t_p}{\sqrt{3\beta(\bar{p}-1)}} \tag{2.6.7}$$

and

$$\dot{w}_o(t_s^-) = \frac{M_o\sqrt{3\beta(\bar{p}-1)}}{N_o\bar{p}t_p}. \tag{2.6.8}$$

Such will be the case if $t_s \leq t_p$, or

$$\beta \geq \frac{4\bar{p}^2}{3(\bar{p}-1)}. \tag{2.6.9}$$

Putting Equations (2.6.1) and (2.6.8) into the initial value problem of Section (2.5.2) gives

$$\begin{aligned} \ddot{w}_o + \frac{N_o\pi^2}{4ml^2}w_o &= \frac{4p_m}{\pi m}, \\ w_o(t_s) &= M_o/N_o, \\ \dot{w}_o(t_s^+) &= \frac{M_o}{N_o\bar{p}t_p}\sqrt{2\beta(\bar{p}-1)}, \end{aligned}$$

for which the solution is

$$\begin{aligned} w_o(t) = \frac{M_o}{N_o}\Bigg\{&\left(1-\frac{32\bar{p}}{\pi^3}\right)\cos\left[\frac{\pi}{2}\sqrt{\frac{p_oN_o}{mM_o}}(t-t_s)\right] \\ &+\frac{4}{\pi}\sqrt{\bar{p}-1}\sin\left[\frac{\pi}{2}\sqrt{\frac{p_oN_o}{mM_o}}(t-t_s)\right]+\frac{32\bar{p}}{\pi^3}\Bigg\}. \end{aligned} \tag{2.6.10}$$

Noting that

$$A\cos\theta + B\sin\theta = \sqrt{A^2+B^2}\cos(\theta+\phi)$$

where

$$\phi = -\tan^{-1}(B/A) - \begin{cases} \pi, & \text{if } A < 0 \\ 0, & \text{if } A \geq 0 \end{cases}$$

and recalling Equation (2.6.5), the response during the loaded string phase can be rewritten as

$$w_o(t) = \frac{M_o}{N_o}\left\{\sqrt{\left(1-\frac{32\bar{p}}{\pi^3}\right)^2 + \frac{16(\bar{p}-1)}{\pi^2}}\right.$$
$$\left.\cos\left[\frac{\pi\sqrt{\beta}}{2\bar{p}}\left(\frac{t-t_s}{t_p}\right) - \tan^{-1}\left(\frac{4\sqrt{\bar{p}-1}}{\pi-32\bar{p}/\pi^2}\right) - \pi\right] + \frac{32\bar{p}}{\pi^3}\right\},$$
$$\dot{w}_o(t) = \frac{M_o\pi\sqrt{\beta}}{2N_o\bar{p}t_p}\sqrt{\left(1-\frac{32\bar{p}}{\pi^3}\right)^2 + \frac{16(\bar{p}-1)}{\pi^2}}$$
$$\sin\left[\tan^{-1}\left(\frac{4\sqrt{\bar{p}-1}}{\pi-32\bar{p}/\pi^2}\right) + \pi - \frac{\pi\sqrt{\beta}}{2\bar{p}}\left(\frac{t-t_s}{t_p}\right)\right]. \tag{2.6.11a, b}$$

The beam's final displacement w_{o_f} will occur at time t_f such that $\dot{w}_o(t_f) = 0$. If the beam comes to rest during the loaded string response phase,

$$w_{o_f} = \frac{M_o}{N_o}\left\{\sqrt{\left(1-\frac{32\bar{p}}{\pi^3}\right)^2 + \frac{16(\bar{p}-1)}{\pi^2}} + \frac{32\bar{p}}{\pi^3}\right\}, \tag{2.6.12}$$

where

$$t_f = \frac{2\bar{p}t_p}{\pi\sqrt{\beta}}\left[\tan^{-1}\left(\frac{4\sqrt{\bar{p}-1}}{\pi-32\bar{p}/\pi^2}\right) + \pi\right] + t_s \leq t_p$$

or

$$\beta \geq 2\bar{p}^2\left[\frac{2}{\pi}\tan^{-1}\left(\frac{4\sqrt{\bar{p}-1}}{\pi-32\bar{p}/\pi^2}\right) + \sqrt{\frac{2}{3(\bar{p}-1)}} + 2\right]^2. \tag{2.6.13}$$

If Equation (2.6.13) is not satisfied the beam will come to rest after the load has been removed.

(b) After The Load Pulse ($t > t_p$)

Hereafter, the load $p(t) = 0$. If the load pulse ends before the beam reaches the plastic string state, *i.e.* if Equation (2.6.9) is not satisfied, the midspan acceleration will be

$$\ddot{w}_o(t) = -\frac{3p_o}{2m} = -\frac{3M_o\beta}{2N_o\bar{p}^2{t_p}^2}. \tag{2.6.14}$$

Integrating in time with the initial conditions at time t_p determined from Equations (2.6.6a,b) gives the deflection response of the beam as

$$\begin{aligned} w_o(t) &= \frac{3M_o\beta}{4N_o\overline{p}^2}\left[-p + 2p\left(\frac{t}{t_p}\right) - \left(\frac{t}{t_p}\right)^2\right], \\ \dot{w}_o(t) &= \frac{3M_o\beta}{2N_o\overline{p}^2 t_p}\left(\overline{p} - \frac{t}{t_p}\right). \end{aligned} \tag{2.6.15a, b}$$

Setting $\dot{w}_o(t_f) = 0$ gives $t_f = \overline{p}t_p$ and hence

$$w_{o_f} = \frac{3M_o\beta}{4N_o}\left(\frac{\overline{p}-1}{\overline{p}}\right), \tag{2.6.16}$$

where the beam comes to rest during the unloaded bending response phase. Setting $w_{o_f} \leq M_o/N_o$, Equation (2.6.16) is found to be valid if

$$\beta \leq \frac{4}{3}\left(\frac{\overline{p}}{\overline{p}-1}\right). \tag{2.6.17}$$

Otherwise the beam will reach the string state at time t_s when $w_o(t_s) = M_o/N_o$, from which it is found that

$$t_s = \overline{p}t_p\left(1 - \sqrt{\frac{\overline{p}-1}{\overline{p}} - \frac{4}{3\beta}}\right) \tag{2.6.18}$$

and

$$\dot{w}_o(t_s^-) = \frac{3M_o\beta}{2N_o\overline{p}t_p}\sqrt{\frac{\overline{p}-1}{\overline{p}} - \frac{4}{3\beta}}. \tag{2.6.19}$$

From time t_s on the beam will respond as a plastic string and this response is governed by the initial value problem

$$\begin{aligned} \ddot{w}_o + \frac{N_o\pi^2}{4ml^2}w_o &= 0, \\ w_o(t_s) &= M_o/N_o, \\ \dot{w}_o(t_s^+) &= \frac{M_o\beta}{N_o\overline{p}t_p}\sqrt{\frac{3}{2}\left(\frac{\overline{p}-1}{\overline{p}}\right) - \frac{2}{\beta}}, \end{aligned}$$

for which the solution is

$$\begin{aligned} w_o(t) = \frac{M_o}{N_o}&\sqrt{1 + \frac{12\beta(\overline{p}-1)}{\pi^2\overline{p}} - \frac{16}{\pi^2}} \\ &\cos\left[\frac{\pi\sqrt{\beta}}{2\overline{p}}\left(\frac{t-t_s}{t_p}\right) - \tan^{-1}\left(\frac{2}{\pi}\sqrt{\frac{3\beta(\overline{p}-1)}{\overline{p}} - 4}\right)\right]. \end{aligned} \tag{2.6.20}$$

The final deflection of the beam is thus obtained as

$$w_{o_f} = \frac{M_o}{N_o}\sqrt{1 + \frac{12\beta(\bar{p}-1)}{\pi^2\bar{p}} - \frac{16}{\pi^2}}. \tag{2.6.21}$$

Finally, if $t_e \leq t_p$ and the beam does not come to rest during the loaded response phase, the beam will deform in the unloaded string response phase according to the initial value problem

$$\ddot{w}_o + \frac{N_o\pi^2}{4ml^2}w_o = 0,$$
$$w_o(t_p) = \frac{M_o}{N_o}\left[\left(1 - \frac{32\bar{p}}{\pi^3}\right)\cos\gamma + \frac{4\sqrt{\bar{p}-1}}{\pi}\sin\gamma + \frac{32\bar{p}}{\pi^3}\right],$$
$$\dot{w}_o(t_p) = \frac{M_o\pi\sqrt{\beta}}{2N_o\bar{p}t_p}\left[\left(\frac{32\bar{p}}{\pi^3} - 1\right)\sin\gamma + \frac{4\sqrt{\bar{p}-1}}{\pi}\cos\gamma\right],$$

where

$$\gamma = \frac{\pi}{2}\left(\sqrt{\frac{\beta}{2\bar{p}^2}} - \sqrt{\frac{2}{3(\bar{p}-1)}}\right), \tag{2.6.22}$$

with the initial conditions determined at t_p from Equations (2.6.10a,b). The midspan displacement of the beam is then found to be

$$\begin{aligned} w_o(t) = {} & \frac{M_o}{N_o}\left[\left(1 - \frac{32\bar{p}}{\pi^3}\right)\cos\gamma + \frac{4\sqrt{\bar{p}-1}}{\pi}\sin\gamma + \frac{32\bar{p}}{\pi^3}\right]\cos\left[\frac{\pi\sqrt{\beta}}{2\bar{p}}(t/t_p - 1)\right] \\ & + \frac{M_o}{N_o}\left[\left(\frac{32\bar{p}}{\pi^3} - 1\right)\sin\gamma + \frac{4\sqrt{\bar{p}-1}}{\pi}\cos\gamma\right]\sin\left[\frac{\pi\sqrt{\beta}}{2\bar{p}}(t/t_p - 1)\right], \end{aligned} \tag{2.6.23}$$

and the final deflection of the beam is

$$\begin{aligned} w_{o_f} = {} & \frac{M_o}{N_o}\left[\left(1 - \frac{32\bar{p}}{\pi^3}\right)^2 + \frac{16(\bar{p}-1)}{\pi^2} + \frac{1024\bar{p}^2}{\pi^6}\right. \\ & \left. + \frac{64\bar{p}}{\pi^3}\left(1 - \frac{32\bar{p}}{\pi^3}\right)\cos\gamma + \frac{256\bar{p}\sqrt{\bar{p}-1}}{\pi^4}\sin\gamma\right]^{1/2}. \end{aligned} \tag{2.6.24}$$

2.6.2 HIGH LOADS ($p_m > 3p_o$)

(a) During The Load Pulse ($t \leq t_p$)

The beam will initially respond with a flat central plastic zone as shown in Figure 2.17. Putting $p(t) = p_m$ into Equations (2.5.4a,b) and (2.5.7) gives the motion of the beam as

$$\begin{aligned} w_o(t) &= \frac{p_m t^2}{2m} = \frac{M_o\beta}{2N_o\bar{p}}\left(\frac{t}{t_p}\right)^2, \\ \dot{w}_o(t) &= \frac{p_m t}{m} = \frac{M_o\beta}{N_o\bar{p}t_p}\left(\frac{t}{t_p}\right), \end{aligned} \tag{2.6.25a, b}$$

and

$$x_o(t) = l\left(1 - \sqrt{3/\bar{p}}\right). \tag{2.6.26}$$

Under the constant load p_m the midspan of the beam continues to deflect and the hinges do not travel along the beam. Setting $w_o(t_s) = M_o/N_o$ yields

$$t_s = t_p\sqrt{2\bar{p}/\beta} \tag{2.6.27}$$

and

$$\dot{w}_o(t_s^-) = \frac{M_o}{N_o t_p}\sqrt{\frac{2\beta}{\bar{p}}}, \tag{2.6.28}$$

which give the initial conditions for the beam response in the loaded string phase. This phase exists if $t_s \leq t_p$ or

$$\beta \geq 2\bar{p}. \tag{2.6.29}$$

In the loaded string response phase the motion of the beam is governed by the initial value problem

$$\begin{aligned}
\ddot{w}_o + \frac{N_o\pi^2}{4ml^2}w_o &= \frac{4p_m}{\pi m},\\
w_o(t_s) &= M_o/N_o,\\
\dot{w}_o(t_s^+) &= \sqrt{\frac{2}{3}\left[1 + 2\left(1 - \sqrt{3/\bar{p}}\right)\right]}\,\dot{w}_o(t_s^-)\\
&= \frac{2M_o}{N_o t_p}\sqrt{\frac{\beta}{\bar{p}}\left(1 - \frac{2}{\sqrt{3\bar{p}}}\right)}.
\end{aligned}$$

Solving the problem as in Section 2.6.1, the deflection response is

$$\begin{aligned}
w_o(t) = \frac{M_o}{N_o}\Bigg\{&\sqrt{\left(1 - \frac{32\bar{p}}{\pi^3}\right)^2 + \frac{32\bar{p}}{\pi^2}\left(1 - \frac{2}{\sqrt{3\bar{p}}}\right)}\\
&\cos\left[\frac{\pi\sqrt{\beta}}{2\bar{p}}\left(\frac{t - t_s}{t_p}\right) - \tan^{-1}\left(\frac{8\sqrt{\frac{\bar{p}}{2} - \sqrt{\frac{\bar{p}}{3}}}}{\pi - 32\bar{p}/\pi^2}\right) - \pi\right] + \frac{32\bar{p}}{\pi^3}\Bigg\},\\
\dot{w}_o(t) = \frac{M_o\pi\sqrt{\beta}}{2N_o\bar{p}t_p}&\sqrt{\left(1 - \frac{32\bar{p}}{\pi^3}\right)^2 + \frac{32\bar{p}}{\pi^2}\left(1 - \frac{2}{\sqrt{3\bar{p}}}\right)}\\
&\sin\left[-\frac{\pi\sqrt{\beta}}{2\bar{p}}\left(\frac{t - t_s}{t_p}\right) + \tan^{-1}\left(\frac{8\sqrt{\frac{\bar{p}}{2} - \sqrt{\frac{\bar{p}}{3}}}}{\pi - 32\bar{p}/\pi^2}\right) + \pi\right],
\end{aligned} \tag{2.6.30a, b}$$

and the final midspan displacement is

$$w_{of} = \frac{M_o}{N_o}\left\{\sqrt{\left(1-\frac{32\overline{p}}{\pi^3}\right)^2 + \frac{32\overline{p}}{\pi^2}\left(1-\frac{2}{\sqrt{3\overline{p}}}\right)} + \frac{32\overline{p}}{\pi^3}\right\}, \tag{2.6.31}$$

where

$$t_f = \frac{2\overline{p}t_p}{\pi\sqrt{\beta}}\left[\tan^{-1}\left(\frac{8\sqrt{\frac{\overline{p}}{2}-\sqrt{\frac{\overline{p}}{3}}}}{\pi - 32\overline{p}/\pi^2}\right) + \pi\right] + t_s \leq t_p$$

or

$$\beta \geq 2\overline{p}^2\left[\frac{2}{\pi}\tan^{-1}\left(\frac{8\sqrt{\frac{\overline{p}}{2}-\sqrt{\frac{\overline{p}}{3}}}}{\pi - 32\overline{p}/\pi^2}\right) + \sqrt{\frac{1}{\overline{p}}} + 2\right]^2. \tag{2.6.32}$$

If Equation (2.6.32) is not satisfied the beam will come to rest after the load has been removed.

(b) After The Load Pulse ($t > t_p$)

If the load is removed before the string state is reached, the beam continues to respond in the travelling hinge mode. The load is zero and therefore so is the midspan acceleration. From Equations (2.5.4a,b),

$$\begin{aligned} w_o(t) &= \frac{M_o\beta}{N_o\overline{p}}\left(\frac{t}{t_p} - \frac{1}{2}\right), \\ \dot{w}_o(t) &= \frac{M_o\beta}{N_o\overline{p}t_p}. \end{aligned} \tag{2.6.33a, b}$$

If $t > t_p$ then $\int_0^t p(\tau)\,d\tau = p_m t_p$ and Equation (2.5.7) gives

$$x_o(t) = l\left(1 - \sqrt{\frac{3t}{\overline{p}t_p}}\right). \tag{2.6.34}$$

This motion will occur until the hinges meet at midspan at the time

$$t_2 = \overline{p}t_p/3 \tag{2.6.35}$$

or the beam reaches the string state at the time

$$t_s = t_p\left(\frac{\overline{p}}{\beta} + \frac{1}{2}\right). \tag{2.6.36}$$

The hinges will meet at midspan before the string state is reached if

$$\beta \leq \frac{6\overline{p}}{2\overline{p}-3}, \tag{2.6.37}$$

and deformation will proceed in the single midspan hinge mode. Equations (2.59a,b) give the resulting deflection response as

$$\begin{aligned} w_o(t) &= \frac{3M_o\beta}{2N_o\overline{p}^2}\left[-\frac{\overline{p}}{3}-\frac{\overline{p}^2}{18}+\overline{p}\left(\frac{t}{t_p}\right)-\frac{1}{2}\left(\frac{t}{t_p}\right)^2\right], \\ \dot{w}_o(t) &= \frac{3M_o\beta}{2N_o\overline{p}^2t_p}\left(\overline{p}-t/t_p\right). \end{aligned} \tag{2.6.38a, b}$$

Setting $\dot{w}_o(t_f) = 0$ gives $t_f = \overline{p}t_p$ and putting this into Equation (2.6.38a) provides the final deflection

$$w_{o_f} = \frac{M_o\beta}{N_o}\left(\frac{2}{3}-\frac{1}{2\overline{p}}\right), \tag{2.6.39}$$

where $w_{o_f} \leq M_o/N_o$, or

$$\beta \leq \frac{6\overline{p}}{4\overline{p}-3}. \tag{2.6.40}$$

If the above inequality is not satisfied, the beam will reach the string state at the time

$$t_s = \overline{p}t_p\left[1-\frac{2}{3}\sqrt{2-3\left(\frac{1}{\beta}+\frac{1}{2\overline{p}}\right)}\right], \tag{2.6.41}$$

with the midspan velocity

$$\dot{w}_o(t_s^-) = \frac{M_o\beta}{N_o\overline{p}t_p}\sqrt{2-3\left(\frac{1}{\beta}+\frac{1}{2\overline{p}}\right)}. \tag{2.6.42}$$

From time t_s on the beam responds as a plastic string and, if $t_2 < t_s$, is governed by the initial value problem

$$\begin{aligned} \ddot{w}_o + \frac{N_o\pi^2}{4ml^2}w_o &= 0, \\ w_o(t_s) &= M_o/N_o, \\ \dot{w}_o(t_s^+) &= \frac{M_o\beta}{N_o\overline{p}t_p}\sqrt{\frac{4}{3}-\frac{2}{\beta}-\frac{1}{\overline{p}}}. \end{aligned}$$

The resulting deflection response is

$$\begin{aligned} w_o(t) = \frac{M_o}{N_o}\Bigg\{ &\cos\left[\frac{\pi\sqrt{\beta}}{2\overline{p}}\left(\frac{t-t_s}{t_p}\right)\right] \\ &+\frac{4}{\pi}\sqrt{\beta\left(\frac{2}{3}-\frac{1}{2\overline{p}}\right)-1}\,\sin\left[\frac{\pi\sqrt{\beta}}{2\overline{p}}\left(\frac{t-t_s}{t_p}\right)\right]\Bigg\}, \end{aligned} \tag{2.6.43}$$

from which the final midspan deflection is seen to be

$$w_{o_f} = \frac{M_o}{N_o}\sqrt{1 + \frac{16}{\pi^2}\left[\beta\left(\frac{2}{3} - \frac{1}{2\overline{p}}\right) - 1\right]}. \tag{2.6.44}$$

If the string state is reached before the hinges neet at midspan, *i.e.* $t_p < t_s \leq t_2$, the initial conditions for the string response come from Equations (2.6.33b), (2.6.34) and (2.6.36). The initial value problem to be solved is then

$$\begin{aligned} \ddot{w}_o + \frac{N_o\pi^2}{4ml^2}w_o &= 0, \\ w_o(t_s) &= M_o/N_o, \\ \dot{w}_o(t_s^+) &= \frac{M_o\beta}{N_o\overline{p}t_p}\sqrt{2 - 4\sqrt{\frac{1}{3\beta} + \frac{1}{2\overline{p}}}}. \end{aligned}$$

The midspan deflection response is then solved to be

$$w_o(t) = \frac{M_o}{N_o}\left\{\cos\left[\frac{\pi\sqrt{\beta}}{2\overline{p}}\left(\frac{t - t_s}{t_p}\right)\right] + \frac{4}{\pi}\sqrt{\beta - \sqrt{\frac{2\beta}{3}(2 + \beta/\overline{p})}}\sin\left[\frac{\pi\sqrt{\beta}}{2\overline{p}}\left(\frac{t - t_s}{t_p}\right)\right]\right\}, \tag{2.6.45}$$

from which the final midspan deflection is seen to be

$$w_{o_f} = \frac{M_o}{N_o}\sqrt{1 + \frac{16\beta}{\pi^2}\left(1 - \sqrt{\frac{4}{3\beta} + \frac{2}{3\overline{p}}}\right)}. \tag{2.6.46}$$

Finally, if the string state is reached before the load is removed, the initial conditions for the unloaded string response come from Equations (2.6.30a,b). Deflection response is then governed by

$$\begin{aligned} \ddot{w}_o + \frac{N_o\pi^2}{4ml^2}w_o &= 0, \\ w_o(t_p) &= \frac{M_o}{N_o}\left[\left(1 - \frac{32\overline{p}}{\pi^3}\right)\cos\gamma + \frac{8}{\pi}\sqrt{\frac{\overline{p}}{2} - \sqrt{\frac{\overline{p}}{3}}}\sin\gamma + \frac{32\overline{p}}{\pi^3}\right], \\ \dot{w}_o(t_p) &= \frac{M_o\pi\sqrt{\beta}}{2N_o\overline{p}t_p}\left[\left(\frac{32\overline{p}}{\pi^3} - 1\right)\sin\gamma + \frac{8}{\pi}\sqrt{\frac{\overline{p}}{2} - \sqrt{\frac{\overline{p}}{3}}}\cos\gamma\right], \end{aligned}$$

where

$$\gamma = \frac{\pi}{2}\left(\sqrt{\frac{\beta}{2\overline{p}^2}} - \sqrt{\frac{1}{\overline{p}}}\right). \tag{2.6.47}$$

The deformation response of the beam is found to be

$$w_o(t) = \frac{M_o}{N_o}\left[\left(1-\frac{32\overline{p}}{\pi^3}\right)\cos\gamma + \frac{8}{\pi}\sqrt{\frac{\overline{p}}{2}-\sqrt{\frac{\overline{p}}{3}}}\sin\gamma + \frac{32\overline{p}}{\pi^3}\right]\cos\left[\frac{\pi\sqrt{\beta}}{2\overline{p}}(t/t_p-1)\right]$$
$$+\frac{M_o}{N_o}\left[\left(\frac{32\overline{p}}{\pi^3}-1\right)\sin\gamma + \frac{8}{\pi}\sqrt{\frac{\overline{p}}{2}-\sqrt{\frac{\overline{p}}{3}}}\cos\gamma\right]\sin\left[\frac{\pi\sqrt{\beta}}{2\overline{p}}(t/t_p-1)\right], \tag{2.6.48}$$

and the final midspan deflection of the beam is

$$w_{o_f} = \frac{M_o}{N_o}\left[\left(1-\frac{32\overline{p}}{\pi^3}\right)^2 + \frac{64}{\pi^2}\left(\frac{\overline{p}}{2}-\sqrt{\frac{\overline{p}}{3}}\right) + \frac{1024\overline{p}^2}{\pi^6}\right.$$
$$\left.+\frac{64\overline{p}}{\pi^3}\left(1-\frac{32\overline{p}}{\pi^3}\right)\cos\gamma + \frac{512\overline{p}}{\pi^4}\sqrt{\frac{\overline{p}}{2}-\sqrt{\frac{\overline{p}}{3}}}\sin\gamma\right]^{1/2}. \tag{2.6.49}$$

The results of the analyses of Sections 2.6.1 and 2.6.2 are summarized in Tables 2.1 and 2.2, in which the solutions for the permanent midspan displacement w_{o_f} are given along with the impulse domains over which they are valid. These results for pinned beams are plotted in Figures 2.19–2.21. Tables 2.3 and 2.4 contain clamped beam results obtained by similar analyses.

2.6.3 COMPARISON WITH PREVIOUS SOLUTIONS

As a check on the credibility of the results derived above, and more critically a check on the accuracy of the underlying assumptions that led to these results, comparisons must be made with the results obtained by analyses of a more rigorous or proven nature.

Recall that the analysis herein assumes that the yield curve of the beam section can be adequately approximated by a linear relation. The yield curves of practical doubly symmetric bending sections were shown in Figure 2.11, in which the rectangular section was seen to be approximated the least well by the linear relation. In this way the rectangular beam can be regarded as a "worst case" for the present analysis. The results of Sections 2.6.1 and 2.6.2 are compared with those of Vaziri's solution for rectangular beams [10] in Figures 2.22 and 2.23. These two analyses are based upon identical sets of assumptions (Section 2.2) with the exception that Vaziri used the correct quadratic yield

Table 2.1 *Final midspan displacement of a pinned beam subjected to a medium load ($\overline{p} \leq 3$) rectangular pulse.*

β	w_{o_f}
$0 \leq \beta \leq \beta_1$	$\dfrac{3M_o\beta}{4N_o}\left(\dfrac{\overline{p}-1}{\overline{p}}\right)$
$\beta_1 < \beta \leq \beta_2$	$\dfrac{M_o}{N_o}\sqrt{1+\dfrac{12\beta(\overline{p}-1)}{\pi^2\overline{p}}-\dfrac{16}{\pi^2}}$
$\beta_2 < \beta \leq \beta_3$	$\dfrac{M_o}{N_o}\left[\left(1-\dfrac{32\overline{p}}{\pi^3}\right)^2+\dfrac{16(\overline{p}-1)}{\pi^2}+\dfrac{1024\overline{p}^2}{\pi^6}+\dfrac{64\overline{p}}{\pi^3}\left(1-\dfrac{32\overline{p}}{\pi^3}\right)\cos\gamma+\dfrac{256\overline{p}\sqrt{\overline{p}-1}}{\pi^4}\sin\gamma\right]^{1/2}$
$\beta > \beta_3$	$\dfrac{M_o}{N_o}\left[\sqrt{\left(1-\dfrac{32\overline{p}}{\pi^3}\right)^2+\dfrac{16(\overline{p}-1)}{\pi^2}}+\dfrac{32\overline{p}}{\pi^3}\right]$

$$\beta_1 = \frac{4\overline{p}}{3(\overline{p}-1)}$$

$$\beta_2 = \frac{4\overline{p}^2}{3(\overline{p}-1)}$$

$$\beta_3 = 2\overline{p}^2\left[\frac{2}{\pi}\tan^{-1}\left(\frac{4\sqrt{\overline{p}-1}}{\pi-32\overline{p}/\pi^2}\right)+\sqrt{\frac{2}{3(\overline{p}-1)}}+2\right]^2$$

$$\gamma = \frac{\pi}{2}\left(\sqrt{\frac{\beta}{2\overline{p}^2}}-\sqrt{\frac{2}{3(\overline{p}-1)}}\right)$$

Table 2.2 *Final midspan displacement of a pinned beam subjected to a high load ($\overline{p} > 3$) rectangular pulse.*

β	w_{o_f}
$0 \le \beta \le \beta_1$	$\dfrac{M_o\beta}{N_o}\left(\dfrac{2}{3} - \dfrac{1}{2\overline{p}}\right)$
$\beta_1 < \beta \le \beta_2$	$\dfrac{M_o}{N_o}\sqrt{1 + \dfrac{16}{\pi^2}\left[\beta\left(\dfrac{2}{3} - \dfrac{1}{2\overline{p}}\right) - 1\right]}$
$\beta_2 < \beta \le \beta_3$	$\dfrac{M_o}{N_o}\sqrt{1 + \dfrac{16\beta}{\pi^2}\left(1 - \sqrt{\dfrac{4}{3\beta} + \dfrac{2}{3\overline{p}}}\right)}$
$\beta_3 < \beta \le \beta_4$	$\dfrac{M_o}{N_o}\left[\left(1 - \dfrac{32\overline{p}}{\pi^3}\right)^2 + \dfrac{64}{\pi^2}\left(\dfrac{\overline{p}}{2} - \sqrt{\dfrac{\overline{p}}{3}}\right) + \dfrac{1024\overline{p}^2}{\pi^6} + \dfrac{64\overline{p}}{\pi^3}\left(1 - \dfrac{32\overline{p}}{\pi^3}\right)\cos\gamma + \dfrac{512\overline{p}}{\pi^4}\sqrt{\dfrac{\overline{p}}{2} - \sqrt{\dfrac{\overline{p}}{3}}}\sin\gamma\right]^{1/2}$
$\beta > \beta_4$	$\dfrac{M_o}{N_o}\left[\sqrt{\left(1 - \dfrac{32\overline{p}}{\pi^3}\right)^2 + \dfrac{64}{\pi^2}\left(\dfrac{\overline{p}}{2} - \sqrt{\dfrac{\overline{p}}{3}}\right)} + \dfrac{32\overline{p}}{\pi^3}\right]$

$$\beta_1 = \frac{6\overline{p}}{4\overline{p} - 3}$$

$$\beta_2 = \frac{6\overline{p}}{2\overline{p} - 3}$$

$$\beta_3 = 2\overline{p}$$

$$\beta_4 = 2\overline{p}^2\left[\frac{2}{\pi}\tan^{-1}\left(\frac{8\sqrt{\overline{p}/2 - \sqrt{\overline{p}/3}}}{\pi - 32\overline{p}/\pi^2}\right) + \sqrt{\frac{1}{\overline{p}}} + 2\right]^2$$

$$\gamma = \frac{\pi}{2}\left(\sqrt{\frac{\beta}{2\overline{p}^2}} - \sqrt{\frac{1}{\overline{p}}}\right)$$

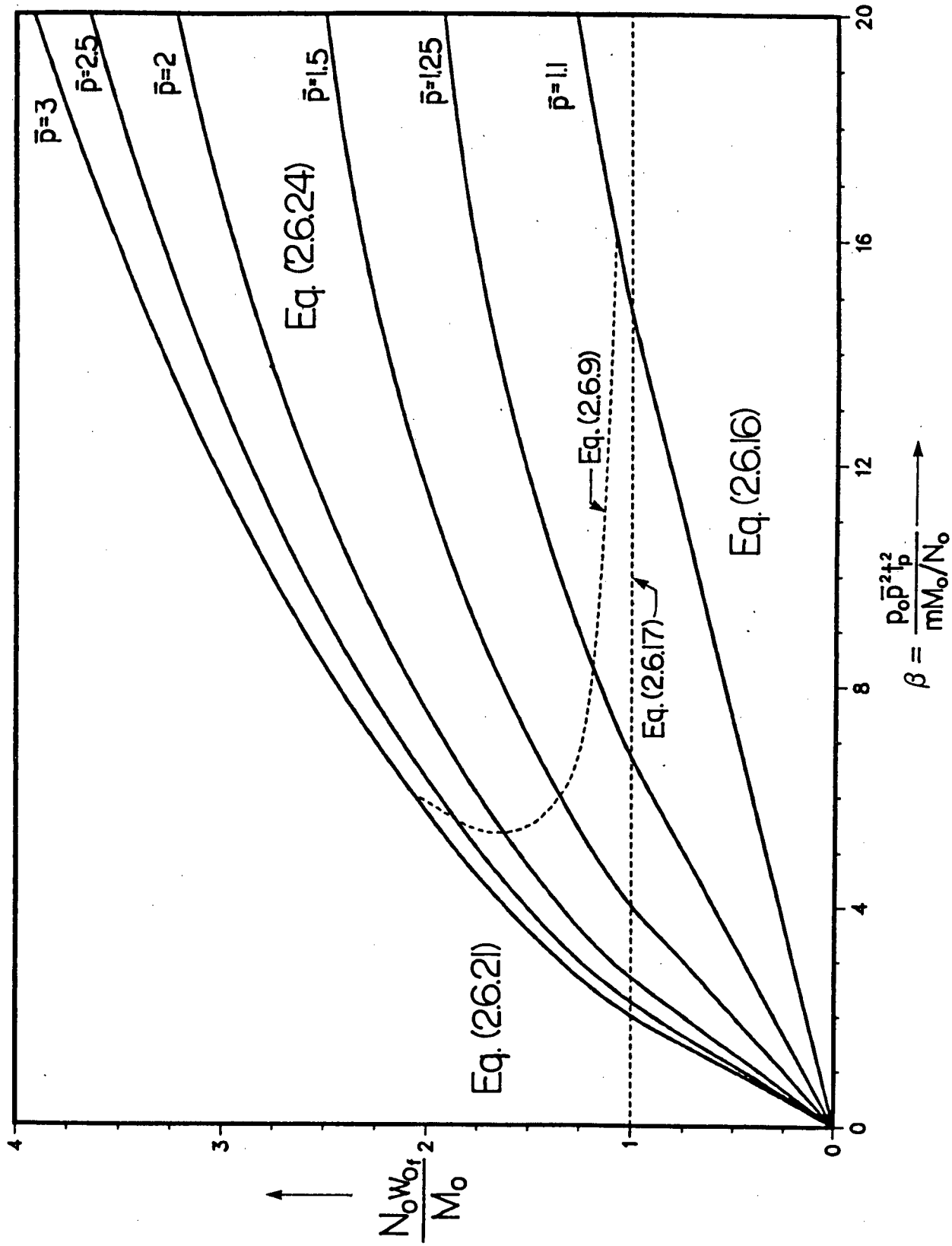

FIGURE 2.19 *Final midspan displacement vs. impulse of a pinned beam subjected to medium intensity rectangular load pulses.*

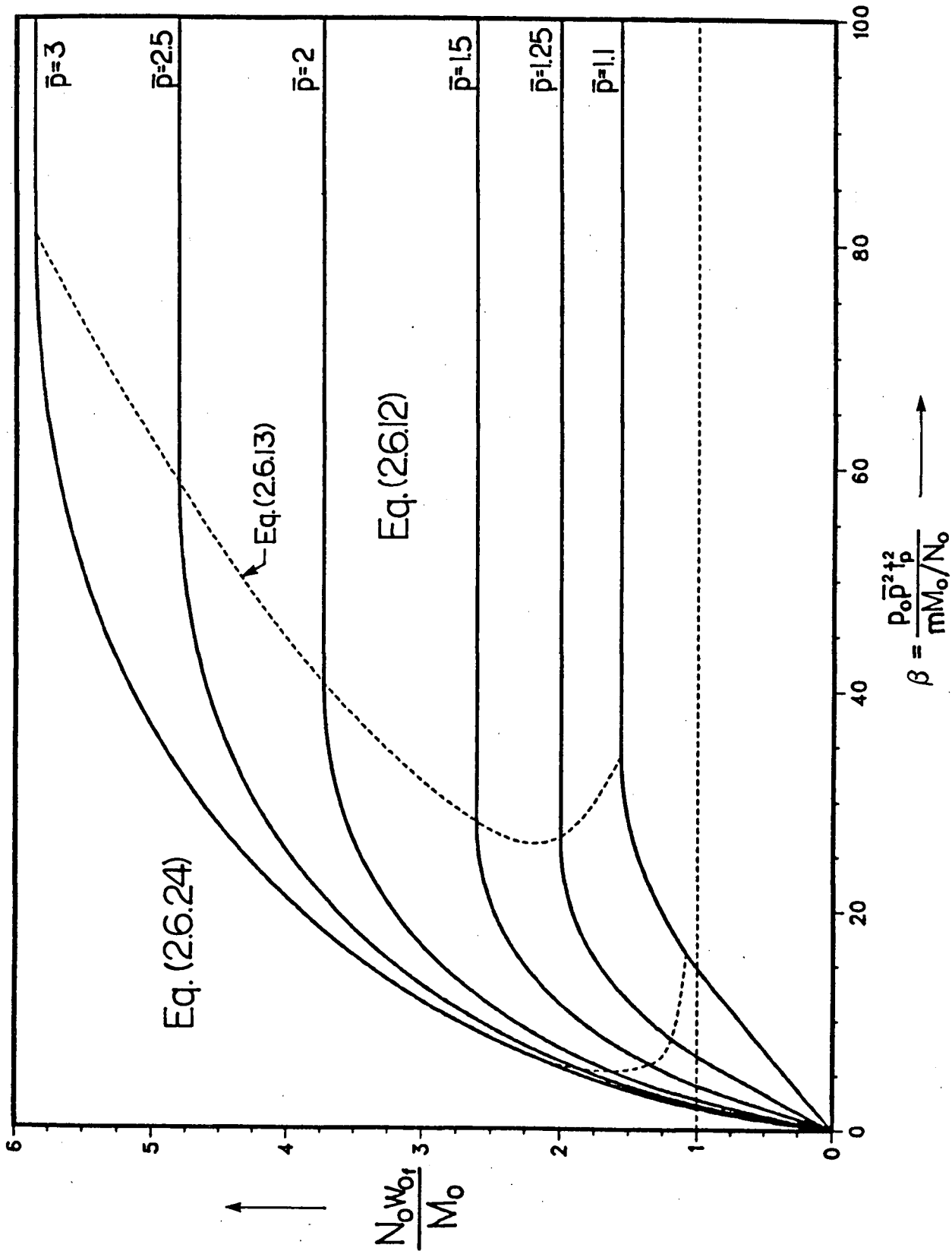

FIGURE 2.20 *Final midspan displacement vs. impulse of a pinned beam subjected to medium intensity rectangular load pulses.*

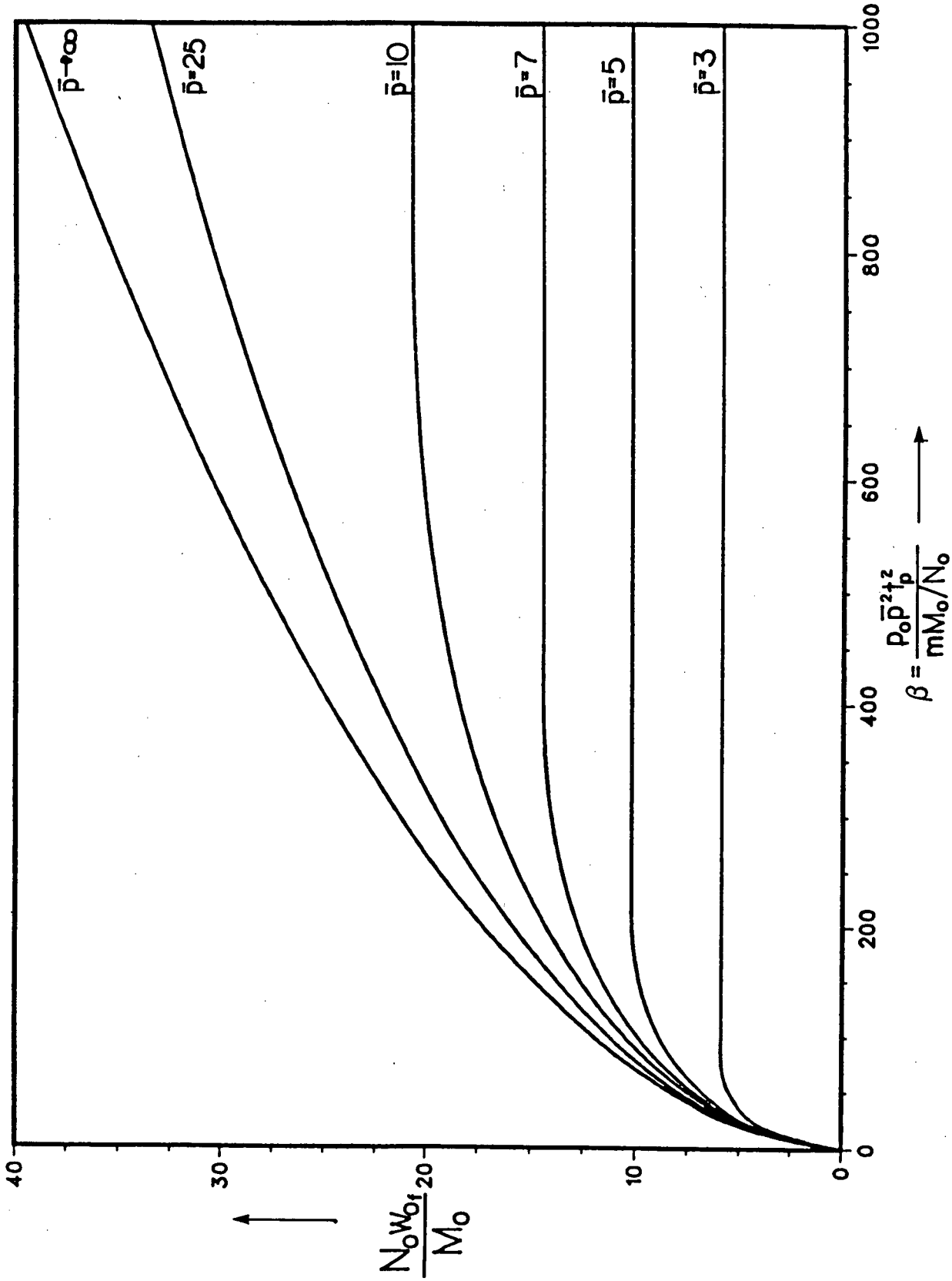

FIGURE 2.21 *Final midspan displacement vs. impulse of a pinned beam subjected to high intensity rectangular load pulses.*

Table 2.3 *Final midspan displacement of a clamped beam subjected to a medium load ($\overline{p} \leq 3$) rectangular pulse.*

β	w_{o_f}
$0 \leq \beta \leq \beta_1$	$\dfrac{3M_o\beta}{4N_o}\left(\dfrac{\overline{p}-1}{\overline{p}}\right)$
$\beta_1 < \beta \leq \beta_2$	$\dfrac{2M_o}{N_o}\sqrt{1+\dfrac{6\beta(\overline{p}-1)}{\pi^2\overline{p}}-\dfrac{16}{\pi^2}}$
$\beta_2 < \beta \leq \beta_3$	$\dfrac{2M_o}{N_o}\left[\left(1-\dfrac{32\overline{p}}{\pi^3}\right)^2+\dfrac{16(\overline{p}-1)}{\pi^2}+\dfrac{1024\overline{p}^2}{\pi^6}+\dfrac{64\overline{p}}{\pi^3}\left(1-\dfrac{32\overline{p}}{\pi^3}\right)\cos\gamma+\dfrac{256\overline{p}\sqrt{\overline{p}-1}}{\pi^4}\sin\gamma\right]^{1/2}$
$\beta > \beta_3$	$\dfrac{2M_o}{N_o}\left[\sqrt{\left(1-\dfrac{32\overline{p}}{\pi^3}\right)^2+\dfrac{16(\overline{p}-1)}{\pi^2}}+\dfrac{32\overline{p}}{\pi^3}\right]$

$$\beta_1 = \frac{8\overline{p}}{3(\overline{p}-1)}$$

$$\beta_2 = \frac{8\overline{p}^2}{3(\overline{p}-1)}$$

$$\beta_3 = 4\overline{p}^2\left[\frac{2}{\pi}\tan^{-1}\left(\frac{4\sqrt{\overline{p}-1}}{\pi-32\overline{p}/\pi^2}\right)+\sqrt{\frac{2}{3(\overline{p}-1)}}+2\right]^2$$

$$\gamma = \frac{\pi}{2}\left(\frac{\sqrt{\beta}}{2\overline{p}}-\sqrt{\frac{2}{3(\overline{p}-1)}}\right)$$

Table 2.4 *Final midspan displacement of a clamped beam subjected to a high load ($\overline{p} > 3$) rectangular pulse.*

β	w_{o_f}
$0 \le \beta \le \beta_1$	$\dfrac{M_o\beta}{N_o}\left(\dfrac{2}{3} - \dfrac{1}{2\overline{p}}\right)$
$\beta_1 < \beta \le \beta_2$	$\dfrac{2M_o}{N_o}\sqrt{1 + \dfrac{16}{\pi^2}\left[\beta\left(\dfrac{1}{3} - \dfrac{1}{4\overline{p}}\right) - 1\right]}$
$\beta_2 < \beta \le \beta_3$	$\dfrac{2M_o}{N_o}\sqrt{1 + \dfrac{8\beta}{\pi^2}\left(1 - \sqrt{\dfrac{8}{3\beta} + \dfrac{2}{3\overline{p}}}\right)}$
$\beta_3 < \beta \le \beta_4$	$\dfrac{2M_o}{N_o}\left[\left(1 - \dfrac{32\overline{p}}{\pi^3}\right)^2 + \dfrac{64}{\pi^2}\left(\dfrac{\overline{p}}{2} - \sqrt{\dfrac{\overline{p}}{3}}\right) + \dfrac{1024\overline{p}^2}{\pi^6} + \dfrac{64\overline{p}}{\pi^3}\left(1 - \dfrac{32\overline{p}}{\pi^3}\right)\cos\gamma + \dfrac{512\overline{p}}{\pi^4}\sqrt{\dfrac{\overline{p}}{2} - \sqrt{\dfrac{\overline{p}}{3}}}\sin\gamma\right]^{1/2}$
$\beta > \beta_4$	$\dfrac{2M_o}{N_o}\left[\sqrt{\left(1 - \dfrac{32\overline{p}}{\pi^3}\right)^2 + \dfrac{64}{\pi^2}\left(\dfrac{\overline{p}}{2} - \sqrt{\dfrac{\overline{p}}{3}}\right)} + \dfrac{32\overline{p}}{\pi^3}\right]$

$$\beta_1 = \frac{12\overline{p}}{4\overline{p} - 3}$$

$$\beta_2 = \frac{12\overline{p}}{2\overline{p} - 3}$$

$$\beta_3 = 4\overline{p}$$

$$\beta_4 = 4\overline{p}^2\left[\frac{2}{\pi}\tan^{-1}\left(\frac{8\sqrt{\overline{p}/2 - \sqrt{\overline{p}/3}}}{\pi - 32\overline{p}/\pi^2}\right) + \sqrt{\frac{1}{\overline{p}}} + 2\right]^2$$

$$\gamma = \frac{\pi}{2}\left(\frac{\sqrt{\beta}}{2\overline{p}} - \sqrt{\frac{1}{\overline{p}}}\right)$$

curve for the rectangular section. Therefore, Figures 2.22 and 2.23 directly represent the accuracy of the linear interaction relation for the worst case rectangular section.

Figure 2.13 showed that the linear interaction approximation gives the poorest results for the rectangular beam's load capacity at midspan deflections of $w_o \approx M_o/N_o$. One could therefore conclude that this study's results are least accurate for final midspan deflections in the order of M_o/N_o. Figure 2.22 supports this conclusion, with the results for $\overline{p} < 1.5$ being somewhat innaccurate and those for $\overline{p} > 1.5$ being reasonably good. The high load results ($\overline{p} > 3$) in Figure 2.23 compare very well. As all other practical, doubly symmetric bending sections would provide an even better comparison, the linear interaction approximation seems well considered.

With the development of numerical solutions based on the finite element method (F.E.M.) the approximation of rigid-plastic material behaviour can also be checked for accuracy. The pinned wide flange section of Figure 2.24 subjected to a rectangular pulse with $p_m = 5p_o = 486lb/in$ and $t_p = 0.01s$ was considered. The midspan displacement history of the beam is plotted in Figure 2.25 for both the rigid plastic-analysis herein and an elastic-plastic F.E.M. analysis by Folz [14]. Neglecting the oscillatory behaviour of Folz's solution which is due to the transient elastic effects of the beam, the two analyses seem to agree strongly with respect to the permanent plastic deformations of the beam. Folz's estimate of permanent midspan displacement, obtained by averaging the values of the "peaks" and "valleys" of the response history, is very close to the result of this study — within a few percent — and the difference could be attributed in part to the linear interaction relation's effect of "softening" the beam. These results seem to confirm the validity of the rigid-plastic idealization, but it must be noted that the loading parameters of this example are, at the least, fortuitous. The load is of high intensity and of short duration, satisfying the validity arguements of assumption (i) in Section 2.2.

A deeper discussion of the validity of this study is contained in Chapter 6.

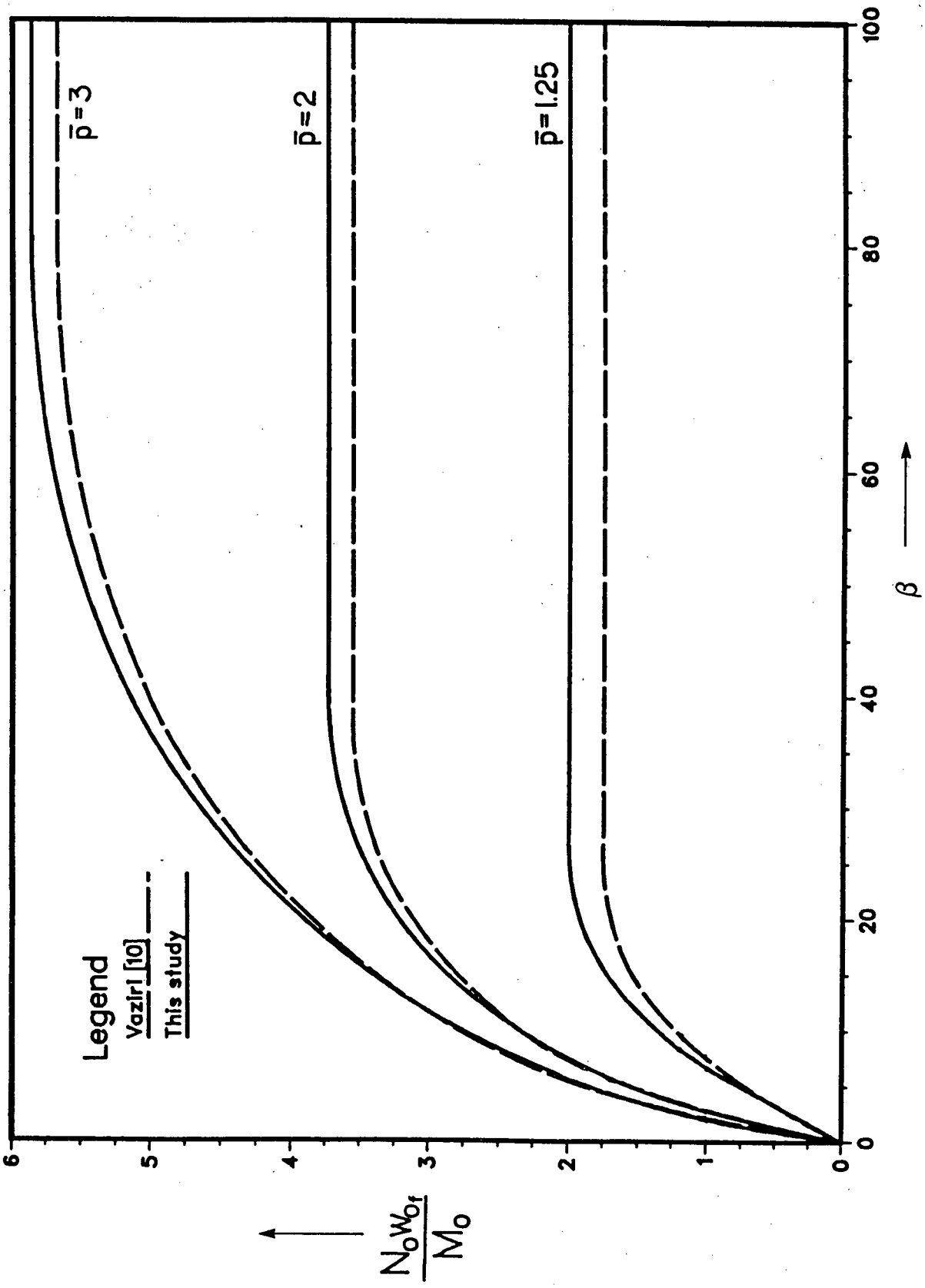

FIGURE 2.22 *Comparison of results of the present study with those of Vaziri [10] for the case of a pinned beam subjected to medium intensity rectangular load pulses.*

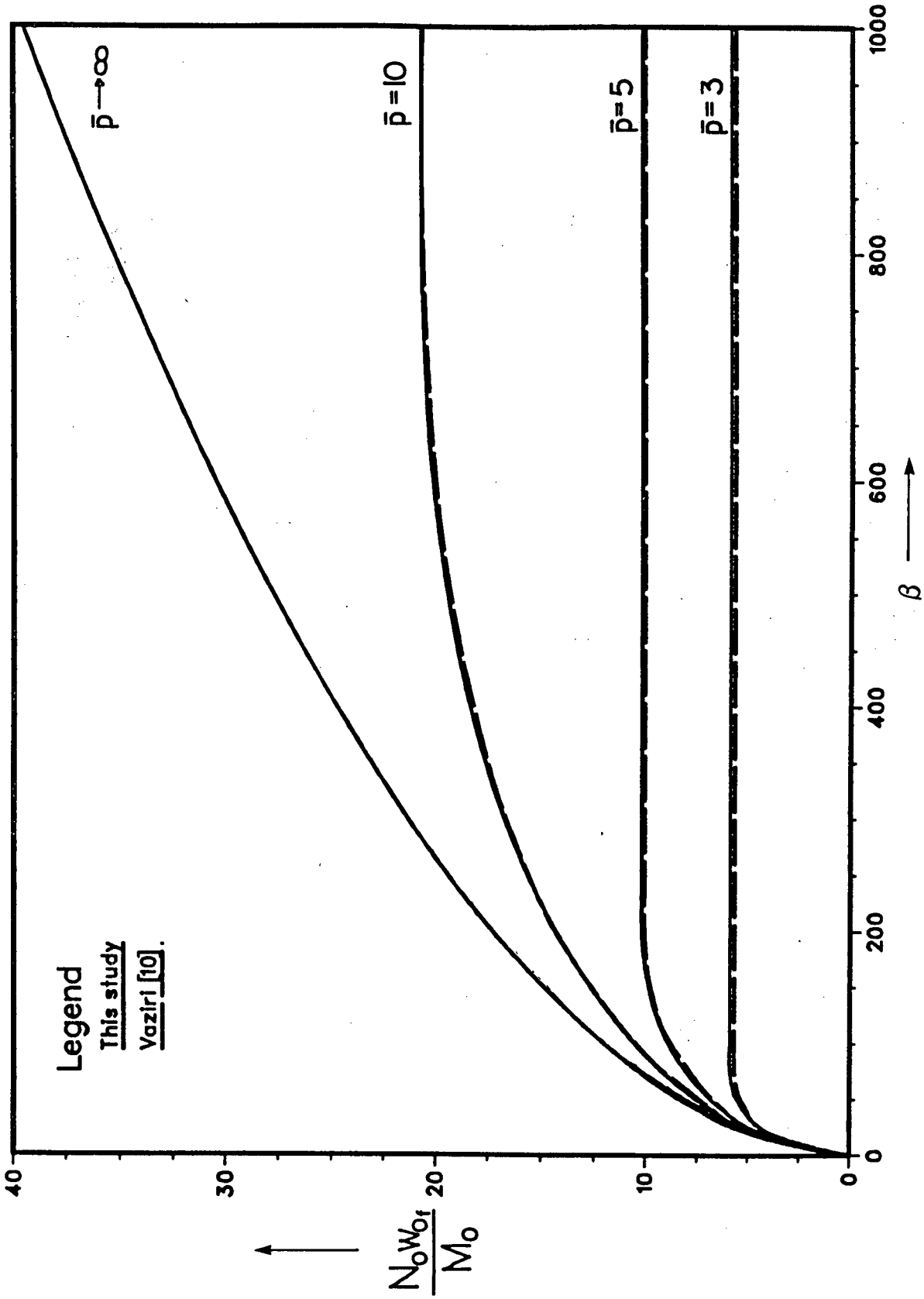

FIGURE 2.23 *Comparison of results of the present study with those of Vaziri [10] for the case of a pinned beam subjected to high intensity rectangular load pulses.*

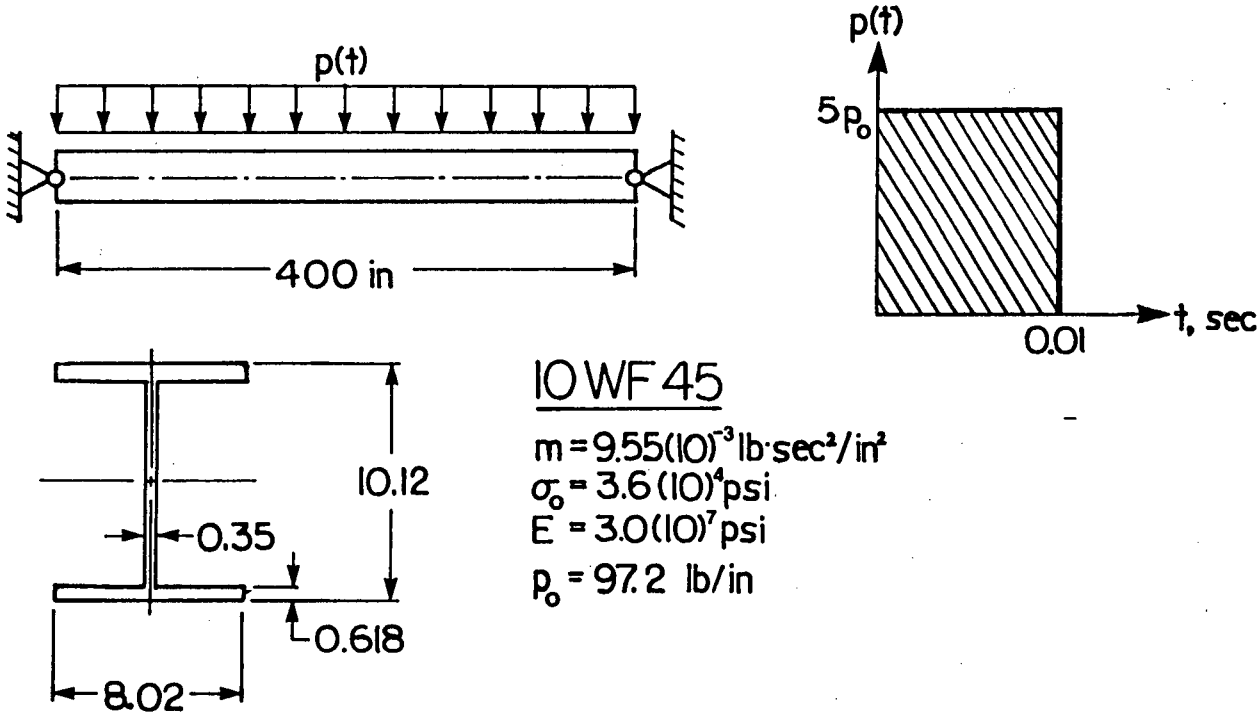

FIGURE 2.24 *Pinned wide flange beam subjected to a rectangular pressure pulse.*

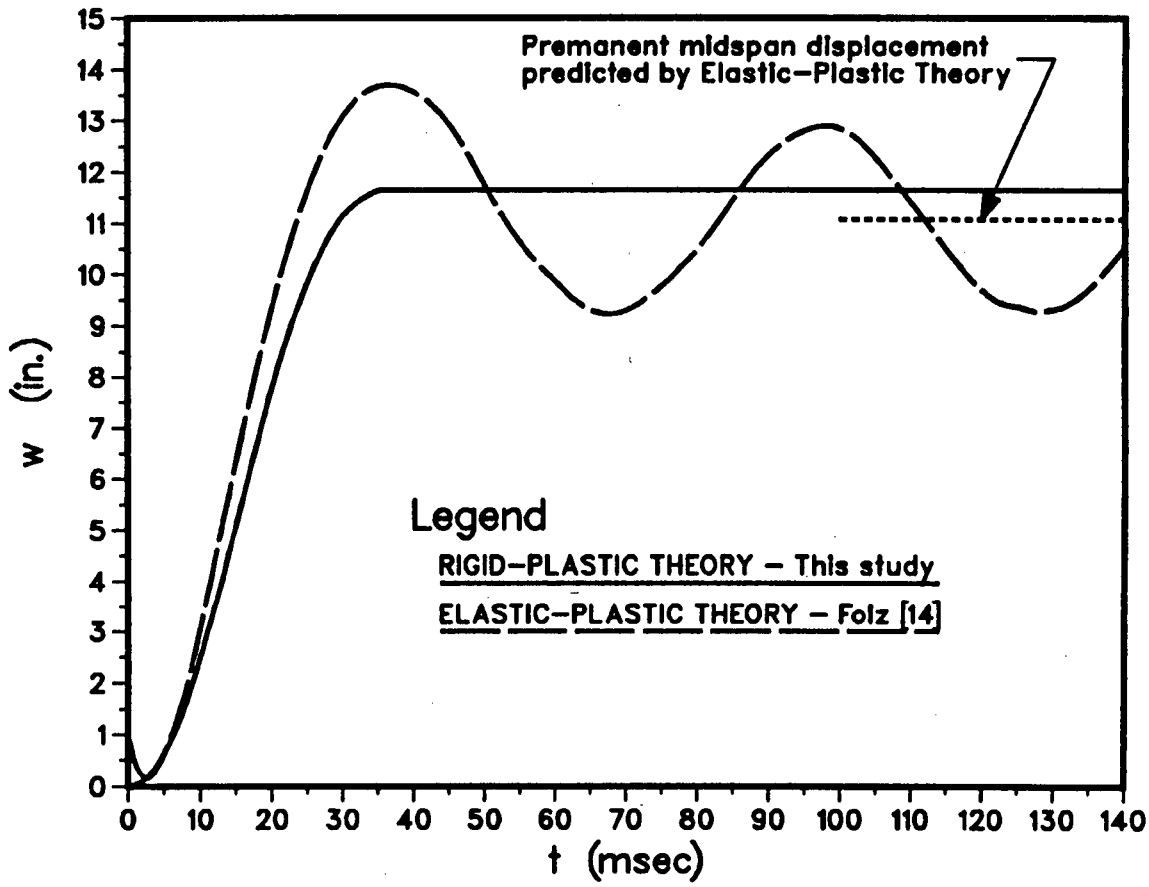

FIGURE 2.25 *Comparison of results between rigid-plastic analysis and elastic-plastic F.E.M. analysis for wide flange beam example.*

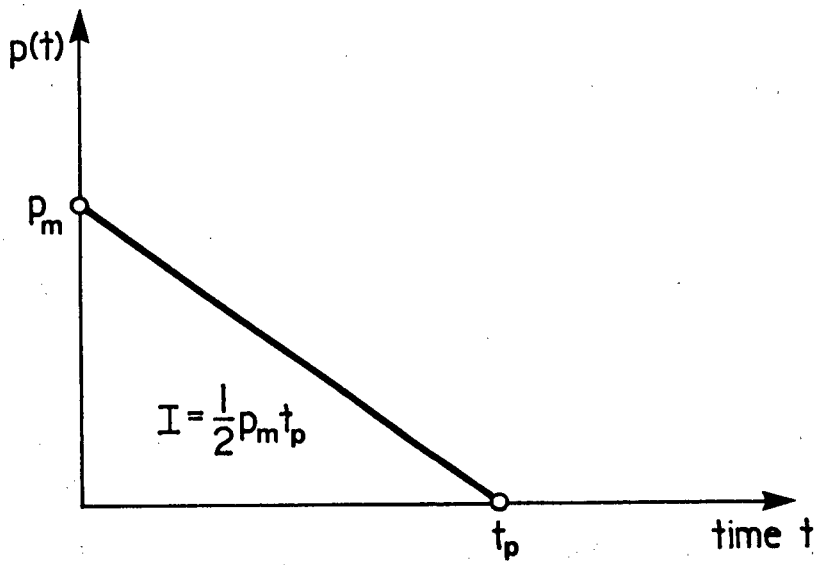

FIGURE 2.26 *Triangular load pulse.*

2.7 TRIANGULAR PULSES

Now consider the case of a pinned beam subjected to a pulse defined by

$$p(t) = \begin{cases} p_m(1 - t/t_p), & \text{if } 0 \le t \le t_p, \\ 0, & \text{if } t > t_p, \end{cases} \tag{2.7.1}$$

and shown in Figure 2.26. The nominal impulse as defined by Equation (2.5.1) is

$$I = \tfrac{1}{2} p_m t_p \tag{2.7.2}$$

and from Equation (2.6.4) the non-dimensional impulse parameter is

$$\beta = \frac{p_o \overline{p}^2 {t_p}^2}{4mM_o/N_o}, \tag{2.7.3}$$

where $\overline{p} = p_m/p_o$ as before.

The displacement response for the triangular pulse is derived in a manner similar to that for the rectangular pulse. With this similarity in mind, this section will not present the complete analysis as did Section 2.6, but only the final results.

2.7.1 MEDIUM LOADS ($p_o < p_m \leq 3p_o$)

(a) During The Load Pulse ($0 \leq t \leq t_p$)

The initial response of the beam will be

$$w_o(t) = \frac{Mo\beta}{N_o\overline{p}}\left[3\left(\frac{\overline{p}-1}{\overline{p}}\right)\left(\frac{t}{t_p}\right)^2 - \left(\frac{t}{t_p}\right)^3\right],$$
$$\dot{w}_o(t) = \frac{3M_o\beta}{N_o\overline{p}t_p}\left[2\left(\frac{\overline{p}-1}{\overline{p}}\right)\frac{t}{t_p} - \left(\frac{t}{t_p}\right)^2\right], \tag{2.7.4a, b}$$

from which the final midspan displacement is found to be

$$w_{o_f} = \frac{4M_o\beta(\overline{p}-1)^3}{N_o\overline{p}^4} \tag{2.7.5}$$

if the beam comes to rest during the loaded bending response phase. This requires that $\overline{p} \leq 2$ and

$$\beta \leq \frac{\overline{p}^4}{4(\overline{p}-1)^3}. \tag{2.7.6}$$

If $\overline{p} > 2$ and

$$\beta < \frac{\overline{p}^2}{2\overline{p}-3} \tag{2.7.7}$$

the beam will proceed to the unloaded bending response phase. Otherwise, subsequent motion of the beam will be in the loaded string response phase with the initial conditions determined by

$$\left(\frac{t_s}{t_p}\right)^3 - 3\left(\frac{\overline{p}-1}{\overline{p}}\right)\left(\frac{t_s}{t_p}\right)^2 + \frac{\overline{p}}{\beta} = 0. \tag{2.7.8}$$

The beam response during the loaded string response phase will be

$$w_o(t) = \sqrt{A^2+B^2}\cos\left[\frac{\pi(t-t_s)}{\overline{p}t_p}\sqrt{\beta/2}+\phi\right] + \frac{32M_o\overline{p}}{\pi^3N_o}\left(1-\frac{t}{t_p}\right),$$
$$\dot{w}_o(t) = -\frac{\pi}{\overline{p}t_p}\sqrt{\frac{\beta}{2}(A^2+B^2)}\sin\left[\frac{\pi(t-t_s)}{\overline{p}t_p}\sqrt{\beta/2}+\phi\right] - \frac{32M_o\overline{p}}{\pi^3N_o}, \tag{2.7.9a, b}$$

where

$$A = \frac{M_o}{N_o}\left[1-\frac{32\overline{p}}{\pi^3}(1-t_s/t_p)\right],$$
$$B = \frac{\overline{p}t_p}{\pi}\sqrt{\frac{2}{\beta}}\left[\sqrt{2/3}\,\dot{w}_o(t_s^-) + \frac{32M_o\overline{p}}{\pi^3N_ot_p}\right], \tag{2.7.10a, b, c}$$
$$\phi = -\tan^{-1}(B/A) - \begin{cases}\pi, & \text{if } A < 0,\\ 0, & \text{if } A \geq 0,\end{cases}$$

and t_s and $\dot{w}_o(t_s^-)$ are given by Equations (2.7.8) and (2.7.4b). The beam will come to rest during the loaded string response phase at the time

$$t_f = \frac{\bar{p}t_p}{\pi}\sqrt{\frac{2}{\beta}}\left\{\sin^{-1}\left[-\frac{32M_o\bar{p}^2}{\pi^4 N_o}\sqrt{\frac{2}{\beta(A^2+B^2)}}\right] - \phi\right\} + t_s \tag{2.7.11}$$

if $t_f < t_p$. Substituting t_f back into Equation (2.7.9a) will give the final midspan displacement w_{o_f}.

(b) After The Load Pulse ($t > t_p$)

As noted in part (a), the beam will deform at some point in the unloaded bending response phase if $\bar{p} > 2$ and $\beta < \bar{p}^2/(2\bar{p} - 3)$. In this phase the response is given by

$$\begin{aligned} w_o(t) &= \frac{M_o\beta}{N_o\bar{p}}\left[-1 + 3\left(\frac{t}{t_p}\right) - \frac{3}{\bar{p}}\left(\frac{t}{t_p}\right)^2\right], \\ \dot{w}_o(t) &= \frac{3M_o\beta}{N_o\bar{p}t_p}\left[1 - \frac{2}{\bar{p}}\left(\frac{t}{t_p}\right)\right]. \end{aligned} \tag{2.7.12a, b}$$

The final midspan displacement is then

$$w_{o_f} = \frac{M_o\beta}{N_o\bar{p}}\left(\frac{3\bar{p}}{4} - 1\right) \tag{2.7.13}$$

if the beam comes to rest before the string state is reached, requiring that

$$\beta \le \frac{4\bar{p}}{3\bar{p} - 4}. \tag{2.7.14}$$

If Equation (2.7.14) is not satisfied, the beam will reach the plastic string state at the time

$$t_s = \frac{\bar{p}t_p}{2}\left(1 - \sqrt{1 - \frac{4}{3\bar{p}} - \frac{4}{3\beta}}\right) \tag{2.7.15}$$

with the midspan velocity

$$\dot{w}_o(t_s^-) = \frac{3M_o\beta}{N_o\bar{p}t_p}\sqrt{1 - \frac{4}{3\bar{p}} - \frac{4}{3\beta}}. \tag{2.7.16}$$

The subsequent motion in the unloaded string response phase is given by

$$w_o(t) = \frac{M_o}{N_o}\left\{\cos\left[\frac{\pi(t - t_s)}{\bar{p}t_p}\sqrt{\frac{\beta}{2}}\right] + \frac{4}{\pi}\sqrt{\frac{3\beta}{4} - \frac{\beta}{\bar{p}} - 1}\sin\left[\frac{\pi(t - t_s)}{\bar{p}t_p}\sqrt{\frac{\beta}{2}}\right]\right\}, \tag{2.7.17}$$

and the final displacement will be

$$w_{o_f} = \frac{M_o}{N_o}\sqrt{1 + \frac{16}{\pi^2}\left(\frac{3\beta}{4} - \frac{\beta}{\overline{p}} - 1\right)}. \tag{2.7.18}$$

Finally, if the beam reaches the string state before the load is removed, the initial conditions of the response will be given by Equations (2.7.9a,b) at time $t = t_p$. The final midspan displacement is eventually found to be

$$\begin{aligned} w_{o_f} = \Bigg\{ & (A^2 + B^2) + \frac{1024 M_o^2 \overline{p}^4}{\pi^8 N_o^2} \\ & + \frac{64 M_o \overline{p}^2}{\pi^4 N_o}\sqrt{\frac{2}{\beta}(A^2 + B^2)}\sin\left[\frac{\pi}{\overline{p}}\left(1 - \frac{t_e}{t_p}\right)\sqrt{\frac{\beta}{2}} + \phi\right]\Bigg\}^{1/2}, \end{aligned} \tag{2.7.19}$$

where A, B and ϕ are given by Equations (2.7.10a,b,c).

2.7.2 HIGH LOADS ($p_m > 3p_o$)

(a) During The Load Pulse ($0 \le t \le t_p$)

The beam will initially respond in the travelling hinge mode described in Section 2.4.1(b). In this mode the midspan displacement response will be

$$\begin{aligned} w_o(t) &= \frac{2M_o\beta}{3N_o\overline{p}}\left[3(t/t_p)^2 - (t/t_p)^3\right], \\ \dot{w}_o(t) &= \frac{2M_o\beta}{N_o\overline{p}t_p}\left[(2(t/t_p) - (t/t_p)^2\right]. \end{aligned} \tag{2.7.20a, b}$$

with no final deflection w_{o_f}. The time t_e at which the beam reaches the string state is found from

$$\left(\frac{t_e}{t_p}\right)^3 - 3\left(\frac{t_e}{t_p}\right)^2 + \frac{3\overline{p}}{2\beta} = 0. \tag{2.7.21}$$

The position of the hinges will be

$$x_o(t) = l\left(1 - \sqrt{\frac{6}{\overline{p}(2 - t/t_p)}}\right), \tag{2.7.22}$$

and by setting $x_o(t_2) = 0$ the time t_2 at which the hinges will meet at mispan is found to be

$$t_2 = 2t_p\left(\frac{\overline{p} - 3}{\overline{p}}\right). \tag{2.7.23}$$

Examining Equations (2.7.21) and (2.7.23), it is found that the hinges will meet during the load pulse (*i.e.* $t_2 \leq t_s, t_p$) if

$$\overline{p} \leq 6 \qquad \text{and} \qquad \beta \leq \frac{3\overline{p}^4}{8(\overline{p}-3)^2(\overline{p}+6)}. \tag{2.7.24}$$

The beam will reach the string state during the loaded travelling hinge mode (*i.e.* $t_s \leq t_2, t_p$) if

$$\beta \geq \begin{cases} \dfrac{3\overline{p}^4}{8(\overline{p}+6)(\overline{p}-3)^2}, & \text{if } \overline{p} \leq 6; \\ 3\overline{p}/4, & \text{if } p > 6. \end{cases} \tag{2.7.25}$$

Finally, if neither of these conditions is satisfied, the beam will begin to deform in the unloaded travelling hinge mode (*i.e.* $t_p < t_2, t_s$).

If Equations (2.7.24) are satisfied, the beam will proceed to deform in the loaded single midspan hinge mode with the displacement response given by

$$\begin{aligned} w_o(t) &= \frac{M_o\beta}{N_o\overline{p}}\left[3\left(\frac{\overline{p}-1}{\overline{p}}\right)\left(\frac{t}{t_p}\right)^2 - \left(\frac{t}{t_p}\right)^3 - \frac{4(\overline{p}-3)^3}{3\overline{p}^3}\right], \\ \dot{w}_o(t) &= \frac{3M_o\beta}{N_o\overline{p}t_p}\left[2\left(\frac{\overline{p}-1}{\overline{p}}\right)\left(\frac{t}{t_p}\right) - \left(\frac{t}{t_p}\right)^2\right], \end{aligned} \tag{2.7.26a, b}$$

with no final deflection w_{o_f} possible in the high load range. The beam will reach the string state at the time t_s determined by

$$\left(\frac{t_s}{t_p}\right)^3 - 3\left(\frac{\overline{p}-1}{\overline{p}}\right)\left(\frac{t_s}{t_p}\right)^2 + \frac{4}{3}\left(\frac{\overline{p}-3}{\overline{p}}\right)^3 + \frac{\overline{p}}{\beta} = 0 \tag{2.7.27}$$

if $t_s \leq t_p$, or

$$\beta \geq \frac{3\overline{p}^4}{6\overline{p}^3 - 9\overline{p}^2 - 4(\overline{p}-3)^3}. \tag{2.7.28}$$

The beam response during the loaded string response phase will again be given by Equations (2.7.9) and (2.7.10), but with Equation (2.7.10b) replaced by

$$B = \frac{\overline{p}t_p}{\pi}\sqrt{\frac{2}{\beta}}\left[\dot{w}_o(t_s^-)\sqrt{\frac{2}{3}\left(1+\frac{2x_o(t_s)}{l}\right)} + \frac{32M_o\overline{p}}{\pi^3 N_o t_p}\right] \tag{2.7.29}$$

if $\overline{p} > 6$. The conditions at time t_s above are determined by Equations (2.7.20) through (2.7.22). The beam will come to rest during the loaded string response phase at the time t_f given by Equation (2.7.11) if $t_f < t_p$.

(b) After The Load Pulse ($t > t_p$)

If the conditions of Equations (2.7.24) and (2.7.25) are not satisfied, the beam will deform in the unloaded travelling hinge mode with the midspan motion

$$\begin{aligned} w_o(t) &= \frac{2M_o\beta}{N_o\overline{p}}\left(\frac{t}{t_p} - \frac{1}{3}\right), \\ \dot{w}_o(t) &= \frac{2M_o\beta}{N_o\overline{p}t_p}, \end{aligned} \tag{2.7.30a, b}$$

and the hinge position

$$x_o(t) = l\left(1 - \sqrt{\frac{6t}{\overline{p}t_p}}\right). \tag{2.7.31}$$

The time t_2 at which the hinges meet at midspan will be

$$t_2 = \frac{\overline{p}t_p}{6}. \tag{2.7.32}$$

The beam will reach the string state at the time

$$t_s = t_p\left(\frac{\overline{p}}{2\beta} + \frac{1}{3}\right) \tag{2.7.33}$$

if $t_s \leq t_2$, or

$$\beta \geq \frac{3\overline{p}}{\overline{p} - 2}. \tag{2.7.34}$$

If the condition of Equation (2.7.34) is not satisfied, the beam will deform in the unloaded single midspan hinge mode as

$$\begin{aligned} w_o(t) &= \frac{3M_o\beta}{N_o\overline{p}^2}\left[-\frac{\overline{p}(\overline{p}+8)}{36} + \overline{p}\left(\frac{t}{t_p}\right) - \left(\frac{t}{t_p}\right)^2\right], \\ \dot{w}_o(t) &= \frac{6M_o\beta}{N_o\overline{p}^2t_p}\left(\frac{\overline{p}}{2} - \frac{t}{t_p}\right). \end{aligned} \tag{2.7.35a, b}$$

The beam will come to rest at the time $t_f = \overline{p}t_p/2$ with the midspan displacement

$$w_{o_f} = \frac{2M_o\beta(\overline{p} - 1)}{3N_o\overline{p}} \tag{2.7.36}$$

if the final displacement lies in the realm of bending response, requiring that $w_{o_f} \leq M_o/N_o$, or

$$\beta \leq \frac{3\overline{p}}{2(\overline{p} - 1)}. \tag{2.7.37}$$

If this is not the case, the beam will proceed to deform in the unloaded string response phase with the initial conditions

$$t_s = \frac{\bar{p}t_p}{2}\left[1 - \sqrt{\frac{8}{9}\left(\frac{\bar{p}-1}{\bar{p}}\right) - \frac{4}{3\beta}}\right] \tag{2.7.38}$$

and

$$\dot{w}_o(t_s) = \frac{3M_o\beta}{N_o\bar{p}t_p}\sqrt{\frac{8}{9}\left(\frac{\bar{p}-1}{\bar{p}}\right) - \frac{4}{3\beta}}. \tag{2.7.39}$$

The resulting motion will be defined by

$$w_o(t) = \frac{M_o}{N_o}\left\{\cos\left[\frac{\pi(t-t_s)}{\bar{p}t_p}\sqrt{\frac{\beta}{2}}\right] + \frac{4}{\pi}\sqrt{\frac{2\beta}{3}\left(\frac{\bar{p}-1}{\bar{p}}\right) - 1}\sin\left[\frac{\pi(t-t_s)}{\bar{p}t_p}\sqrt{\frac{\beta}{2}}\right]\right\} \tag{2.7.40}$$

with the final midspan deflection

$$w_{o_f} = \frac{M_o}{N_o}\sqrt{1 + \frac{16}{\pi^2}\left[\frac{2\beta}{3}\left(\frac{\bar{p}-1}{\bar{p}}\right) - 1\right]}. \tag{2.7.41}$$

If the condition of Equation (2.7.34) is satisfied, the beam will deform in the unloaded string response phase with the initial conditions of Equations (2.7.30b) and (2.7.33), resulting in the midspan displacement

$$w_o(t) = \frac{M_o}{N_o}\left\{\cos\left[\frac{\pi(t-t_s)}{\bar{p}t_p}\sqrt{\frac{\beta}{2}}\right] + \frac{4}{\pi}\sqrt{\beta - \frac{2\beta}{3}\sqrt{\frac{3}{\beta} + \frac{2}{\bar{p}}}}\sin\left[\frac{\pi(t-t_s)}{\bar{p}t_p}\sqrt{\frac{\beta}{2}}\right]\right\}. \tag{2.7.42}$$

The final midspan deflection will then be

$$w_{o_f} = \frac{M_o}{N_o}\sqrt{1 + \frac{16\beta}{\pi^2}\left(1 - \frac{2}{3}\sqrt{\frac{3}{\beta} + \frac{2}{\bar{p}}}\right)}. \tag{2.7.43}$$

Another possibility is that the beam will deform in the loaded single midspan hinge mode with the load removed before the string state is reached, *i.e.* $t_2 < t_p < t$. At the time t_p the beam will begin to deform in the unloaded single midspan hinge mode with the motion

$$\begin{aligned} w_o(t) &= \frac{3M_o\beta}{N_o\bar{p}^2}\left\{-\frac{\bar{p}}{3}\left[1 + \frac{4}{3}\left(\frac{\bar{p}-3}{\bar{p}}\right)^3\right] + \bar{p}\left(\frac{t}{t_p}\right) - \left(\frac{t}{t_p}\right)^2\right\}, \\ \dot{w}_o(t) &= \frac{6M_o\beta}{N_o\bar{p}^2t_p}\left(\frac{\bar{p}}{2} - \frac{t}{t_p}\right). \end{aligned} \tag{2.7.44a, b}$$

The beam will come to rest at the time $t_f = \overline{p}t_p/2$ with the midspan displacement

$$w_{o_f} = \frac{3M_o\beta}{N_o\overline{p}}\left[\frac{\overline{p}}{4} - \frac{1}{3} - \frac{4}{9}\left(\frac{\overline{p}-3}{\overline{p}}\right)^3\right] \tag{2.7.45}$$

if the final displacement lies within the realm of bending response, requiring that $w_{o_f} \leq M_o/N_o$, or

$$\beta \leq \frac{12\overline{p}^4}{9\overline{p}^4 - 12\overline{p}^3 - 16(\overline{p}-3)^3}. \tag{2.7.46}$$

Otherwise, the beam will proceed to deform in the unloaded string response phase with the initial conditions

$$t_s = \frac{\overline{p}t_p}{2}\left[1 - \sqrt{1 - \frac{4}{3\beta} - \frac{4}{3\overline{p}} - \frac{16(\overline{p}-3)^3}{9\overline{p}^4}}\right] \tag{2.7.47}$$

and

$$\dot{w}_o(t_s) = \frac{3M_o\beta}{N_o\overline{p}t_p}\sqrt{1 - \frac{4}{3\beta} - \frac{4}{3\overline{p}} - \frac{16(\overline{p}-3)^3}{9\overline{p}^4}}. \tag{2.7.48}$$

The resulting deflection response will be given by

$$w_o(t) = \frac{M_o}{N_o}\left\{\cos\left[\frac{\pi(t-t_s)}{\overline{p}t_p}\sqrt{\frac{\beta}{2}}\right] + \frac{4}{\pi}\sqrt{\beta\left[\frac{3}{4} - \frac{1}{\overline{p}} - \frac{4(\overline{p}-3)^3}{3\overline{p}^4}\right] - 1}\sin\left[\frac{\pi(t-t_s)}{\overline{p}t_p}\sqrt{\frac{\beta}{2}}\right]\right\}, \tag{2.7.49}$$

with the final midspan deflection

$$w_{o_f} = \frac{M_o}{N_o}\sqrt{1 + \frac{16\beta}{\pi^2}\left[\frac{3}{4} - \frac{1}{\overline{p}} - \frac{4(\overline{p}-3)^3}{3\overline{p}^4}\right] - \frac{16}{\pi^2}}. \tag{2.7.50}$$

Finally, if the beam reaches the string state before the load is removed, the initial conditions of the response will be given by Equations (2.7.9a,b) at time $t = t_p$. The final midspan displacement will again be given by Equation (2.7.19) with A and ϕ given by Equations (2.7.10a,c) and B coming from Equation (2.7.10b) or (2.7.29).

The results of this section for w_{o_f} are plotted in Figures (2.27 and (2.28) as functions of $\overline{p}$ and β.

2.7.3 COMPARISON WITH RECTANGULAR PULSE SOLUTION

Results for the displacement response of a beam subjected to a triangular pulse are of similar character to those of a beam subjected to a rectangular pulse. As

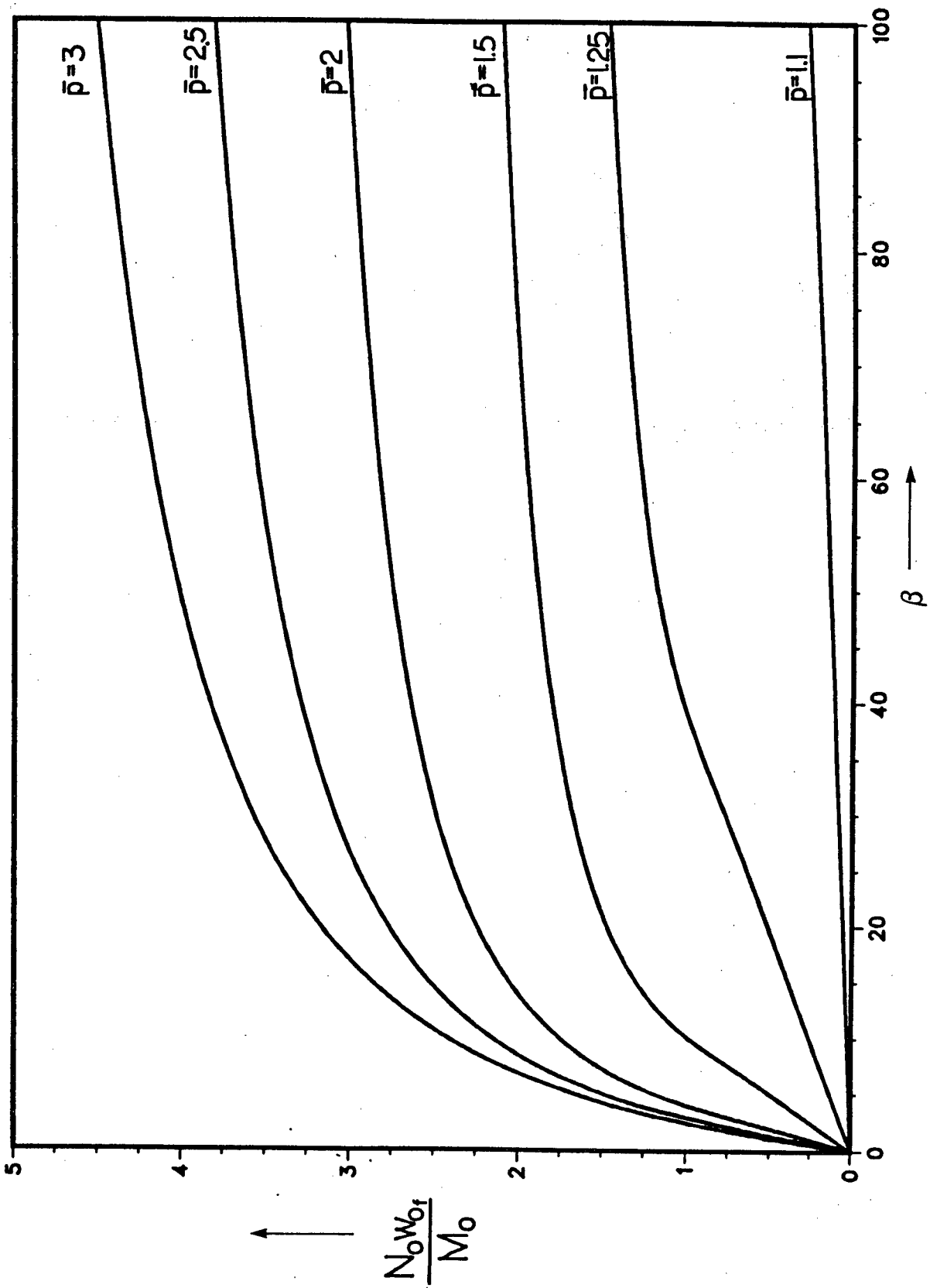

FIGURE 2.27 *Final midspan displacement vs. impulse of a pinned beam subjected to medium intensity triangular load pulses.*

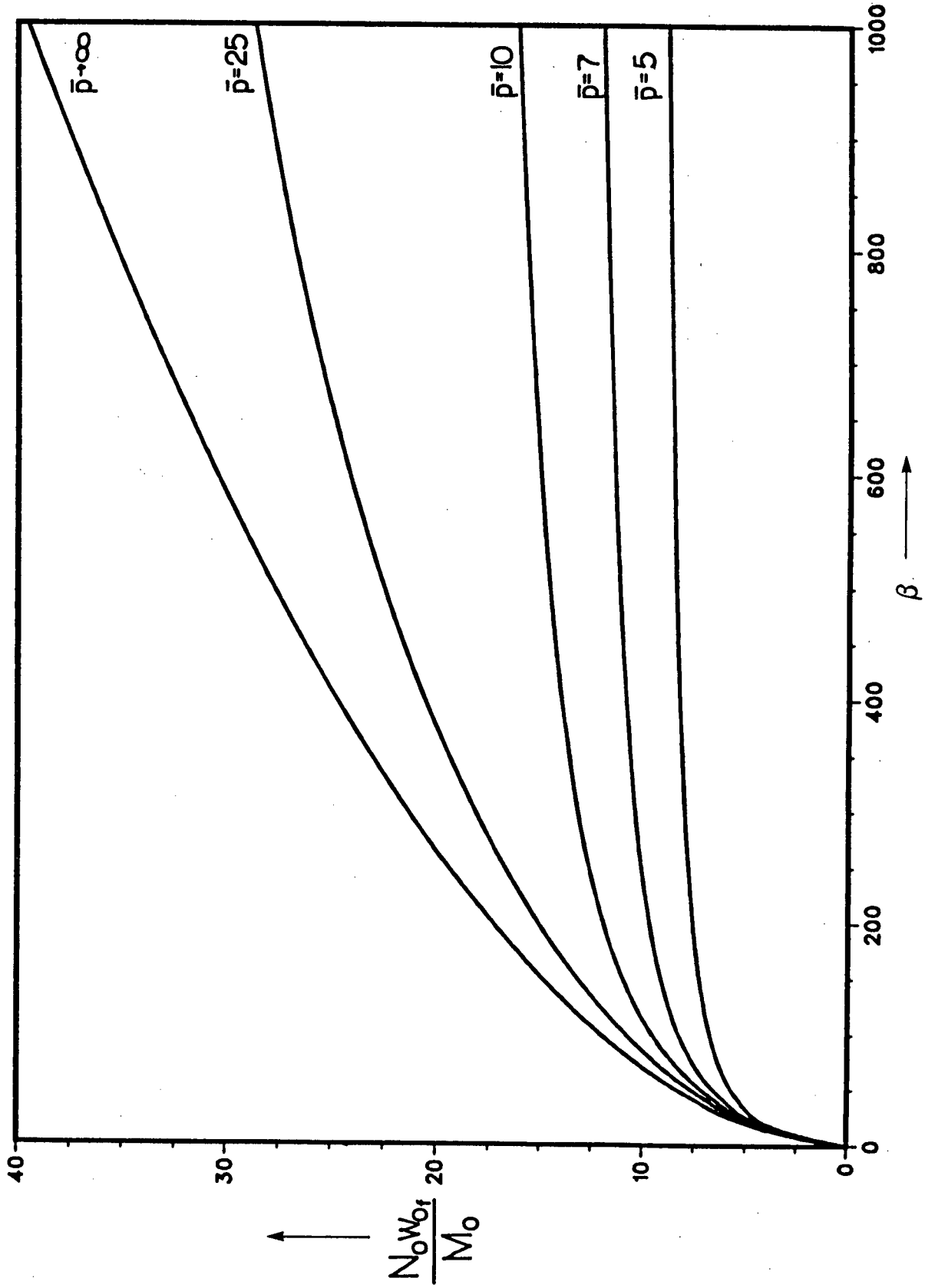

FIGURE 2.28 *Final midspan displacement vs. impulse of a pinned beam subjected to high intensity triangular load pulses.*

might be expected, for pulses with equal maximum intensity p_m and equal impulse I, final midspan deflection due to a rectangular pulse is greater than that for a triangular pulse, with the results tending to be equal as the loading duration t_p or the peak pressure p_m tends to infinity. As the load duration t_p, and hence the impulse I, approaches infinity the intensity of the triangular pulse of Figure 2.26 is seen to decrease at the rate $dp(t)/dt = -p_m/t_p \rightarrow 0$ and the pulse tends to become a step load identical to the rectangular pulse of infinite duration. As the peak pressure p_m approaches infinity for both pulse shapes, t_p must approach zero and the pulses become ideal impulses, equivalently represented by Dirac delta functions at time $t = 0$. Results for all other blast-type pulses will compare similarly.

CHAPTER 3

GENERAL PULSES

3.1 STATEMENT OF THE PROBLEM

In Chapter 2 the response of doubly symmetric beams subjected to blast-type pulses was investigated. Blast-type pulses are characterized by an instantaneous rise to the peak load p_m followed by monotonic decay of the load to zero. For the case of a pulse with peak load $p_m > 3p_o$, these blast-type pulse characteristics result in the instantaneous formation of two plastic hinges located symmetrically about the beam midspan followed by the monotonic convergence of these hinges towards midspan. With the hinges moving inward only, the plastic segment between the hinges is known to be flat and the analysis of such motion is straightforward.

In considering a blast-type pulse, the analyst assumes that the load rise time is very small in comparison to the pulse duration. However, measurements of experimental air blast pulses have shown that the load rise time can be of considerable duration. These experimental measurements have led some researchers to question the validity of the blast-type pulse approximation for structural design procedures.

The effect of load rise time, and hence the validity of the blast-type pulse approximation, will be studied in this chapter by subjecting the same doubly symmetric,

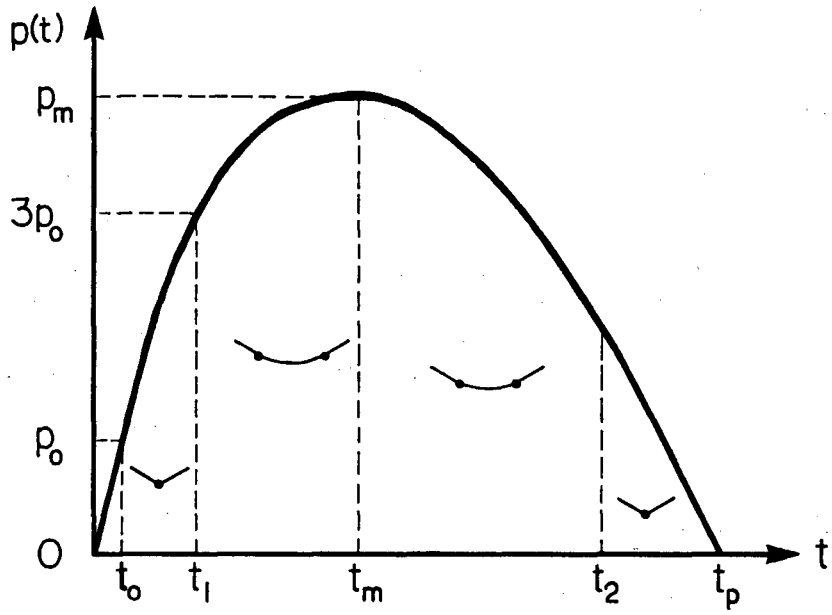

FIGURE 3.1 *Load pulse of general load-time history.*

axially restrained beam of Chapter 2 to a uniformly distributed pulse of more general load-time history.

3.2 RESPONSE TO AN ARBITRARY PULSE

The axially restrained beam will be analysed as it was in Chapter 2 by applying the concepts of plastic limit analysis and the assumptions of Section 2.2. The yield curves of doubly symmetric beam sections will again be approximated by the linear interaction relation of Figure 2.12, uncoupling the beam response into phases of pure bending response and pure string response.

3.2.1 BENDING RESPONSE

For small deflections the bending moment in fully plastic sections will be equal to the plastic moment M_o and the axial force will be zero. Linear bending-only theory will apply and the axial constraints will have no effect on the beam response.

Krajcinovic [15] derived the bending response of a rigid-plastic, simply supported beam subjected to uniformly distributed pulse loads of general load-time history.

He found that, for some arbitrary load pulse as in Figure 3.1, there exist five distinct phases of loaded bending response. During the time $0 \leq t < t_o$, when the load $p(t)$ is less than the static collapse load p_o, there are insufficient fully plastic sections for a mechanism to form, and the beam will not deform. When the load reaches p_o at the time t_o the midspan section becomes fully plastic and the beam begins to deform in the single midspan hinge mode of Figure 2.15. At the time t_1 the load reaches the value $3p_o$ and, as discussed in Section 2.4.1, continued deformation in the single midspan hinge mode would violate the plasticity condition. Satisfaction of the plasticity condition requires that the midspan hinge extend outward to become a finite plastic segment whose length increases with the load. At the time t_m the load reaches its maximum intensity p_m and then begins to decrease. Correspondingly, the travelling boundaries of the plastic segment begin to slow and eventually reverse the direction of their motion. The plastic segment recedes until some time t_2 when it has reduced once again to a single midspan hinge. Beyond the time t_2 the beam again deforms in the single midspan hinge mode of Figure 2.15.

(a) Rising Load—Midspan Hinge ($t_o \leq t < t_1$)

During the time when the load $p(t)$ is greater than the static collapse load p_o but less than three times the latter value, the beam will deform in the single midspan hinge mode just as it did for the medium load case of blast-type pulse loading. It follows that the midspan acceleration of the beam will again be given by Equation (2.4.7) as

$$\ddot{w}_o(t) = \frac{3}{2m}\left[p(t) - p_o\right]$$

and that the midspan displacement and velocity will be given by variations of Equations (2.5.2a,b) as

$$\begin{aligned} w_o(t) &= \frac{3}{2m}\int_{t_o}^{t} (t-\tau)\left[p(\tau) - p_o\right] d\tau, \\ \dot{w}_o(t) &= \frac{3}{2m}\int_{t_o}^{t} \left[p(\tau) - p_o\right] d\tau. \end{aligned} \tag{3.2.1a, b}$$

The beam will come to rest at the time t_f given by

$$t_f = t_o + \int_{t_o}^{t_f} \frac{p(t)}{p_o}\, dt \tag{3.2.2}$$

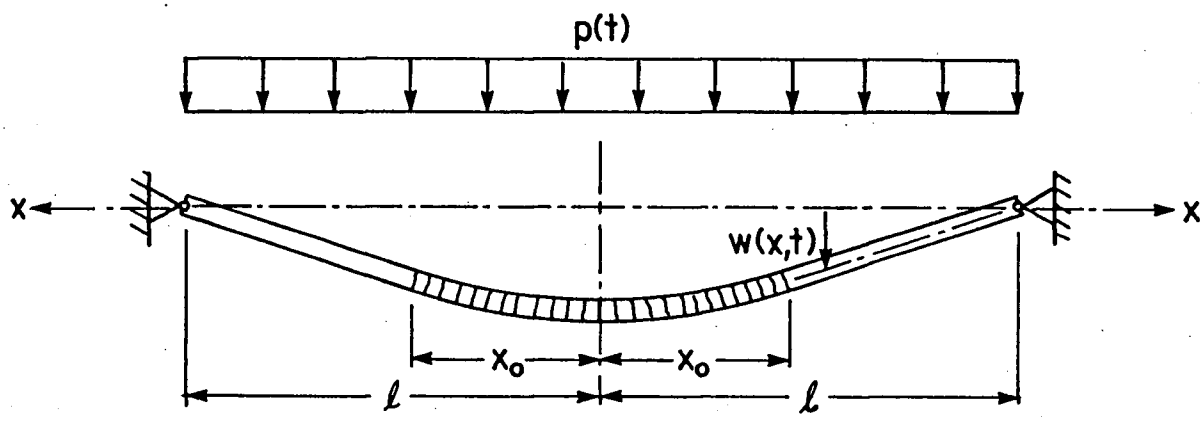

FIGURE 3.2 *Displaced configuration of a beam subjected to a rising high intensity load.*

if the load pulse begins its decay before exceeding $3p_o$ (*i.e.* $p_m \leq 3p_o$).

(b) Rising Load—Plastic Segment ($t_1 \leq t \leq t_m$)

As the load increases beyond the value $3p_o$, the moment distribution of the single midspan hinge mode will exceed the plastic moment M_o along a portion of the beam, violating the plasticity condition. The midspan plastic hinge must extend outward with increasing load. The beam will thus be comprised of a central plastic segment of finite length and two rigid end segments as in Figure 3.2.

In the midspan plastic segment the moment is constant at M_o, and there can be no shear. Hence there are no forces to resist the applied load $p(t)$ except the inertia load $m\ddot{w}(x,t)$ so that the acceleration is given by $\ddot{w}(x,t) = p(t)/m$ for $0 \leq x \leq x_o(t)$.

The outer segments of the beam respond as rigid bars. The free body diagram of a pinned beam's rigid end segment is given in Figure 3.3. The segment will rotate about the support point A. In Section 2.4 it was shown that in order to just prevent violation of the plasticity condition the inertia load must equal the applied load, which in this case demands that the transverse acceleration of a point at the plastic boundary be $p(t)/m$.

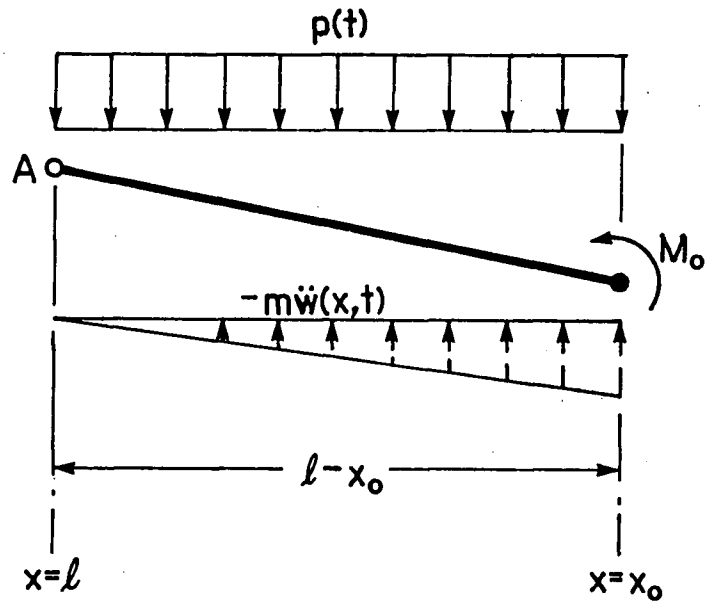

FIGURE 3.3 *Free body diagram of a pinned beam's rigid end segment.*

From dynamic moment equilibrium,

$$\tfrac{1}{2}(l - x_o)^2 p(t) = M_o + \tfrac{1}{3}(l - x_o)^2 p(t),$$

$$\tfrac{1}{6}(l - x_o)^2 p(t) = M_o.$$

Recalling that $p_o = 2M_o/l^2$ for a pinned beam, it is seen that the boundary between the plastic and rigid segments is located at

$$x_o(t) = l\left(1 - \sqrt{\frac{3p_o}{p(t)}}\right). \tag{3.2.3}$$

Transverse acceleration $\ddot{w}(x,t)$ must vary linearly with x on the rigid end segments so that the beam's acceleration field must be

$$\ddot{w}(x,t) = \begin{cases} p(t)/m, & \text{if } 0 \le x \le x_o(t); \\ \dfrac{p(t)}{m} \cdot \dfrac{l - x}{l - x_o(t)}, & \text{if } x_o(t) < x \le l. \end{cases} \tag{3.2.4}$$

A point x of the beam will initially deflect as part of the single midspan hinge mode until the time t_1. The point will then deflect as part of a rigid end segment of length $l - x_o(t)$ until the time at which the plastic boundary reaches the considered point, after which the

point will deflect as part of the plastic segment. This latter time, denoted as $g(x)$, can be determined as a function of x by rearranging Equation (3.1.2). Keeping these different phases of motion of the point in mind, recalling Equations (3.2.1a,b) and Equation(3.2.4) yields the velocity field

$$\dot{w}(x,t) = \begin{cases} \dfrac{l-x}{m}\left[\dfrac{3}{2l}\displaystyle\int_{t_o}^{t_1}[p(t)-p_o]\,dt + \int_{t_1}^{t}\frac{p(\tau)}{l-x_o(\tau)}d\tau\right], & \text{if } x_o \le x \le l; \\ \dfrac{l-x}{m}\left[\dfrac{3}{2l}\displaystyle\int_{t_o}^{t_1}[p(t)-p_o]\,dt + \int_{t_1}^{g(x)}\frac{p(\tau)}{l-x_o(\tau)}d\tau\right] & \\ \qquad\qquad + \displaystyle\int_{g(x)}^{t}\frac{p(\tau)}{m}d\tau, & \text{if } 0 \le x \le x_o. \end{cases} \tag{3.2.5}$$

A further integration yields the dispacement field

$$w(x,t) = \begin{cases} \dfrac{l-x}{m}\left[\dfrac{3}{2l}\displaystyle\int_{t_o}^{t_1}(t-\tau)\,[p(\tau)-p_o]\,d\tau + \int_{t_1}^{t}\frac{(t-\tau)p(\tau)}{l-x_o(\tau)}d\tau\right], & \text{if } x_o \le x \le l; \\ \dfrac{l-x}{m}\left[\dfrac{3}{2l}\displaystyle\int_{t_o}^{t_1}(t-\tau)\,[p(\tau)-p_o]\,d\tau + \int_{t_1}^{g(x)}\frac{(t-\tau)p(\tau)}{l-x_o(\tau)}d\tau\right] & \\ \qquad\qquad + \displaystyle\int_{g(x)}^{t}\frac{(t-\tau)p(\tau)}{m}d\tau, & \text{if } 0 \le x \le x_o. \end{cases} \tag{3.2.6}$$

It can be seen that the displacement and velocity profiles are smooth and continuous through the plastic boundary — the boundaries are not hinges. Krajcinovic [15] has shown that this response satisfies the kinematics of the beam. The midspan response can be found by setting $x = 0$ and noting that $g(0) = t_1$. Hence,

$$\begin{aligned} w_o(t) &= \frac{3}{2m}\int_{t_o}^{t_1}(t-\tau)\,[p(\tau)-p_o]\,d\tau + \frac{1}{m}\int_{t_1}^{t}(t-\tau)p(\tau)\,d\tau, \\ \dot{w}_o(t) &= \frac{3}{2m}\int_{t_o}^{t_1}[p(\tau)-p_o]\,d\tau + \frac{1}{m}\int_{t_1}^{t}p(\tau)\,d\tau. \end{aligned} \tag{3.2.7a, b}$$

During this phase of motion the load $p(t)$ is increasing and the midspan plastic segment has no load resistance. Therefore the beam cannot come to rest. Identical results are obtained for clamped beams.

(c) Decaying Load—Plastic Segment ($t_m \leq t \leq t_2$)

At some point during this phase the plastic segment boundaries will momentarily come to rest and then begin to travel back toward midspan. It can be reasoned that the position x_o of the boundaries will no longer depend solely upon the satisfaction of the plasticity condition but also upon the previous boundary motion — x_o will depend upon the complete load history and not just the intensity of the load at the time considered. Consequently Equation (3.2.3) will no longer apply. Again considering the free body diagram of Figure 3.3, the dynamic moment equilibrium of a pinned beam's rigid end segment can be written as

$$\tfrac{1}{2}(l - x_o)^2 p(t) = M_o + \tfrac{1}{3}m(l - x_o)^2 \ddot{w}(x_o, t). \tag{3.2.8}$$

Since the plastic segment boundary position is not necessarily determined by the plasticity condition, the transverse acceleration can no longer be assumed to be continuous across the boundaries (which will now be true plastic hinges) and hence $\ddot{w}(x_o, t)$ is undetermined. However, the rigid end segments force the velocity field to be linear in $x_o \leq x \leq l$ so that

$$\begin{aligned}
\dot{w}(x,t) &= \dot{w}(x_o,t) \cdot \frac{l - x}{l - x_o}, \\
\ddot{w}(x,t) &= (l - x)\frac{d}{dt}\left[\frac{\dot{w}(x_o,t)}{l - x_o(t)}\right], \\
\ddot{w}(x_o,t) &= (l - x_o)\frac{d}{dt}\left[\frac{\dot{w}(x_o,t)}{l - x_o(t)}\right].
\end{aligned} \tag{3.2.9}$$

Combining Equations (3.2.8) and (3.2.9) and rewriting M_o as $\frac{1}{2}p_o l^2$ gives

$$m\frac{d}{dt}\left[\frac{\dot{w}(x_o,t)}{l - x_o(t)}\right] = \frac{3}{2(l - x_o)^3}\left[p(t)(l - x_o)^2 - p_o l^2\right]. \tag{3.2.10}$$

Some differences between the present phase and the previous phase of motion have been discussed. The response of the plastic segment of the beam ($0 \leq x \leq x_o$) will be unaffected by these differences, however, and Equations (3.2.5) and (3.2.6) will continue to be valid (for the plastic segment only), as will Equations (3.2.7a,b). From Equation (3.2.5),

$$\begin{aligned}
m\left[\frac{\dot{w}(x_o,t)}{l - x_o}\right] &= \frac{1}{l - x_o}\int_{g(x_o)}^{t} p(\tau)\,d\tau \\
&\quad + \underbrace{\frac{3}{2l}\int_{t_o}^{t_1}[p(t) - p_o]\,dt + \int_{t_1}^{g(x_o)} \frac{p(t)}{l - x_o(t)}dt}_{\text{constant for } x_o}.
\end{aligned}$$

For some uniquely defined $x_o(t)$, the last two terms in the above equation will be constant in time so that differentiating in time gives

$$m\frac{d}{dt}\left[\frac{\dot{w}(x_o,t)}{l-x_o(t)}\right] = \frac{\dot{x}_o(t)}{(l-x_o)^2}\int_{g(x_o)}^{t} p(\tau)\,d\tau + \frac{p(t)}{l-x_o}. \tag{3.2.11}$$

Combining Equations (3.2.10) and (3.2.11) gives

$$\frac{3}{2(l-x_o)^3}\left[p(t)(l-x_o)^2 - p_o l^2\right] = \frac{\dot{x}_o(t)}{(l-x_o)^2}\int_{g(x_o)}^{t} p(\tau)\,d\tau + \frac{p(t)}{l-x_o},$$

which can be rewritten as

$$2\dot{x}_o(l-x_o)\int_{g(x_o)}^{t} p(\tau)\,d\tau - p(t)(l-x_o)^2 + 3p_o l^2 = 0,$$

$$-\frac{d}{dt}\left[(l-x_o)^2\right]\cdot\int_{g(x_o)}^{t} p(\tau)\,d\tau - p(t)(l-x_o)^2 + 3p_o l^2 = 0.$$

Integrating in time from $g(x_o)$ to t, an expression from which x_o may be determined is found:

$$\int_{g(x_o)}^{t} p(\tau)\,d\tau = \frac{3p_o l^2\,[t-g(x_o)]}{(l-x_o)^2}. \tag{3.2.12}$$

The travelling hinges will rejoin at midspan at the time t_2. Setting $x_o = 0$ and noting that $g(0) = t_1$, it is found that

$$t_2 = t_1 + \frac{1}{3p_o}\int_{t_1}^{t_2} p(t)\,dt. \tag{3.2.13}$$

Recalling that velocity varies linearly with x on the rigid end segments, the velocity field for this phase of motion is found to be

$$\dot{w}(x,t) = \begin{cases} \dfrac{l-x}{m}\left[\dfrac{3}{2l}\displaystyle\int_{t_o}^{t_1}\left[p(t)-p_o\right]dt + \int_{t_1}^{g(x)}\frac{p(t)}{l-x_o(t)}\,dt\right] & \text{if } 0 \le x \le x_o; \\ \qquad\qquad + \displaystyle\int_{g(x)}^{t}\frac{p(\tau)}{m}\,d\tau, & \\ \dfrac{l-x}{m}\left[\dfrac{3}{2l}\displaystyle\int_{t_o}^{t_1}\left[p(t)-p_o\right]dt + \int_{t_1}^{g(x_o)}\frac{p(t)}{l-x_o(t)}\,dt\right. & \text{if } x_o \le x \le l. \\ \qquad\qquad \left. + \dfrac{1}{l-x_o}\displaystyle\int_{g(x_o)}^{t} p(\tau)\,d\tau\right], & \end{cases} \tag{3.2.14}$$

Identical results are found for clamped beams.

(d) Decaying Load—Midspan Hinge ($t > t_2$)

After the hinges have met at time t_2, the beam will once again deform in the single midspan hinge mode of Figure 2.15, with the midspan acceleration again given by Equation (2.4.7) as

$$\ddot{w}_o(t) = \frac{3}{2m}\left[p(t) - p_o\right].$$

The initial conditions of this phase of motion can be determined by setting $t = t_2$ in Equations (3.2.7a,b), and are found to be

$$w_o(t_2) = \frac{3}{2m}\int_{t_o}^{t_1}(t_2 - t)\left[p(t) - p_o\right]dt + \frac{1}{m}\int_{t_1}^{t_2}(t_2 - t)p(t)\,dt,$$

$$\begin{aligned}\dot{w}_o(t_2) &= \frac{3}{2m}\int_{t_o}^{t_1}\left[p(t) - p_o\right]dt + \frac{1}{m}\int_{t_1}^{t_2}p(t)\,dt,\\ &= \frac{3}{2m}\int_{t_o}^{t_2}\left[p(t) - p_o\right]dt.\end{aligned}$$

Integrating Equation (2.4.7) with the above initial conditions, the midspan response of the beam is derived as

$$\begin{aligned}w_o(t) &= \frac{3}{2m}\int_{t_o}^{t}(t - \tau)\left[p(\tau) - p_o\right]d\tau + \frac{1}{2m}\int_{t_1}^{t_2}(t_2 - t)\left[3p_o - p(t)\right]dt,\\ \dot{w}_o(t) &= \frac{3}{2m}\int_{t_o}^{t}\left[p(\tau) - p_o\right]d\tau.\end{aligned} \tag{3.2.15a, b}$$

The beam will come to rest at the time t_f, again given by Equation (3.2.2) as

$$t_f = t_o + \int_{t_o}^{t_f}\frac{p(t)}{p_o}\,dt.$$

Once again, identical results will be obtained for clamped beams and pinned beams.

At this point it is worthwhile to note that the blast-type pulses of Chapter 2 are special cases of the general pulses discussed in this chapter. The instantaneous rise of the blast-type pulse implies that t_o, t_1, t_m and $g(x)$ are all equal to zero. The reader may verify that, by setting these variables to zero, the equations of this section reduce to the corresponding equations of Sections 2.4 and 2.5.

3.2.2 STRING RESPONSE

The blast-type pulse assumption of Chapter 2 has been seen to significantly affect the bending response of the beam. During string response, however, the entire length of the beam is plastic and the load $p(t)$ has no effect on the deflection mode. Again using the first mode approximation of Section 2.4.2, Equations (2.4.16) and (2.4.17) give the initial value problem which governs the beam's motion:

$$\ddot{w}_o + \frac{N_o\pi^2}{4ml^2}w_o = \frac{4p(t)}{\pi m},$$

$$w_o(t_s) = \begin{cases} M_o/N_o, & \text{for a pinned beam;} \\ 2M_o/N_o, & \text{for a clamped beam,} \end{cases}$$

$$\dot{w}_o(t_s^+) = \begin{cases} \sqrt{2/3}\,\dot{w}_o(t_s^-), & \text{if } p_m \le 3p_o \text{ or } t_s \le t_1 \text{ or } t_s \ge t_2; \\ \sqrt{\frac{2}{l}\int_0^l \left[\dot{w}(x,t_s^-)\right]^2 dx}, & \text{if } p_m > 3p_o \text{ and } t_1 \le t_s \le t_2. \end{cases}$$

Equation (2.5.10) will again give the solution to this problem as

$$w_o(t) = A\cos\left[\frac{\pi}{2}\sqrt{\frac{p_oN_o}{mM_o}}(t-t_s)\right] + B\sin\left[\frac{\pi}{2}\sqrt{\frac{p_oN_o}{mM_o}}(t-t_s)\right] + w_{o_p}(t),$$

where A and B are constants to be determined by the initial conditions and $w_{o_p}(t)$ is the particular solution unique to the load function $p(t)$.

3.3 TRIANGULAR PULSE WITH FINITE RISE TIME

Consider the case of a pinned beam subjected to a triangular load pulse with a rise time $t_m = \varsigma t_p$ defined by

$$p(t) = \begin{cases} \frac{p_m t}{\varsigma t_p}, & \text{if } 0 \le t \le \varsigma t_p; \\ \frac{p_m}{1-\varsigma}(1 - t/t_p), & \text{if } \varsigma t_p < t \le t_p; \\ 0, & \text{if } t > t_p. \end{cases} \tag{3.3.1}$$

and shown in Figure 3.4. As for the blast-type triangular pulse, Equations (2.7.2) and (2.7.3) give the impulse $I = \frac{1}{2}p_m t_p$ and the non-dimensional impulse parameter

$$\beta = \frac{p_o\bar{p}^2 {t_p}^2}{4mM_o/N_o},$$

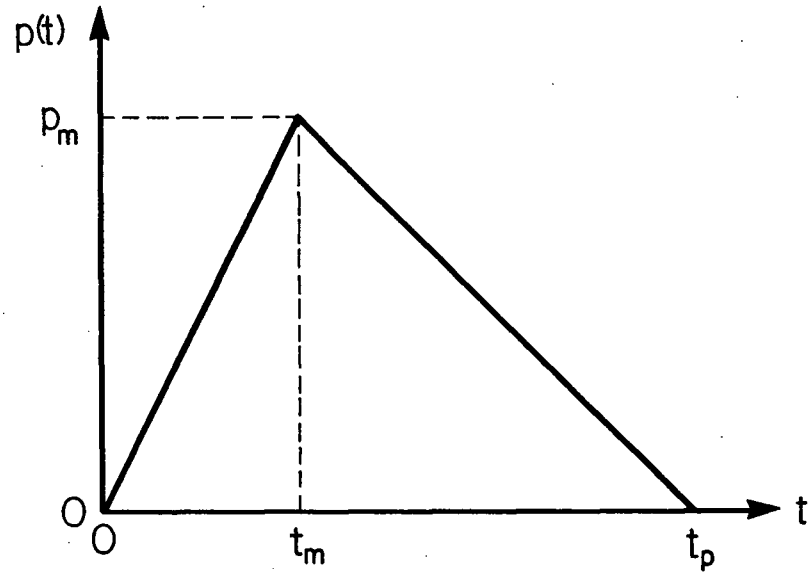

FIGURE 3.4 *Triangular load pulse with finite rise time.*

where, as before, $\bar{p} = p_m/p_o$.

3.3.1 MEDIUM LOADS ($p_m \leq 3p_o$)

(a) During The Load Rise ($t_o \leq t \leq t_m$)

During the load rise the time-varying load is defined by $p(t) = p_m t/\varsigma t_p$. Hence, Equation (2.4.7) gives the midspan acceleration

$$\ddot{w}_o(t) = \frac{3p_m}{2m\varsigma}\left(\frac{t}{t_p} - \frac{\varsigma}{\bar{p}}\right), \tag{3.3.2}$$

and Equations (3.2.1a,b) give

$$\begin{aligned} w_o(t) &= \frac{p_m {t_p}^2}{4m\varsigma}\left(\frac{t}{t_p} - \frac{\varsigma}{\bar{p}}\right)^3 = \frac{M_o\beta}{N_o\bar{p}\varsigma}\left(\frac{t}{t_p} - \frac{\varsigma}{\bar{p}}\right)^3, \\ \dot{w}_o(t) &= \frac{3p_m t_p}{4m\varsigma}\left(\frac{t}{t_p} - \frac{\varsigma}{\bar{p}}\right)^2 = \frac{3M_o\beta}{N_o\bar{p}\varsigma t_p}\left(\frac{t}{t_p} - \frac{\varsigma}{\bar{p}}\right)^2. \end{aligned} \tag{3.3.3a, b}$$

The beam will not come to rest during this phase of motion, but it may reach the string state. Setting $w_o(t_s) = M_o/N_o$ yields

$$\frac{t_s}{t_p} = \frac{\varsigma}{\bar{p}} + \left(\frac{\bar{p}\varsigma}{\beta}\right)^{1/3} \tag{3.3.4}$$

where t_s exists if $t_s \leq t_m = \varsigma t_p$, or

$$\beta \geq \frac{\overline{p}^4}{\varsigma^2(\overline{p}-1)^3}. \tag{3.3.5}$$

If such is the case, the beam will reach the string state with the midspan velocity

$$\dot{w}_o(t_s^-) = \frac{3M_o}{N_o t_p}\left(\frac{\beta}{\overline{p}\varsigma}\right)^{1/3}. \tag{3.3.6}$$

The ensuing string response will be governed by the initial value problem

$$\ddot{w}_o + \frac{N_o\pi^2}{4ml^2}w_o = \frac{4p_m t}{\pi m\varsigma t_p},$$

$$w_o(t_s) = M_o/N_o,$$

$$\dot{w}_o(t_s^+) = \sqrt{2/3}\,\dot{w}_o(t_s^-) = \frac{M_o\sqrt{6}}{N_o t_p}\left(\frac{\beta}{\overline{p}\varsigma}\right)^{1/3}.$$

Solving the initial value problem, the response is

$$\begin{aligned} w_o(t) &= A\cos\left[\frac{\pi(t-t_s)}{\overline{p}t_p}\sqrt{\frac{\beta}{2}}\right] + B\sin\left[\frac{\pi(t-t_s)}{\overline{p}t_p}\sqrt{\frac{\beta}{2}}\right] + \frac{32M_o\overline{p}}{\pi^3 N_o\varsigma}(t/t_p), \\ \dot{w}_o(t) &= \frac{\pi}{\overline{p}t_p}\sqrt{\frac{\beta}{2}}\left\{-A\sin\left[\frac{\pi(t-t_s)}{\overline{p}t_p}\sqrt{\frac{\beta}{2}}\right] + B\cos\left[\frac{\pi(t-t_s)}{\overline{p}t_p}\sqrt{\frac{\beta}{2}}\right]\right\} + \frac{32M_o\overline{p}}{\pi^3 N_o\varsigma t_p}, \end{aligned} \tag{3.3.7a, b}$$

where

$$\begin{aligned} A &= \frac{M_o}{N_o}\left[1 - \frac{32\overline{p}}{\pi^3\varsigma}(t_s/t_p)\right], \\ B &= \frac{\overline{p}t_p}{\pi}\sqrt{\frac{2}{\beta}}\left[\dot{w}_o(t_s^+) - \frac{32M_o\overline{p}}{\pi^3 N_o\varsigma t_p}\right]. \end{aligned} \tag{3.3.8a, b}$$

Rewriting Equations (3.3.7a,b) as

$$\begin{aligned} w_o(t) &= \sqrt{A^2+B^2}\cos\left[\frac{\pi(t-t_s)}{\overline{p}t_p}\sqrt{\frac{\beta}{2}} + \phi\right] + \frac{32M_o\overline{p}}{\pi^3 N_o\varsigma}(t/t_p), \\ \dot{w}_o(t) &= -\frac{\pi}{\overline{p}t_p}\sqrt{\frac{\beta}{2}(A^2+B^2)}\sin\left[\frac{\pi(t-t_s)}{\overline{p}t_p}\sqrt{\frac{\beta}{2}} + \phi\right] + \frac{32M_o\overline{p}}{\pi^3 N_o\varsigma t_p}, \end{aligned} \tag{3.3.9a, b}$$

where

$$\phi = -\tan^{-1}(B/A) - \begin{cases} \pi, & \text{if } A < 0; \\ 0, & \text{if } A \geq 0, \end{cases} \tag{3.3.10}$$

it is found that the beam will come to rest at the time t_f given by

$$t_f = \frac{\overline{p}t_p}{\pi}\sqrt{\frac{2}{\beta}}\left\{\sin^{-1}\left[\frac{32M_o\overline{p}^2}{\pi^4 N_o\varsigma\sqrt{\frac{\beta}{2}(A^2+B^2)}}\right]-\phi\right\}+t_s \tag{3.3.11}$$

if $t_f \leq t_m = \varsigma t_p$.

(b) During The Load Decay ($t_m < t \leq t_p$)

If the inequality of Equation (3.3.5) is not satisfied, the beam will undergo bending response as the load pulse begins to decay. From Equation (2.4.7) the midspan acceleration is

$$\ddot{w}_o(t) = \frac{3}{2m}\left[\frac{p_m}{1-\varsigma}\left(1-\frac{t}{t_p}\right)-p_o\right]. \tag{3.3.12}$$

Integrating the Equations (3.3.2) and (3.3.12) as specified by Equations (3.2.15a,b) gives the midspan response

$$w_o(t) = \frac{M_o\beta}{N_o\overline{p}(1-\varsigma)}\left[\varsigma^2\left(\frac{\overline{p}^3+\varsigma-1}{\overline{p}^3}\right)-3\varsigma\left(\frac{\overline{p}^2+\varsigma-1}{\overline{p}^2}\right)\frac{t}{t_p}\right.$$
$$\left.+3\left(\frac{\overline{p}+\varsigma-1}{\overline{p}}\right)\left(\frac{t}{t_p}\right)^2-\left(\frac{t}{t_p}\right)^3\right], \tag{3.3.13a, b}$$

$$\dot{w}_o(t) = \frac{3M_o\beta}{N_o\overline{p}(1-\varsigma)t_p}\left[\frac{\varsigma(1-\varsigma-\overline{p}^2)}{\overline{p}^2}+2\left(\frac{\overline{p}+\varsigma-1}{\overline{p}}\right)\frac{t}{t_p}-\left(\frac{t}{t_p}\right)^2\right].$$

The time at which the beam will come to rest is determined by Equation (3.2.2) to be

$$t_f = \left[\left(\frac{\overline{p}-1}{\overline{p}}\right)\left(1+\sqrt{1-\varsigma}\right)+\frac{\varsigma}{\overline{p}}\right]t_p, \tag{3.3.14}$$

and inserting t_f into Equation (3.3.13a) gives the final midspan deflection

$$w_{o_f} = \frac{M_o\beta(\overline{p}-1)^3}{N_o\overline{p}^4}\left[2\left(1+\sqrt{1-\varsigma}\right)-\varsigma\right]. \tag{3.3.15}$$

For the beam to come to rest during this phase the inequalities $t_f \leq t_p$ and $w_{o_f} \leq M_o/N_o$ must be satisfied. These restrictions may be equivalently stated as

$$\overline{p} \leq 1+\sqrt{1-\varsigma} \tag{3.3.16}$$

and

$$\beta \leq \frac{\overline{p}^4}{(\overline{p}-1)^3\left[2(1+\sqrt{1-\varsigma})-\varsigma\right]}. \tag{3.3.17}$$

If either of the above inequalities is not satisfied the beam may reach the string state at the time t_s determined by

$$\begin{aligned}\left(\frac{t_s}{t_p}\right)^3 - 3\left(\frac{\overline{p}+\varsigma-1}{\overline{p}}\right)\left(\frac{t_s}{t_p}\right)^2 + 3\varsigma\left(\frac{\overline{p}^2+\varsigma-1}{\overline{p}^2}\right)\left(\frac{t_s}{t_p}\right)\\ -\varsigma^2\left(\frac{\overline{p}^3+\varsigma-1}{\overline{p}^3}\right) + \frac{\overline{p}(1-\varsigma)}{\beta} = 0\end{aligned} \tag{3.3.18}$$

where t_s exists in this phase if

$$\beta \geq \begin{cases} \dfrac{\overline{p}^4}{\overline{p}^3(2-\varsigma)-3\overline{p}^2+3\varsigma\overline{p}-\varsigma^2}, & \text{if } \overline{p} > 1+\sqrt{1-\varsigma}; \\ \dfrac{\overline{p}^4}{(\overline{p}-1)^3\left[2(1+\sqrt{1-\varsigma})-\varsigma\right]}, & \text{if } \overline{p} \leq 1+\sqrt{1-\varsigma}. \end{cases} \tag{3.3.19}$$

The beam will then proceed to deform in the string state according to the initial value problem

$$\ddot{w}_o + \frac{N_o\pi^2}{4ml^2}w_o = \frac{4p_m}{\pi m(1-\varsigma)}(1-t/t_p),$$

$$w_o(t_s) = M_o/N_o,$$

$$\dot{w}_o(t_s^+) = \sqrt{2/3}\,\dot{w}_o(t_s^-),$$

where $\dot{w}_o(t_s^-)$ is determined by inserting t_s into Equation (3.3.13b). The response is then solved to be

$$\begin{aligned} w_o(t) &= \sqrt{A^2+B^2}\cos\left[\frac{\pi(t-t_s)}{\overline{p}t_p}\sqrt{\frac{\beta}{2}}+\phi\right] + \frac{32M_o\overline{p}}{\pi^3N_o(1-\varsigma)}\left(1-\frac{t}{t_p}\right), \\ \dot{w}_o(t) &= \sqrt{\frac{\beta}{2}A^2+B^2}\sin\left[\frac{\pi(t-t_s)}{\overline{p}t_p}\sqrt{\frac{\beta}{2}}+\phi\right] - \frac{32M_o\overline{p}}{\pi^3N_o(1-\varsigma)t_p}, \end{aligned} \tag{3.3.20a, b}$$

where

$$\begin{aligned} A &= \frac{M_o}{N_o}\left[1-\frac{32\overline{p}}{\pi^3(1-\varsigma)}\left(1-\frac{t_s}{t_p}\right)\right], \\ B &= \frac{\overline{p}t_p}{\pi}\sqrt{\frac{2}{\beta}}\left[\dot{w}_o(t_s^+)+\frac{32M_o\overline{p}}{\pi^3N_o(1-\varsigma)t_p}\right], \\ \phi &= -\tan^{-1}(B/A) - \begin{cases}\pi, & \text{if } A<0; \\ 0, & \text{if } A \geq 0.\end{cases} \end{aligned} \tag{3.3.21a, b, c}$$

Setting the velocity equal to zero, the time at which the beam comes to rest is found to be

$$t_f = \frac{\overline{p}t_p}{\pi}\sqrt{\frac{2}{\beta}}\left\{\sin^{-1}\left[-\frac{32M_o\overline{p}^2}{N_o\pi^4(1-\varsigma)\sqrt{\frac{\beta}{2}(A^2+B^2)}}\right]-\phi\right\}+t_s \tag{3.3.22}$$

if $t_f \leq t_p$.

If the inequality of Equation (3.3.5) is satisfied and the beam reaches the string state during the load rise, the beam will deform during the load decay according to the differential equation

$$\ddot{w}_o + \frac{N_o\pi^2}{4ml^2}w_o = \frac{4p_m}{\pi m(1-\varsigma)}(1-t/t_p)$$

with the initial conditions at time t_m given by Equations (3.3.9a,b). The response will again be given by Equations (3.3.20a,b) but, because the initial conditions have changed, t_s is replaced by $t_m = \varsigma t_p$ and the coefficients are now

$$\begin{aligned} A &= w_o(t_m) - \frac{32M_o\overline{p}}{N_o\pi^3(1-\varsigma)t_p}, \\ B &= \frac{\overline{p}t_p}{\pi}\sqrt{\frac{2}{\beta}}\left[\dot{w}_o(t_m) + \frac{32M_o\overline{p}}{N_o\pi^3(1-\varsigma)t_p}\right], \\ \phi &= -\tan^{-1}(B/A) - \begin{cases}\pi, & \text{if } A<0; \\ 0, & \text{if } A \geq 0.\end{cases} \end{aligned} \tag{3.3.23a, b, c}$$

Setting the velocity equal to zero yields

$$\frac{t_f}{t_p} = \frac{\overline{p}}{\pi}\sqrt{\frac{2}{\beta}}\left\{\sin^{-1}\left[-\frac{32M_o\overline{p}^2}{N_o\pi^4(1-\varsigma)\sqrt{\frac{\beta}{2}(A^2+B^2)}}\right]-\phi\right\}+\varsigma \tag{3.3.24}$$

if $t_f \leq t_p$.

(c) After The Load Pulse ($t > t_p$)

If $\overline{p} > 1+\sqrt{1-\varsigma}$ and the inequality of Equation (3.3.19) is not satisfied, the beam will deform in the unloaded bending response phase with the midspan acceleration $\ddot{w}_o(t) = -3p_o/2m$. Integration gives the response

$$\begin{aligned} w_o(t) &= \frac{M_o\beta}{N_o\overline{p}^4}\left[-(1+\varsigma)\overline{p}^3 - \varsigma^2 + 3\overline{p}(\overline{p}^2+\varsigma)t/t_p - 3\overline{p}^2\left(\frac{t}{t_p}\right)^2\right], \\ \dot{w}_o(t) &= \frac{3M_o\beta}{N_o\overline{p}^3t_p}\left(\overline{p}^2+\varsigma-2\overline{p}\frac{t}{t_p}\right). \end{aligned} \tag{3.3.25a, b}$$

The beam will come to rest at the time $t_f = (\overline{p}^2+\varsigma)t_p/2\overline{p}$ with the final midspan deflection

$$w_{o_f} = \frac{M_o\beta}{N_o\overline{p}^4}\left[\frac{3}{4}(\overline{p}^2+\varsigma)^2 - (1+\varsigma)\overline{p}^3 - \varsigma^2\right] \tag{3.3.26}$$

if $w_{o_f} \leq M_o/N_o$, or

$$\beta \leq \frac{\overline{p}^4}{\frac{3}{4}(\overline{p}^2+\varsigma)^2 - (1+\varsigma)\overline{p}^3 - \varsigma^2}. \tag{3.3.27}$$

If the beam does not come to rest as above it will reach the string state at the time t_s when $w_o(t_s) = M_o/N_o$. From Equation (3.3.25a) it is found that

$$\frac{t_s}{t_p} = \frac{\overline{p}^2+\varsigma}{2\overline{p}}\left\{1 - \sqrt{1 - \frac{4}{3\beta(\overline{p}^2+\varsigma)^2}\left[\beta\varsigma^2 + \beta(1+\varsigma)\overline{p}^3 + \overline{p}^4\right]}\right\}, \tag{3.3.28}$$

and, hence,

$$\dot{w}_o(t_s^-) = \frac{3M_o\beta}{N_o\overline{p}^3 t_p}\sqrt{\left(1 - \frac{4}{3\beta}\right)\overline{p}^4 - \frac{4(1+\varsigma)}{3}\overline{p}^3 + 2\varsigma\overline{p}^2 - \frac{\varsigma^2}{3}}. \tag{3.3.29}$$

The beam will then proceed to deform in the unloaded string response phase according to the initial value problem

$$\ddot{w}_o + \frac{N_o\pi^2}{4ml^2}w_o = 0,$$

$$w_o(t_s) = M_o/N_o,$$

$$\dot{w}_o(t_s^+) = \sqrt{2/3}\,\dot{w}_o(t_s^-).$$

The response is solved to be

$$w_o(t) = \sqrt{A^2+B^2}\cos\left[\frac{\pi(t-t_s)}{\overline{p}t_p}\sqrt{\frac{\beta}{2}} - \tan^{-1}(B/A)\right] \tag{3.3.30}$$

where

$$A = M_o/N_o,$$

$$B = \frac{\overline{p}t_p}{\pi}\sqrt{\frac{2}{\beta}}\,\dot{w}_o(t_s^+),$$

and the final midspan deflection is

$$w_{o_f} = \sqrt{\left(\frac{M_o}{N_o}\right)^2 + \frac{2\overline{p}^2 t_p{}^2}{\pi^2\beta}\left[\dot{w}_o(t_s^+)\right]^2}. \tag{3.3.31}$$

If the beam reaches the string state during the load pulse with t_s given by Equation (3.3.4) or (3.3.18), it will deform in the unloaded string response phase according

to an initial value problem similar to the immediately previous one, but with the initial conditions given at the time t_p. The response will be given by

$$w_o(t) = \sqrt{A^2 + B^2} \cos \left[\frac{\pi}{\overline{p}} \sqrt{\frac{\beta}{2}} \left(\frac{t}{t_p} - 1 \right) - \tan^{-1}(B/A) \right] \tag{3.3.32}$$

where

$$A = w_o(t_p)$$
$$B = \frac{\overline{p} t_p}{\pi} \sqrt{\frac{2}{\beta}} \dot{w}_o(t_p),$$

as determined by Equations (3.3.20) and (3.3.21) or (3.3.23). The final midspan deflection for this case will be

$$w_{o_f} = \sqrt{A^2 + B^2}. \tag{3.3.33}$$

3.3.2 HIGH LOADS ($p_m > 3p_o$)

(a) During The Load Rise ($t_o \leq t \leq t_m$)

Until the time t_1 when the load $p(t) = 3p_o$, the initial beam response will be the same as for the medium load case, given by Equations (3.3.3a,b). The time t_s at which the string state is reached and the midspan velocity at that time are again given by Equations (3.3.4) and (3.3.6) respectively, but will now only be valid if $t_s \leq t_1 = 3\varsigma t_p/\overline{p}$, or

$$\beta \geq \frac{\overline{p}^4}{8\varsigma^2}. \tag{3.3.34}$$

If Equation (3.3.34) is satisfied, the ensuing string response during the load rise will again be given by Equations (3.3.7) through (3.3.11).

If Equation (3.3.34) is not satisfied, the midspan plastic hinge will extend outward into a finite plastic segment as the load rises above $3p_o$. The location of the boundaries of this plastic segment are found from Equation (3.2.3) to be

$$x_o(t) = l \left(1 - \sqrt{\frac{3\varsigma t_p}{\overline{p} t}} \right). \tag{3.3.35}$$

Expressing this another way, a section of the beam at the point x will be crossed by the plastic segment boundary (and hence will become fully plastic itself) at the time

$$g(x) = \frac{3\varsigma t_p}{\overline{p}(1 - x/l)^2}. \tag{3.3.36}$$

Equations (3.2.7a,b) give the midspan response of the beam as

$$\begin{aligned} w_o(t) &= \frac{2M_o\beta}{3N_o\overline{p}\varsigma}\left[\left(\frac{t}{t_p}\right)^3 - \frac{9\varsigma^2}{\overline{p}^2}\left(\frac{t}{t_p}\right) + \frac{12\varsigma^3}{\overline{p}^3}\right], \\ \dot{w}_o(t) &= \frac{2M_o\beta}{N_o\overline{p}\varsigma t_p}\left[\left(\frac{t}{t_p}\right)^2 - \frac{3\varsigma^2}{\overline{p}^2}\right]. \end{aligned} \tag{3.3.37a, b}$$

The beam may reach the string state during the load rise. Setting $w_o(t_s) = M_o/N_o$ yields

$$\left(\frac{t_s}{t_p}\right)^3 - \frac{9\varsigma^2}{\overline{p}^2}\left(\frac{t_s}{t_p}\right) + \frac{12\varsigma^3}{\overline{p}^3} - \frac{3\overline{p}\varsigma}{2\beta} = 0 \tag{3.3.38}$$

which will be true if $t_s \le t_m = \varsigma t_p$, or

$$\beta \ge \frac{3\overline{p}^4}{2\varsigma^2(\overline{p}^3 - 9\overline{p} + 12)}. \tag{3.3.39}$$

Just prior to the onset of string response, the beam will have the velocity profile

$$\dot{w}(x, t_s^-) = \begin{cases} \left(1 - \frac{x}{l}\right)\frac{p_o}{m}\left[\frac{3}{2}\int_{t_o}^{t_1}\left(\frac{\overline{p}t}{\varsigma t_p} - 1\right)dt + \int_{t_1}^{g(x)}\sqrt{\frac{1}{3}\left(\frac{\overline{p}t}{\varsigma t_p}\right)^3}\,dt\right], & \text{if } 0 \le x \le x_o(t_s); \\ \qquad\qquad + \frac{p_o}{m}\int_{g(x)}^{t_s}\frac{\overline{p}t}{\varsigma t_p}\,dt & \\ \left(1 - \frac{x}{l}\right)\frac{p_o}{m}\left[\frac{3}{2}\int_{t_o}^{t_1}\left(\frac{\overline{p}t}{\varsigma t_p} - 1\right)dt + \int_{t_1}^{t_s}\sqrt{\frac{1}{3}\left(\frac{\overline{p}t}{\varsigma t_p}\right)^3}\,dt\right], & \text{if } x_o(t_s) \le x \le l, \end{cases}$$

as given by Equation (3.2.5). Carrying out the integration with $g(x)$ given by Equation (3.3.36),

$$\dot{w}(x, t_s^-) = \frac{4M_o\beta\varsigma}{5N_o\overline{p}^3 t_p}\begin{cases} \frac{5\overline{p}^2}{2\varsigma^2}\left(\frac{t_s}{t_p}\right)^2 - \frac{9}{2}\left(1 - \frac{x}{l}\right)^{-4} - 3\left(1 - \frac{x}{l}\right), & \text{if } 0 \le x \le x_o(t_s); \\ \left[\frac{2}{\sqrt{3}}\left(\frac{\overline{p}t_s}{\varsigma t_p}\right)^{5/2} - 3\right]\left(1 - \frac{x}{l}\right), & \text{if } x_o(t_s) \le x \le l. \end{cases} \tag{3.3.40}$$

In the transition from bending to string response, the kinetic energy of the beam must be continuous. Equation (2.4.17) expresses this continuity as

$$w_o(t_s^+) = \sqrt{\frac{2}{l}\int_0^l \left[\dot{w}(x,t_s^-)\right]^2 dx}$$

and hence

$$\begin{aligned}\dot{w}_o(t_s^+) = \frac{4M_o\beta\varsigma}{N_o\bar{p}^3 t_p}\Bigg\{ & \frac{x_o}{2l}\left(\frac{\bar{p}t_s}{\varsigma t_p}\right)^4 - \frac{3}{5}\left(\frac{\bar{p}t_s}{\varsigma t_p}\right)^2\left[1-\left(1-\frac{x_o}{l}\right)^2\right] \\ & + \frac{6}{25}\left[1-\left(1-\frac{x_o}{l}\right)^3\right] - \frac{27}{25}\left[1-\left(1-\frac{x_o}{l}\right)^{-2}\right] \\ & + \frac{3}{5}\left(\frac{\bar{p}t_s}{\varsigma t_p}\right)^2\left[1-\left(1-\frac{x_o}{l}\right)^{-3}\right] - \frac{81}{350}\left[1-\left(1-\frac{x_o}{l}\right)^{-7}\right] \\ & + 2\left[\frac{2}{15}\left(\frac{\bar{p}t_s}{\varsigma t_p}\right)^{5/2} - \frac{\sqrt{3}}{5}\right]^2\left(1-\frac{x_o}{l}\right)^3\Bigg\}^{1/2}.\end{aligned} \tag{3.3.41}$$

Once again, the string response during the load rise will be given by Equations (3.3.7) through (3.3.11).

(b) During The Load Decay ($t_m \le t \le t_p$)

If Equation (3.3.39) is not satisfied the load will begin to decrease according to the function $p(t) = p_m(1 - t/t_p)/(1-\varsigma)$ before the beam reaches the string state. The plastic segment boundaries will become hinges and will travel back towards midspan. From Equation (3.2.12),

$$\int_{g(x_o)}^{t_m} \frac{p_m t}{\varsigma t_p}\,dt + \int_{t_m}^{t} \frac{p_m}{1-\varsigma}\left(1-\frac{\tau}{t_p}\right)d\tau = \frac{3p_o\left[t-g(x_o)\right]}{(1-x_o/l)^2}.$$

With $g(x_o)$ given by Equation (3.3.36), the position of the hinges is found to be

$$x_o = l\left\{1-\sqrt{\frac{3(1-\varsigma)}{\bar{p}}\left[\frac{(t/t_p)+(t/t_p-\varsigma)/\sqrt{1-\varsigma}}{(1-\varsigma)-(1-t/t_p)^2}\right]}\right\}. \tag{3.3.42}$$

The hinges will meet at midspan at the time t_2 given by

$$\frac{t_2}{t_p} = \left(\frac{\bar{p}-3}{\bar{p}}\right)\left(1+\sqrt{1-\varsigma}\right) + \frac{3\varsigma}{\bar{p}} \tag{3.3.43}$$

if $t_2 \le t_p$, or $\bar{p} \le 3(1+\sqrt{1-\varsigma})$. Equations (3.2.7a,b) again give the midspan response of the beam which, during the load decay, is

$$w_o(t) = \frac{2M_o\beta}{3N_o\bar{p}(1-\varsigma)}\left\{-\left(\frac{t}{t_p}\right)^3 + 3\left(\frac{t}{t_p}\right)^2 - 3\varsigma\left[1+\frac{3(1-\varsigma)}{\bar{p}^2}\right]\left(\frac{t}{t_p}\right) + \varsigma^2\left[1+\frac{12(1-\varsigma)}{\bar{p}^3}\right]\right\}, \tag{3.3.44a, b}$$

$$\dot{w}_o(t) = \frac{2M_o\beta}{N_o\bar{p}(1-\varsigma)t_p}\left\{-\left(\frac{t}{t_p}\right)^2 + 2\left(\frac{t}{t_p}\right) - \varsigma\left[1+\frac{3(1-\varsigma)}{\bar{p}^2}\right]\right\}.$$

Setting $w_o(t_s) = M_o/N_o$, t_s is given by

$$\left(\frac{t_s}{t_p}\right)^3 - 3\left(\frac{t_s}{t_p}\right)^2 + 3\varsigma\left[1+\frac{3(1-\varsigma)}{\bar{p}^2}\right]\left(\frac{t_s}{t_p}\right) - \varsigma^2\left[1+\frac{12(1-\varsigma)}{\bar{p}^3}\right] + \frac{3\bar{p}(1-\varsigma)}{2\beta} = 0, \tag{3.3.45}$$

where $t_s \le t_p$ if $\bar{p} \ge 3(1+\sqrt{1-\varsigma})$ and $t_s \le t_2$ if $\bar{p} < 3(1+\sqrt{1-\varsigma})$, or

$$\beta \ge \begin{cases} \dfrac{3\bar{p}(1-\varsigma)}{2\varsigma^2 - 6\varsigma\left[1+\frac{3(1-\varsigma)}{\bar{p}^2}\right]\frac{t_2}{t_p} + 6\left(\frac{t_2}{t_p}\right)^2 - 2\left(\frac{t_2}{t_p}\right)^3 + \frac{24\varsigma(1-\varsigma)}{\bar{p}^3}}, & \text{if } \bar{p} < 3(1+\sqrt{1-\varsigma}); \\ \dfrac{3\bar{p}^4}{2\left[(2-\varsigma)\bar{p}^3 - 9\varsigma\bar{p} + 12\varsigma^2\right]}, & \text{if } \bar{p} \ge 3(1+\sqrt{1-\varsigma}). \end{cases} \tag{3.3.46}$$

Just before the onset of string response, the beam will have the velocity profile given by Equation (3.2.14) as

$$\dot{w}(x,t_s^-) = \frac{4M_o\beta}{N_o\bar{p}^3 t_p}\cdot\begin{cases} \dfrac{\bar{p}^2}{2}\left(1-\dfrac{(1-t_s/t_p)^2}{1-\varsigma}\right) - \dfrac{3\varsigma}{5}\left(1-\dfrac{x}{l}\right) - \dfrac{9\varsigma}{10}\left(1-\dfrac{x}{l}\right)^{-4}, & \text{if } 0 \le x \le x_o(t_s); \\ \left[\dfrac{\bar{p}^2}{2}\left(1-\dfrac{(1-t_s/t_p)^2}{1-\varsigma}\right)\left(1-\dfrac{x_o}{l}\right)^{-1} - \dfrac{3\varsigma}{5} - \dfrac{9\varsigma}{10}\left(1-\dfrac{x}{l}\right)^{-5}\right]\left(1-\dfrac{x}{l}\right), & \text{if } x_o(t_s) \le x \le l. \end{cases} \tag{3.3.47}$$

From Equation (2.4.17) the midspan velocity just at the onset of string response is

$$\dot{w}_o(t_s^+) = \frac{4M_o\beta}{N_o\bar{p}^3 t_p}\left\{\frac{6\varsigma^2}{25}\left[1-\left(1-\frac{x_o}{l}\right)^3\right] - \frac{3\varsigma\bar{p}^2}{5}\left[1-\frac{(1-t_s/t_p)^2}{1-\varsigma}\right]\left[1-\left(1-\frac{x_o}{l}\right)^2\right]\right.$$
$$+\frac{\bar{p}^4}{2}\left[1-\frac{(1-t_s/t_p)^2}{1-\varsigma}\right]^2\left(\frac{x_o}{l}\right) - \frac{27\varsigma^2}{25}\left[1-\left(1-\frac{x_o}{l}\right)^{-2}\right]$$
$$+\frac{3\varsigma\bar{p}^2}{5}\left[1-\frac{(1-t_s/t_p)^2}{1-\varsigma}\right]\left[1-\left(1-\frac{x_o}{l}\right)^{-3}\right] - \frac{81\varsigma^2}{350}\left[1-\left(1-\frac{x_o}{l}\right)^{-7}\right]$$
$$+\frac{2}{3}\left[\frac{\bar{p}^2}{2}\left(1-\frac{(1-t_s/t_p)^2}{1-\varsigma}\right)\left(1-\frac{x_o}{l}\right)^{-1}\right.$$
$$\left.\left.-\frac{3\varsigma}{5}-\frac{9\varsigma}{10}\left(1-\frac{x_o}{l}\right)^{-5}\right]^2\left(1-\frac{x_o}{l}\right)^3\right\}^{1/2}. \tag{3.3.48}$$

If Equation (3.3.46) is not satisfied for $\bar{p} < 3(1+\sqrt{1-\varsigma})$, the hinges will meet at midspan before the load is removed or the string state is reached. From Equations (3.2.15a,b) the midspan response of the beam is

$$w_o(t) = \frac{M_o\beta}{3N_o\bar{p}(1-\varsigma)}\left\{\left(\frac{t_2}{t_p}\right)^3 + \frac{3(3-3\varsigma-\bar{p})}{\bar{p}}\left(\frac{t_2}{t_p}\right)^2 + \frac{3\varsigma(\bar{p}^2-9+9\varsigma)}{\bar{p}^2}\left(\frac{t_2}{t_p}\right)\right.$$
$$+2\varsigma^2\left[1+\frac{12(1-\varsigma)}{\bar{p}^3}\right] + \frac{9\varsigma(1-\varsigma-\bar{p}^2)}{\bar{p}^2}\left(\frac{t}{t_p}\right)$$
$$\left.+\frac{9(\bar{p}+\varsigma-1)}{\bar{p}}\left(\frac{t}{t_p}\right)^2 - 3\left(\frac{t}{t_p}\right)^3\right\},$$

$$\dot{w}_o(t) = \frac{3M_o\beta}{N_o\bar{p}(1-\varsigma)t_p}\left[\frac{\varsigma(1-\varsigma-\bar{p}^2)}{\bar{p}^2} + \frac{2(\bar{p}+\varsigma-1)}{\bar{p}}\left(\frac{t}{t_p}\right) - \left(\frac{t}{t_p}\right)^2\right]. \tag{3.3.49a, b}$$

In setting $\dot{w}_o(t_f) = 0$ it is discovered that a time t_f cannot be found within the allowable time domain $t_m \le t_f \le t_p$ — the beam cannot come to rest during this phase of motion. However, the beam may reach the string state at the time t_s given by

$$\left(\frac{t_s}{t_p}\right)^3 - \frac{3(\bar{p}+\varsigma-1)}{\bar{p}}\left(\frac{t_s}{t_p}\right)^2 + \frac{3\varsigma(\bar{p}^2+\varsigma-1)}{\bar{p}^2}\left(\frac{t_s}{t_p}\right)$$
$$-\frac{2\varsigma^2}{3\bar{p}^3}\left[\bar{p}^3+12(1-\varsigma)\right] - \frac{\varsigma(\bar{p}^2-9+9\varsigma)}{\bar{p}^2}\left(\frac{t_2}{t_p}\right) \tag{3.3.50}$$
$$+\frac{\bar{p}-3+3\varsigma)}{\bar{p}}\left(\frac{t_2}{t_p}\right)^2 - \frac{1}{3}\left(\frac{t_2}{t_p}\right)^3 + \frac{\bar{p}(1-\varsigma)}{\beta} = 0$$

if $t_s \leq t_p$. The beam will have the midspan velocity $\dot{w}_o(t_s^-)$ just prior to the onset of string response and $\dot{w}_o(t_s^+) = \sqrt{2/3}\,\dot{w}_o(t_s^-)$ just after.

If the beam reaches the string state during the load decay, the string response is given by Equations (3.3.20) through (3.3.22). If the beam reaches the string state during the load rise, the string response is given by Equations (3.3.20) with t_s replaced by $t_m = \varsigma t_p$, and Equations (3.3.23) and (3.3.24), as was the case for medium loads.

(c) After The Load Pulse ($t > t_p$)

If $\bar{p} < 3(1+\sqrt{1-\varsigma})$ and the beam doesn't reach the string state during the load pulse, the beam will deform in the unloaded bending response phase with a single midspan hinge as

$$w_o(t) = \frac{M_o\beta}{3N_o\bar{p}^4}\left[\frac{\bar{p}^3}{1-\varsigma}\left(\frac{t_2}{t_p}\right)^3 + \left(9\bar{p}^2 - \frac{3\bar{p}^3}{1-\varsigma}\right)\left(\frac{t_2}{t_p}\right)^2 + \varsigma\left(\frac{3\bar{p}^3}{1-\varsigma} + 9\bar{p}\right)\left(\frac{t_2}{t_p}\right)\right.$$
$$\left. + \left(\frac{2\varsigma^2-3}{1-\varsigma}\right)\bar{p}^3 + 24\varsigma^2 + 9\bar{p}(\bar{p}^2+\varsigma)\frac{t}{t_p} - 9\bar{p}^2\left(\frac{t}{t_p}\right)^2\right],$$
$$\dot{w}_o(t) = \frac{3M_o\beta}{N_o\bar{p}^3 t_p}\left[\bar{p}^2 + \varsigma - 2\bar{p}\left(\frac{t}{t_p}\right)\right]. \tag{3.3.51a, b}$$

The beam will come to rest at the time

$$t_f = \frac{t_p}{2}\left(\bar{p} + \frac{\varsigma}{\bar{p}}\right), \tag{3.3.52}$$

if $w_{o_f} = w_o(t_f) \leq M_o/N_o$. Otherwise the beam will reach the string state at the time t_s. Setting $w_o(t_s) = M_o/N_o$, it is found that

$$\frac{t_s}{t_p} = \frac{\bar{p}^2+2\varsigma}{2\bar{p}} - \left\{\frac{(\bar{p}^2+2\varsigma)^2}{4\bar{p}^2} - \frac{(3-2\varsigma^2)\bar{p}}{9(1-\varsigma)} + \frac{8\varsigma^2}{3\bar{p}^2} - \frac{\bar{p}^2}{3\beta} + \varsigma\left[\frac{\bar{p}}{3(1-\varsigma)} + \frac{1}{\bar{p}}\right]\left(\frac{t_2}{t_p}\right)\right.$$
$$\left. - \left[\frac{\bar{p}}{3(1-\varsigma)} - 1\right]\left(\frac{t_2}{t_p}\right)^2 + \frac{\bar{p}}{9(1-\varsigma)}\left(\frac{t_2}{t_p}\right)^3\right\}^{1/2}. \tag{3.3.53}$$

With the beam deforming in the single hinge mode, the transition to string response will be such that $\dot{w}_o(t_s^+) = \sqrt{2/3}\dot{w}_o(t_s^-)$.

If $\bar{p} > 3(1+\sqrt{1-\varsigma})$ and the beam doesn't reach the string state during the load pulse, the beam will respond in the travelling hinge mode. Because there is no load

the midspan acceleration must be zero. Matching the conditions at time t_p with those of Equations (3.3.44a,b), the midspan response is found to be

$$w_o(t) = \frac{2M_o\beta}{3N_o\bar{p}}\left[3\left(1-\frac{3\varsigma}{\bar{p}^2}\right)\frac{t}{t_p} - 1 - \varsigma + \frac{12\varsigma^2}{\bar{p}^3}\right],$$
$$\dot{w}_o(t) = \frac{2M_o\beta}{N_o\bar{p}t_p}\left(1-\frac{3\varsigma}{\bar{p}^2}\right). \tag{3.3.54a, b}$$

From Equation (3.2.12) the hinge location is

$$x_o = l\left\{1 - \sqrt{\frac{3}{\bar{p}}\left[\frac{t}{t_p} + \sqrt{\left(\frac{t}{t_p}\right)^2 - \varsigma}\right]}\right\}, \tag{3.3.55}$$

and the hinges will meet at midspan at the time

$$t_2 = t_p\left(\frac{\bar{p}}{6} + \frac{3\varsigma}{2\bar{p}}\right). \tag{3.3.56}$$

Setting $w_o(t_s) = M_o/N_o$ yields

$$t_s = \frac{t_p}{\bar{p}^2 - 3\varsigma}\left[\frac{\bar{p}^3}{2\beta} + \frac{\bar{p}^2}{3}(1+\varsigma) - \frac{4\varsigma^2}{\bar{p}}\right] \tag{3.3.57}$$

if $t_s \le t_2$, or

$$\beta \ge \frac{3\bar{p}^4}{\bar{p}^4 - 2(1+\varsigma)\bar{p}^3 + 6\varsigma\bar{p}^2 - 3\varsigma^2}. \tag{3.3.58}$$

Putting t_s into Equation (3.2.14) gives the velocity profile at an instant before the onset of string response:

$$\dot{w}(x, t_s^-) = \frac{4M_o\beta}{N_o\bar{p}^3 t_p}\begin{cases} \dfrac{\bar{p}^2}{2} - \dfrac{3\varsigma}{5}\left(1-\dfrac{x}{l}\right) - \dfrac{9\varsigma}{10}\left(1-\dfrac{x}{l}\right)^{-4}, & \text{if } 0 \le x \le x_o(t_s); \\ \left[\dfrac{\bar{p}^2}{2}\left(1-\dfrac{x_o}{l}\right)^{-1} - \dfrac{3\varsigma}{5} - \dfrac{9\varsigma}{10}\left(1-\dfrac{x_o}{l}\right)^{-5}\right]\left(1-\dfrac{x}{l}\right), & \text{if } x_o(t_s) \le x \le l, \end{cases} \tag{3.3.59}$$

so that

$$\begin{aligned}\dot{w}_o(t_s^+) = \frac{4M_o\beta}{N_o\bar{p}^3 t_p}\Bigg\{&\frac{6\varsigma^2}{25}\left[1-\left(1-\frac{x_o}{l}\right)^3\right] - \frac{3\varsigma\bar{p}^2}{5}\left[1-\left(1-\frac{x_o}{l}\right)^2\right] \\ &+ \frac{\bar{p}^4}{2}\left(\frac{x_o}{l}\right) - \frac{27\varsigma^2}{25}\left[1-\left(1-\frac{x_o}{l}\right)^{-2}\right] \\ &+ \frac{3\varsigma\bar{p}^2}{5}\left[1-\left(1-\frac{x_o}{l}\right)^{-3}\right] - \frac{81\varsigma^2}{350}\left[1-\left(1-\frac{x_o}{l}\right)^{-7}\right] \\ &+ \frac{2}{3}\left[\frac{\bar{p}^2}{2}\left(1-\frac{x_o}{l}\right)^{-1} - \frac{3\varsigma}{5} - \frac{9\varsigma}{10}\left(1-\frac{x_o}{l}\right)^{-5}\right]^2\left(1-\frac{x_o}{l}\right)^3\Bigg\}^{1/2}.\end{aligned} \tag{3.3.60}$$

If Equation (3.3.58) is not satisfied (so that the hinges meet at midspan before the string state is reached) the beam will proceed to deform in the single midspan hinge mode. The midspan response will be

$$w_o(t) = \frac{M_o\beta}{3N_o\overline{p}^3}\left[\frac{96\varsigma^2 - 8\overline{p}^3(1+\varsigma) - (\overline{p}^2+9\varsigma)^2}{4\overline{p}} + 9(\overline{p}^2+\varsigma)\frac{t}{t_p} - 9\overline{p}\left(\frac{t}{t_p}\right)^2\right],$$
$$\dot{w}_o(t) = \frac{3M_o\beta}{N_o\overline{p}^3 t_p}\left[\overline{p}^2+\varsigma - 2\overline{p}\left(\frac{t}{t_p}\right)\right]. \qquad (3.3.61a,b)$$

Equation (3.3.52) again gives the time t_f at which the beam comes to rest. Setting $w_o(t_s) = M_o/N_o$, it is found that

$$\frac{t_s}{t_p} = \frac{\overline{p}^2+\varsigma}{2\overline{p}}\left\{1 - \sqrt{1 + \frac{96\varsigma^2 - 8\overline{p}^3(1+\varsigma) - (\overline{p}^2+9\varsigma)^2 - 12\overline{p}^4/\beta}{9(\overline{p}^2+9\varsigma)^2}}\right\}. \qquad (3.3.62)$$

The transition from bending to string response is such that $\dot{w}_o(t_s^+) = \sqrt{2/3}\dot{w}_o(t_s^-)$.

The response of the beam in the unloaded string state is the same as that for the medium load case. If the beam reaches the string state after the load pulse, the response is given by Equations (3.3.30) and (3.3.31). If the beam reaches the string state during the load pulse, the response is given by Equations (3.3.32) and (3.3.33).

3.3.3 COMPARISON WITH BLAST-TYPE PULSE RESULTS

The results of this section are plotted in Figures 3.5 and 3.6 for various amounts of time rise given by the ratio $\varsigma = t_m/t_p$. Included are the results for $\varsigma = 0$ which are equivalent to the blast-type triangular pulse results of Section 2.7. It is seen in these figures that the final midspan deflection changes very slightly with a change in the ς-value of the pulse. It might therefore be concluded that the effect of finite load rise time is small enough to use the blast-type approximation with confidence and with economy of effort and time.

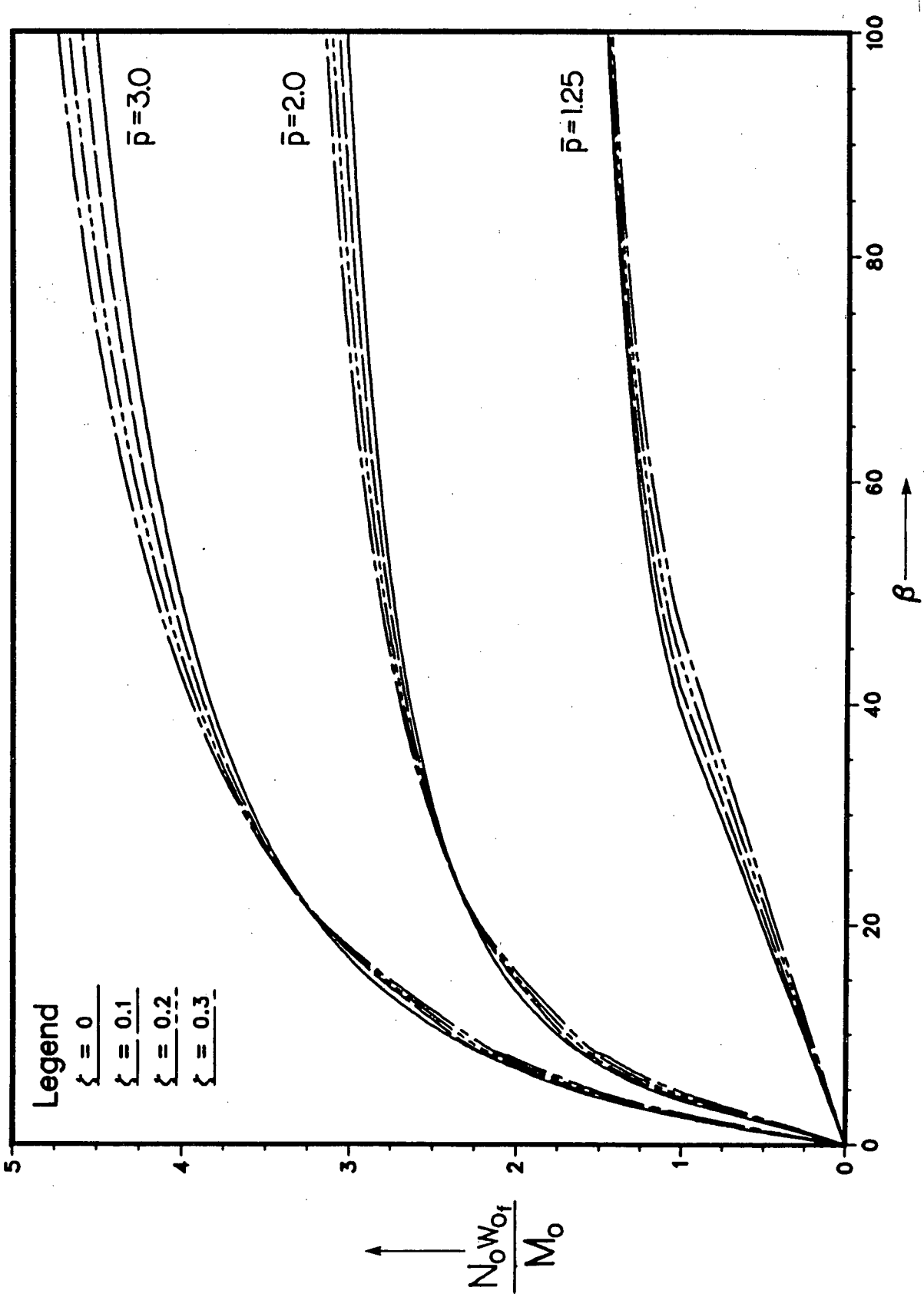

FIGURE 3.5 *Final midspan displacement vs. impulse of a pinned beam subjected to medium intensity triangular load pulses with varying rise times.*

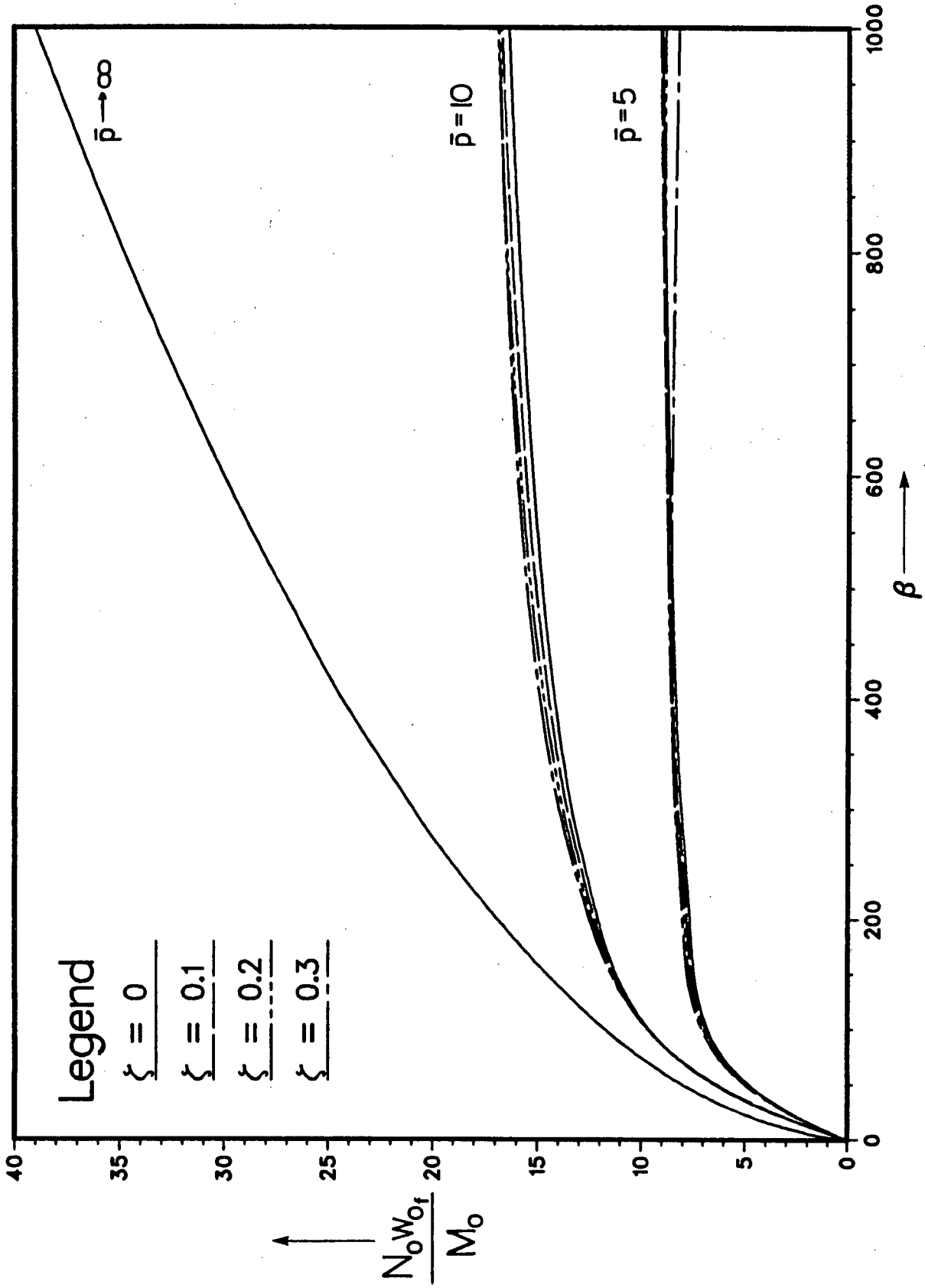

FIGURE 3.6 *Final midspan displacement vs. impulse of a pinned beam subjected to high intensity triangular load pulses with varying rise times.*

CHAPTER 4

ELIMINATING THE EFFECT OF PULSE SHAPE

4.1 SIMPLIFYING THE ANALYSIS

The analytical procedure developed in the two preceeding chapters can be used to solve for the deflection response of a beam subjected to any arbitrary load pulse. However, it was also evident from these two chapters that the applied pulse need not become overly complex for the ensuing analysis to become so. It would therefore be desirable to have a method of reducing arbitrary pulses to equivalent, easily analysed rectangular pulses. Pulses shall be considered equivalent if they produce an equivalent response characteristic, which for the purposes of this study shall be the final midspan displacement of the beam.

4.2 EQUIVALENT RECTANGULAR PULSES

Consider once again the rigid-plastic, pinned, doubly symmetric beam of Figure 2.1(a). Work formulations have been used to derive the differential equations of motion of this beam subjected to a uniformly distributed pulse load. Work formulations can also be used to solve for the final deformation of the beam.

The external work done by the pulse load in some increment of time dt is

$$dW_{ext} = p(t)\frac{d}{dt}\left(\int_{-l}^{l} w(x,t)\,dt\right)dt = p(t)\dot{S}\,dt,$$

where S is the displaced area of the beam (as defined in Figure 2.5) and $\dot{()}$ denotes differentiation in time. Hence, the total external work done by the load through the beam's deformation is

$$W_{ext} = \int_{t_o}^{t_f} p(t)\dot{S}\,dt. \tag{4.2.1}$$

The internal work dissipated by the beam in some increment of time dt during the bending response is $dW_{int} = M_o\dot{\theta}\,dt$ where θ is the angle through which the midspan plastic hinge or finite segment is rotated. During string response the increment in internal work is $dW_{int} = N_o\dot{\Delta}\,dt$ where Δ is the extension of the beam caused by transverse deflections. Hence, the total internal work dissipated by the beam through the plastic deformation is

$$W_{int} = \int_{t_o}^{t_s} M_o\dot{\theta}\,dt + \int_{t_s}^{t_f} N_o\dot{\Delta}\,dt. \tag{4.2.2}$$

The beam is at rest at the times t_o and t_f. The external work and internal work done between these times can therefore be equated to yield

$$\int_{t_o}^{t_f} p(t)\dot{S}\,dt = \int_{t_o}^{t_s} M_o\dot{\theta}\,dt + \int_{t_s}^{t_f} N_o\dot{\Delta}\,dt. \tag{4.2.3}$$

Equation (4.2.3) is really just another way of expressing the direct integration of accelerations obtained by d'Alembert's principle, as was done in Chapters 2 and 3. As such, this equation does not provide the analyst with any new information, but it does conveniently and concisely express the energy principles and means of energy input and dissipation which govern the motion of the beam, and will prove to be of some benefit in this present study.

4.2.1 BENDING RESPONSE

In Chapters 2 and 3 the final midspan displacement w_{o_f} of the beam was obtained by direct integration of the accelerations derived from d'Alembert's principle.

These expressions for w_{o_f} can be used directly to find rectangular pulses that are equivalent to the true ones.

(a) Medium Loads ($p_m \leq 3p_o$)

From Equations (3.2.1) and (3.2.2), the final midspan displacement of a pinned beam subjected to an arbitrary pulse of medium intensity is

$$w_{o_f} = \frac{3p_o}{2m}\int_{t_o}^{t_f}(t_f - t)\left[\frac{p(t)}{p_o} - 1\right]dt,$$

where

$$t_f = t_o + \int_{t_o}^{t_f}\frac{p(t)}{p_o}dt.$$

These two equations can be combined to yield the expression

$$w_{o_f} = \frac{3p_o}{2m}\left[\tfrac{1}{2}(t_f - t_o)^2 - \int_{t_o}^{t_f}\frac{p(t)}{p_o}(t - t_o)\,dt\right]. \tag{4.2.4}$$

Equation (2.6.16) gives the final midspan displacement of a rectangular pulse. Consider the equivalent rectangular pulse with an intensity of p_e and a duration of t_{p_e}. The final midspan displacement due to this pulse will occur at the time $t_{f_e} = \overline{p}_e t_{p_e}$ and will be

$$(w_{o_f})_e = \frac{3M_o\beta_e}{4N_o}\left(\frac{\overline{p}_e - 1}{\overline{p}_e}\right) = \frac{3p_e}{4m}(\overline{p}_e - 1){t_{p_e}}^2, \tag{4.2.5}$$

where $\overline{p}_e = p_e/p_o$.

If the equivalent rectangular pulse is to cause the same final midspan displacement as the true pulse, combining Equations (4.2.4) and (4.2.5) so that $(w_{o_f})_e = w_{o_f}$ gives

$$\overline{p}_e(\overline{p}_e - 1){t_{p_e}}^2 = (t_f - t_o)^2 - 2\int_{t_o}^{t_f}\frac{p(t)}{p_o}(t - t_o)\,dt. \tag{4.2.6}$$

With two unknown variables ($\overline{p}_e$ and t_{p_e}), one variable can be made dependent upon the other by some convenient means, and the independent variable can then be solved from Equation (4.2.6). For convenience the nominal impulse I (and hence β) of the effective rectangular pulse can be made equal to that of the true pulse, giving

$$p_e t_{p_e} = \int_0^{t_p} p(t)\,dt = I. \tag{4.2.7}$$

With this relationship, Equation (4.2.6) can be simplified to give the intensity of the equivalent pulse as

$$\overline{p}_e = \frac{I^2}{I^2 - p_o^2(t_f - t_o)^2 + 2p_o \int_{t_o}^{t_f} p(t)(t - t_o)\, dt}. \tag{4.2.8}$$

(b) High Loads ($p_m > 3p_o$)

From Equations (3.2.2), (3.2.13), and (3.2.15), the final midspan displacement of a beam subjected to an arbitrary pulse of high intensity is

$$w_{o_f} = \frac{3p_o}{2m}\int_{t_o}^{t_f}(t_f - t)\left[\frac{p(t)}{p_o} - 1\right] dt - \frac{3p_o}{2m}\int_{t_1}^{t_2}(t_2 - t)\left[\frac{p(t)}{3p_o} - 1\right] dt,$$

where

$$t_f = t_o + \int_{t_o}^{t_f} \frac{p(t)}{p_o} dt$$

and

$$t_2 = t_1 + \int_{t_1}^{t_2} \frac{p(t)}{3p_o} dt.$$

These three equations can be combined to give

$$w_{o_f} = \frac{3p_o}{2m}\left[\tfrac{1}{2}(t_f - t_o)^2 - \int_{t_o}^{t_f} \frac{p(t)}{p_o}(t - t_o)\, dt - \tfrac{1}{2}(t_2 - t_1)^2 + \int_{t_1}^{t_2} \frac{p(t)}{3p_o}(t - t_1)\, dt\right]. \tag{4.2.9}$$

From Equation (2.6.39) the final midspan displacement of an equivalent rectangular pulse occurs at the time $t_{f_e} = \overline{p}_e t_{p_e}$ and is

$$(w_{o_f})_e = \frac{M_o\beta}{N_o}\left(\frac{2}{3} - \frac{1}{2\overline{p}_e}\right) = \left(\frac{2}{3} - \frac{1}{2\overline{p}_e}\right)\overline{p}_e^2 {t_{p_e}}^2. \tag{4.2.10}$$

Again setting the nominal impulse of the rectangular pulse equal to that of the true pulse, Equations (4.2.9) and (4.2.10) combine to give the intensity of the equivalent rectangular pulse as

$$\overline{p}_e = \left\{\frac{4}{3} + \frac{3\int_{t_o}^{t_f} \frac{p(t)}{p_o}(t - t_o)\, dt - \frac{3}{2}(t_f - t_o)^2 - \int_{t_1}^{t_2} \frac{p(t)}{p_o}(t - t_1)\, dt + \frac{3}{2}(t_2 - t_1)^2}{\left(\frac{I}{p_o}\right)^2}\right\}^{-1}. \tag{4.2.11}$$

The above equation is valid if the equivalent rectangular pulse is of high intensity (*i.e.* $\overline{p}_e > 3$). If such is not the case, Equation (4.2.9) must be combined with Equation (4.2.5) to yield

$$\overline{p}_e = \left\{ 1 - \frac{(t_f - t_o)^2 - 2\int_{t_o}^{t_f} \frac{p(t)}{p_o}(t - t_o)\,dt - (t_2 - t_1)^2 + 2\int_{t_1}^{t_2} \frac{p(t)}{3p_o}(t - t_1)\,dt}{\left(\frac{I}{p_o}\right)^2} \right\}^{-1}, \quad (4.2.12)$$

which is valid if $\overline{p}_e \leq 3$ and $\overline{p} > 3$.

4.2.2 STRING RESPONSE

The string response of the beam, although dependent upon the load function $p(t)$, can not in general be written strictly in terms of $p(t)$. A closed form method to determine the equivalent rectangular pulse is not available as it was for bending response. Approximations must be made, and consideration of Equation (4.2.3) can be of benefit.

In string response, the beam has been assumed in this study to deform in a simple sinusoidal profile. In this mode the displaced area of the beam is $S = 4lw_o/\pi$ and the extension is $\Delta = \pi^2 w_o^2/8l$. Equation (4.2.3) can then be written as

$$\begin{aligned}\int_{t_o}^{t_s} p(t)\dot{S}\,dt + \frac{4l}{\pi}\int_{t_s}^{t_f} p(t)\dot{w}_o\,dt &= M_o\theta(t_s) + \int_{t_s}^{t_f} \frac{N_o\pi^2}{8l}(\dot{w_o}^2)\,dt \\ &= \frac{2{M_o}^2}{N_o[l - x_o(t_s)]} + \frac{N_o\pi^2}{8l}\left({w_{o_f}}^2 - \frac{{M_o}^2}{{N_o}^2}\right).\end{aligned}$$

Noting that the final term in the above equation is constant for some predetermined w_{o_f}, an equivalent rectangular pulse which causes the same final midspan displacement as the true pulse must satisfy the expression

$$\begin{aligned}p_e\int_0^{t_{se}} \dot{S}_e dt + \frac{4p_e l}{\pi}\left(w_{o_f} - \frac{M_o}{N_o}\right) - \frac{2{M_o}^2}{N_o[l - x_o(t_s)]_e} = \\ \int_{t_o}^{t_s} p(t)\dot{S}\,dt + \frac{4l}{\pi}\int_{t_s}^{t_f} p(t)\dot{w}_o\,dt - \frac{2{M_o}^2}{N_o[l - x_o(t_s)]}.\end{aligned} \quad (4.2.13)$$

In the above equation, the term $\int_{t_s}^{t_f} p(t)\dot{w}_o\,dt$ can not be determined analytically without actually solving the problem as before. Equation (4.2.13) can only be solved approximately. To do this, an iterative numerical solution scheme could be develoed. Alternatively one could assume that the distribution of work done on the beam in the bending and string phases is roughly the same for the true and equivalent pulses, and solve the approximate expression

$$p_e \int_0^{t_{se}} \dot{S}_e dt - \frac{2M_o^2}{N_o[l - x_o(t_s)]_e} \approx \int_{t_o}^{t_s} p(t)\dot{S}\,dt - \frac{2M_o^2}{N_o[l - x_o(t_s)]}.$$

Either of these methods, and perhaps others, could provide reasonably good approximations for the equivalent pulse. However it is readily apparent that these methods are ungainly and as potentially tedious as the complete analyses of Chapters 2 and 3. Even the closed form results for bending response in Section 4.2.1 are unsettling to the analyst looking for a quick approximation of the permanent beam deformations. The use of energy methods to eliminate the effect of the pulse shape does not appear promising.

4.3 YOUNGDAHL'S CORRELATION PARAMETERS

Youngdahl [16] has developed correlation parameters to convert an arbitrary load pulse to an equivalent "effective" rectangular load pulse. Youngdahl's procedure is a general one, applicable to all forms of pulse loaded structures, but intended only for bending response of the structure.

Youngdahl's effective rectangular pulse has the same true impulse as the arbitrary pulse considered. The true impulse I^* is defined to be the area under the load-time relation from the onset to the cessation of deformation, † *i.e.*

$$I^* = \int_{t_o}^{t_f} p(t)\,dt. \tag{4.3.1}$$

The centroid of the considered pulse is at the time t_{mean} defined as

$$t_{mean} = \frac{1}{I^*}\int_{t_o}^{t_f} p(t)(t - t_o)\,dt. \tag{4.3.2}$$

† Note that this definition differs from that of the nominal impulse I in Equation (2.5.1).

The effective pulse has the same centroid t_{mean} and hence has the duration $t_{p_e} = 2t_{mean}$. As a result of this, the intensity of the effective pulse must be

$$p_e = \frac{I^*}{2t_{mean}}. \tag{4.3.3}$$

In general, the time t_f at which motion ceases is not known a *priori*. Youngdahl assumed that in all cases t_f is given by

$$t_f = t_o + \int_{t_o}^{t_f} \frac{p(t)}{p_o} dt,$$

which is in fact true for bending-only response of the beam and corresponds to Equation (3.2.2). In summary, an arbitrary pulse is replaced by a rectangular pulse with an equivalent true impulse and an equivalent impulsive centroid. Notice that the effective rectangular pulse's nominal impulse I_e is equal to its true impulse I_e^*.

Youngdahl asserted that the effective rectangular pulse induces permanent deformations that compare well with those derived from arbitrary pulse shapes, especially for loads in the medium range ($1 < \bar{p} \leq 3$). In fact, if in the closed form analysis of Section 4.2.1(a) the true impulse I^* had been held constant instead of the nominal impulse I, Equation (4.3.3) would have been obtained instead of Equation (4.2.8).

As has been previously stated, Youngdahl's method is intended only for bending response of the structure. With little regard for this limitation, the procedure was applied to the axially restrained beam problem at hand, string response included. The triangular pulse of Section 2.7 was replaced by an effective rectangular pulse as per Equations (4.3.1) through (4.3.3) and analysed as in Section 2.6. Because I^* is held constant rather than I, the β-value of the effective pulse (β_e) must be $(I^*/I)^2$ times the β-value of the true pulse. For example, if the triangular pulse has $\bar{p} \leq 2$, Equation (3.2.2) gives the time of final deformation as $t_f = 2t_p(\bar{p}-1)/\bar{p} \leq t_p$. From Equation (4.3.1) the true impulse is $I^* = 2p_m t_p(\bar{p}-1)/\bar{p}^2$ (as compared to $I = \frac{1}{2}p_m t_p$) which is set equal to I_e^* and I_e. Hence, $\beta_e = (I^*/I)^2\beta = [4(\bar{p}-1)/\bar{p}^2]^2\beta$ and this effective impulse parameter β_e is used in the subsequent rectangular pulse analysis. The results of this approximate

analysis are shown in Figures 4.1 and 4.2 along with the results of the complete analysis of Section 2.7. The results are plotted in terms of β, the non-dimensional impulse parameter of the true triangular pulse. Comparison of the two analyses is quite good for this example, with discrepancies in the final midspan displacement results limited to about ten percent.

Though having little basis in theory for the axially restrained beam problem where string response can predominate, Youngdahl's correlation parameters seem to provide a quick and tidy means by which the effects of a complex load pulse may be approximated.

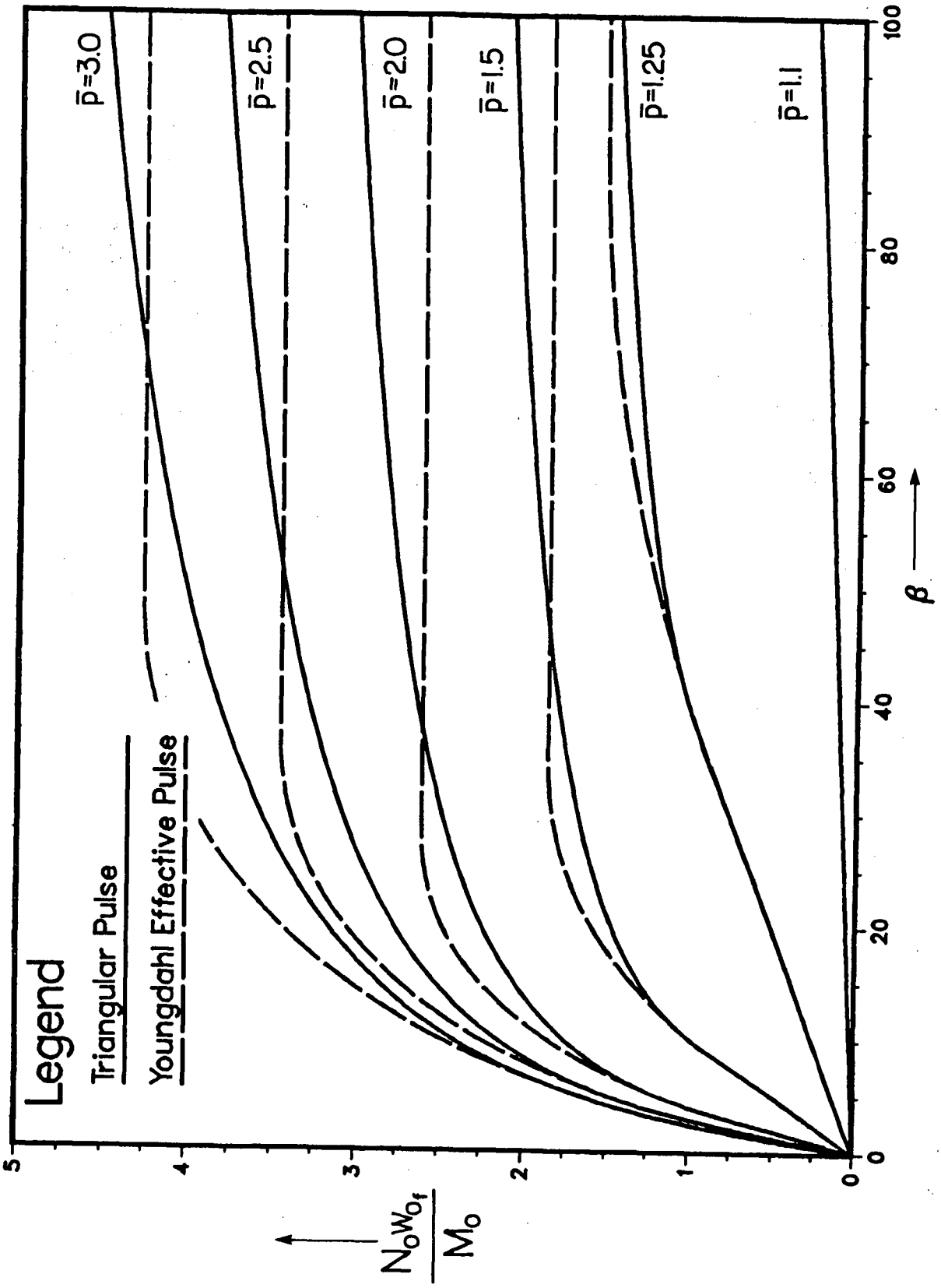

FIGURE 4.1 *Final midspan displacement of a pinned beam subjected to a medium intensity triangular load pulse as computed using Youngdahl's correlation parameters.*

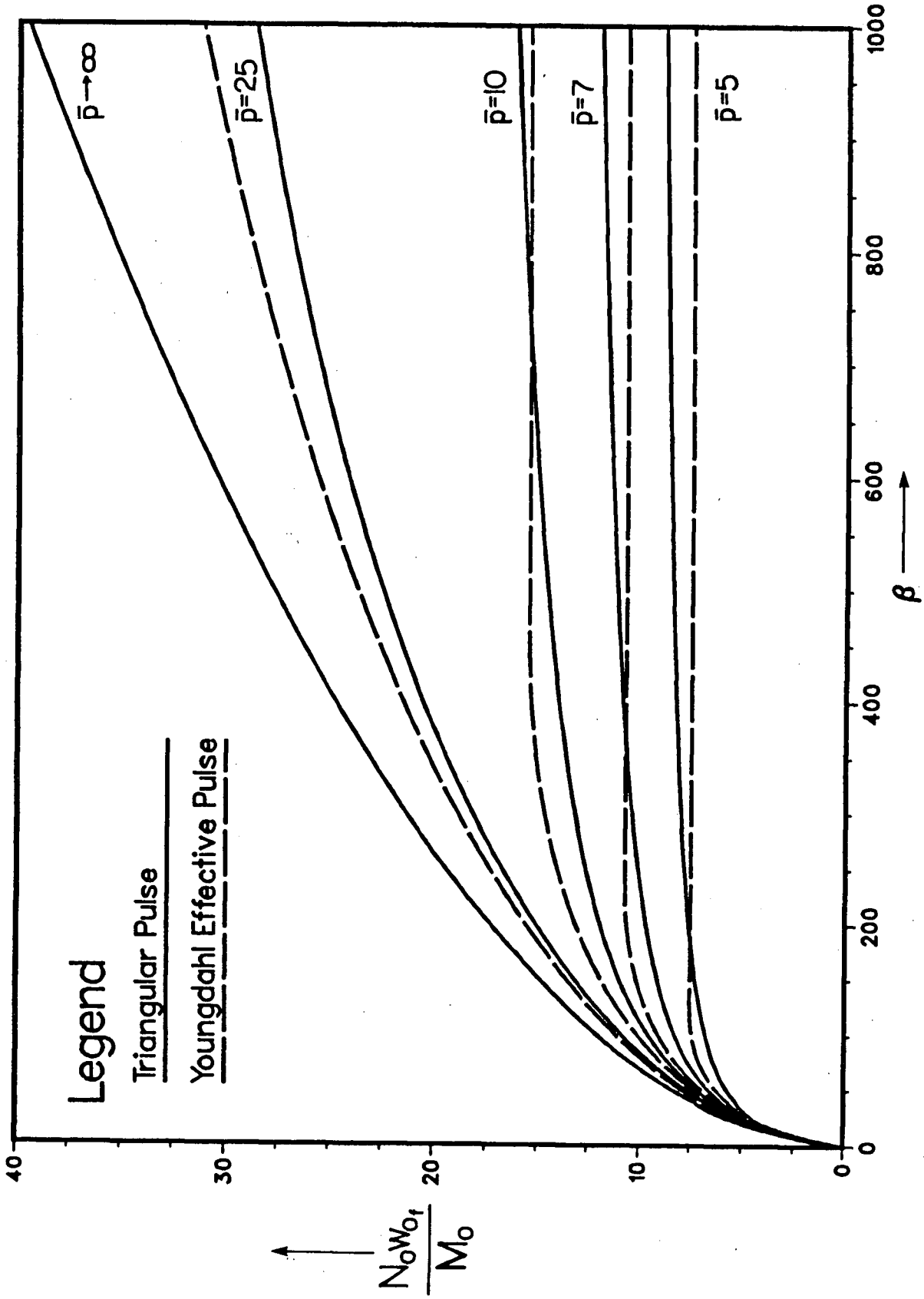

FIGURE 4.2 *Final midspan displacement of a pinned beam subjected to a high intensity triangular load pulse as computed using Youngdahl's correlation parameters.*

CHAPTER 5

RESPONSE OF SINGLY SYMMETRIC BEAMS

5.1 STATEMENT OF THE PROBLEM

Previous chapters have dealt with the response of doubly symmetric beams subjected to uniformly distributed pulse loads. In many instances, however, beam sections of only a single degree of symmetry such as T-beams and non-symmetric I-beams are employed. In this chapter, a beam of *singly* symmetric cross-section with a mass per unit length of m will be considered. As before, the ends of the beam are symmetrically supported at the section's centroidal axis with constraints against axial displacements. The beam is subjected to a uniformly distributed pressure pulse which acts through the beam's axis of symmetry, as in Figure 5.1. The solution to this problem shall proceed in a manner similar to that for the doubly symmetric beam — discussion will begin with the response of the singly symmetric beam to static loading.

5.2 STATIC ANALYSIS

In Section 2.3 it was shown that the static load capacity of a symmetrically supported, axially restrained beam subjected to a uniformly distributed load can be found

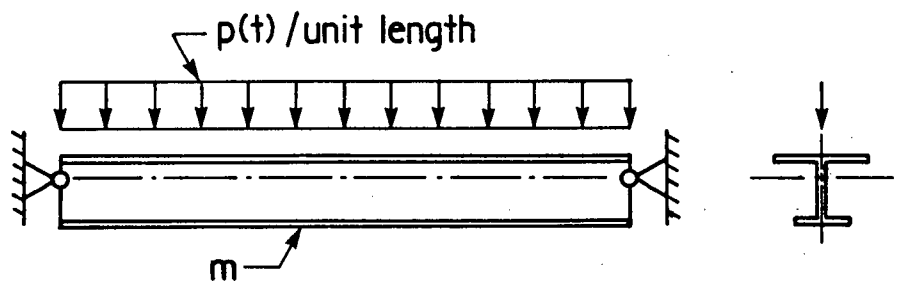

FIGURE 5.1 *Singly symmetric beam subjected to a uniformly distributed pulse load.*

by using Haythornwaite's [11] approximate deformation mode. For small deflections the beam responds in the single midspan hinge mode of Figure 2.4(a). The beam retains its bending stiffness and the load capacity for a pinned beam is given by Equation (2.3.10) as

$$\left(\frac{p}{p_o}\right)_{pinned} = \overline{m} + \left(\frac{N_o w_o}{M_o}\right)\overline{n},$$

and the load capacity for a clamped beam is given by Equation (2.3.10a) as

$$\left(\frac{p}{p_o}\right)_{clamped} = \overline{m} + \frac{1}{2}\left(\frac{N_o w_o}{M_o}\right)\overline{n}.$$

As deflections become large the beam responds as a plastic string as in Figure 2.4(b) and the load capacities for pinned and clamped beams are given by Equations (2.3.24) and (2.3.24a) as

$$\left(\frac{p}{p_o}\right)_{pinned} = \frac{N_o w_o}{M_o}$$

and

$$\left(\frac{p}{p_o}\right)_{pinned} = \frac{N_o w_o}{2M_o}.$$

As was pointed out in Section 2.3, $\overline{m}$ and $\overline{n}$ must be known in order to solve for the load capacity, and this requires that the yield curve for the section be defined.

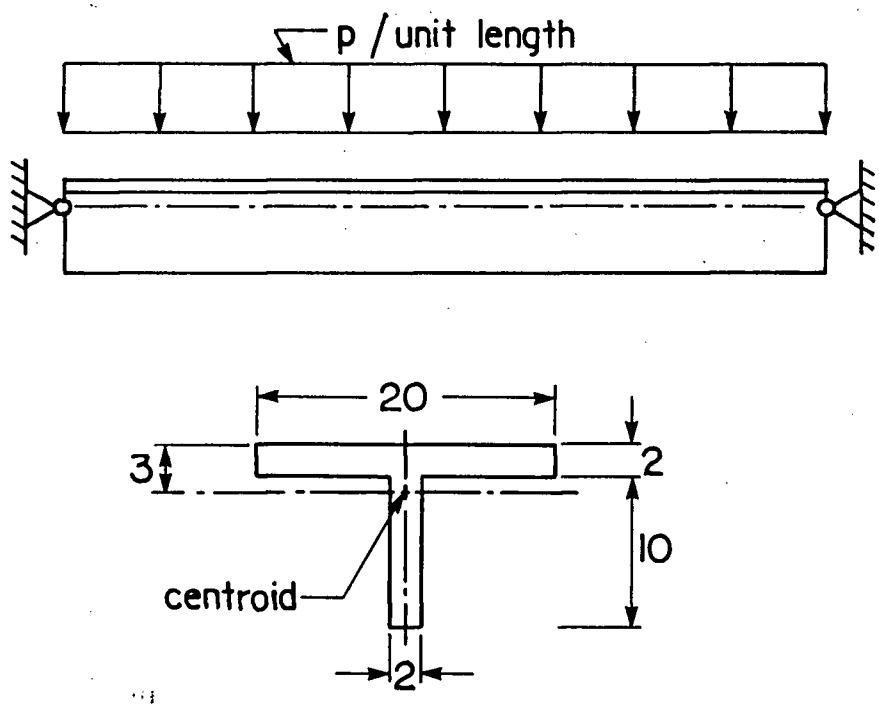

FIGURE 5.2 *Pinned T-beam example.*

Consider for example the pinned T-beam of Figure 5.2. As before, N_o is defined to be the axial load capacity of the beam section, which is equal to the beam's cross-sectional area multiplied by the beam material's uniaxial yield stress σ_o. For the T-beam presently considered, $N_o = 60\sigma_o$. Previously, the maximum moment that could be carried by the beam was the plastic moment — the moment due to a fully plastic stress distribution with the neutral axis at the section's equal area axis. However, in the case of an axially restrained, singly symmetric beam, axial forces can be induced and a larger moment — one due to a fully plastic stress distribution with the neutral axis at the section's centroidal axis — can be carried. This latter ultimate moment shall hereafter be defined as M_o. For the present T-beam example, $M_o = 162\sigma_o$ while the plastic moment is only $135\sigma_o$. The beam will not begin to deform until the ultimate moment M_o is reached at the midspan section, which for the pinned beam considered here will occur at the static

collapse load $p_o = 2M_o/l^2$. The yield curve for this section is defined by

$$\overline{m} = \begin{cases} \frac{5}{9}(1 - 4\overline{n} - 5\overline{n}^2), & \text{if } \overline{n} < -1/3; \\ \frac{5}{18}(3 - 2\overline{n} - \overline{n}^2), & \text{if } \overline{n} \geq -1/3, \end{cases} \tag{5.2.1}$$

where, as before, $\overline{n} = N/N_o$ and $\overline{m} = M/M_o$. Equation (2.3.12) states the flow rule to be

$$\frac{M_o \delta\psi}{N_o \delta\varepsilon} \cdot \frac{d\overline{m}}{d\overline{n}} = -1$$

where, for the single midspan hinge mode, $\delta\varepsilon/\delta\psi = \delta\Delta/\delta\theta = w_o$. Inserting the interaction relation into the flow rule yields

$$\overline{n} = \begin{cases} \frac{9}{50}\left(\frac{N_o w_o}{M_o}\right) - \frac{2}{5}, & \text{if } 0 \leq \frac{N_o w_o}{M_o} \leq \frac{10}{27}; \\ \frac{9}{5}\left(\frac{N_o w_o}{M_o}\right) - 1, & \text{if } \frac{10}{27} < \frac{N_o w_o}{M_o} \leq \frac{10}{9}, \end{cases} \tag{5.2.2}$$

and

$$\overline{m} = \begin{cases} 1 - \frac{9}{100}\left(\frac{N_o w_o}{M_o}\right)^2, & \text{if } 0 \leq \frac{N_o w_o}{M_o} \leq \frac{10}{27}; \\ \frac{10}{9} - \frac{9}{10}\left(\frac{N_o w_o}{M_o}\right)^2, & \text{if } \frac{10}{27} < \frac{N_o w_o}{M_o} \leq \frac{10}{9}. \end{cases} \tag{5.2.3}$$

Combining these results with Equations (2.3.10) and (2.3.24) gives the static load capacity of the T-beam as

$$\frac{p}{p_o} = \begin{cases} 1 - \frac{2}{5}\left(\frac{N_o w_o}{M_o}\right) + \frac{9}{100}\left(\frac{N_o w_o}{M_o}\right)^2, & \text{if } 0 \leq \frac{N_o w_o}{M_o} \leq \frac{10}{27}; \\ \frac{10}{9} - \frac{N_o w_o}{M_o} + \frac{9}{10}\left(\frac{N_o w_o}{M_o}\right)^2, & \text{if } \frac{10}{27} < \frac{N_o w_o}{M_o} \leq \frac{10}{9}; \\ \frac{N_o w_o}{M_o}, & \text{if } \frac{N_o w_o}{M_o} > \frac{10}{9}. \end{cases} \tag{5.2.4}$$

It was demonstrated in Section 2.3.3 that the yield curves of doubly symmetric beams could be adequately approximated by linear relations. The same is true for singly symmetric sections. The yield curve of the T-beam presently considered can be approximated by linear segments connecting nodes at $(\overline{n}, \overline{m}) \equiv (-1, 0)$, $(\overline{n}, \overline{m}) \equiv (-\frac{2}{5}, 1)$, and $(\overline{n}, \overline{m}) \equiv (1, 0)$. Figure 5.3 shows this linear approximation along with the section's true yield curve. From consideration of the flow rule it is seen that the stress state of

a plastic section must always be at one of the nodes. As a result, $(\overline{n}, \overline{m}) \equiv (-\frac{2}{5}, 1)$ for $0 \leq N_o w_o / M_o \leq 5/7$ and $(\overline{n}, \overline{m}) \equiv (1, 0)$ for $N_o w_o / M_o > 5/7$. Putting the first stress state into Equation (2.3.10) and the second into Equation (2.3.24), the static load capacity of the T-beam (as approximated by the linear interaction relation) is found to be

$$\frac{p}{p_o} = \begin{cases} 1 - \dfrac{2}{5}\left(\dfrac{N_o w_o}{M_o}\right), & \text{if } 0 \leq \dfrac{N_o w_o}{M_o} \leq \dfrac{5}{7}; \\ \dfrac{N_o w_o}{M_o}, & \text{if } \dfrac{N_o w_o}{M_o} > \dfrac{5}{7}. \end{cases} \tag{5.2.5}$$

The static load capacity of the pinned T-beam is plotted in Figure 5.4 for both the true interaction relation and the linear approximation. The load capacity as computed using the approximate linear interaction relation is slightly smaller than that computed using the true relation for small deflections ($N_o w_o / M_o < 1$), but the two results are identical for larger deflections. The use of a linear interaction relation provides a good estimate of the load capacity of the T-beam of Figure 5.2 and should do so for any singly symmetric beam. As was the case for doubly symmetric beams, linear interaction relations can be used to advantage in the dynamic analysis of singly symmetric beams.

5.3 RESPONSE TO BLAST-TYPE PULSES

The dynamic response of singly symmetric, axially restrained beams subjected to uniformly distributed pulse loads will now be studied. In deriving the differential equations of motion of the singly symmetric beam the assumptions of Section 2.2 will again be made. Since it was shown in Chapter 3 that the effect of finite load rise time is small, pulses will henceforth be of the so-called blast-type. Furthermore, the yield curves of singly symmetric sections will be approximated by linear interaction relations as in Section 5.2. The dynamic analysis of singly symmetric beams is then similar to that of doubly symmetric beams. There is, however, one significant difference in the analyses. The response of singly symmetric beams does not uncouple to include a phase of pure bending response

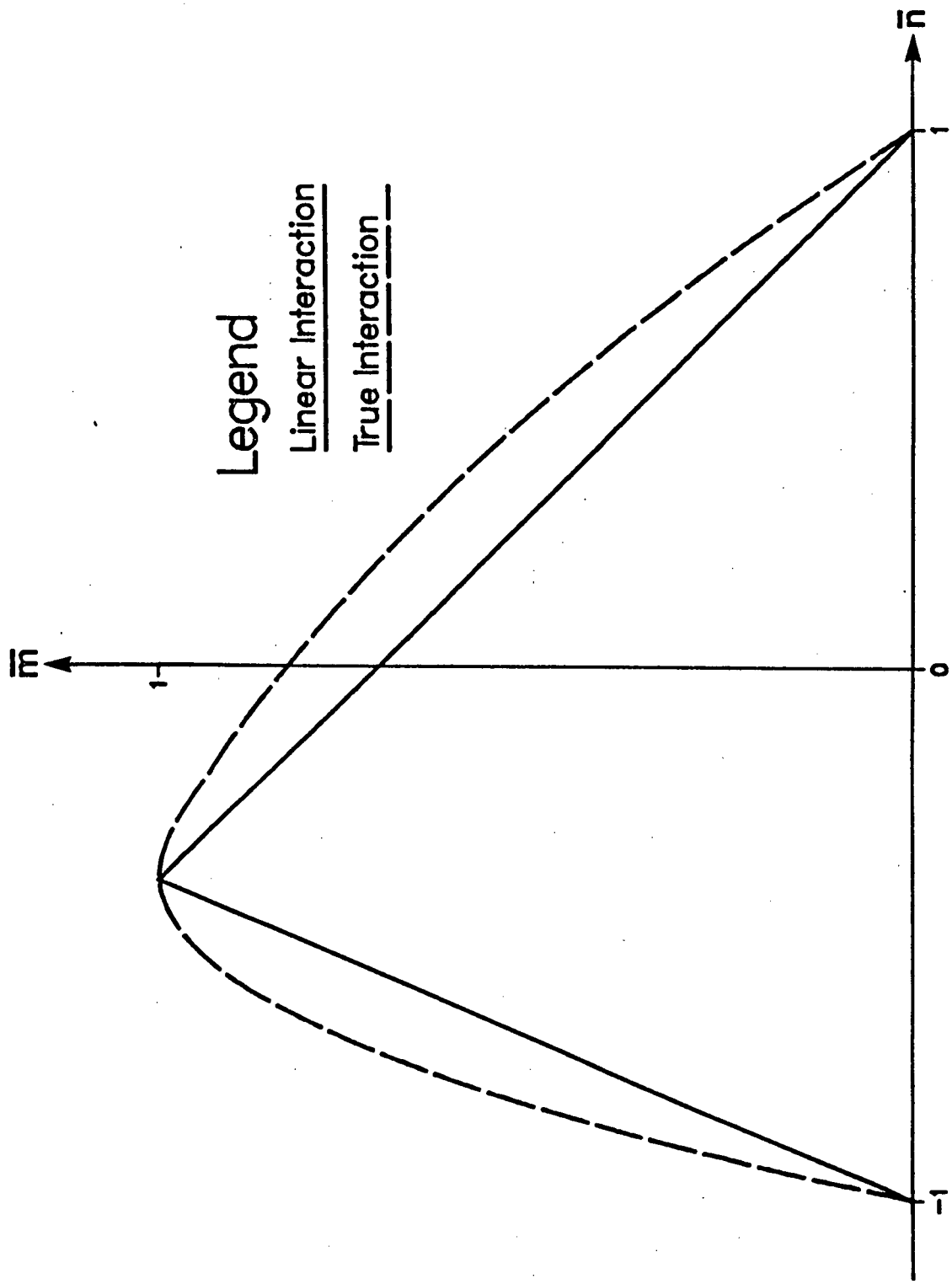

FIGURE 5.3 *True and approximate linear yield curves for the T-beam.*

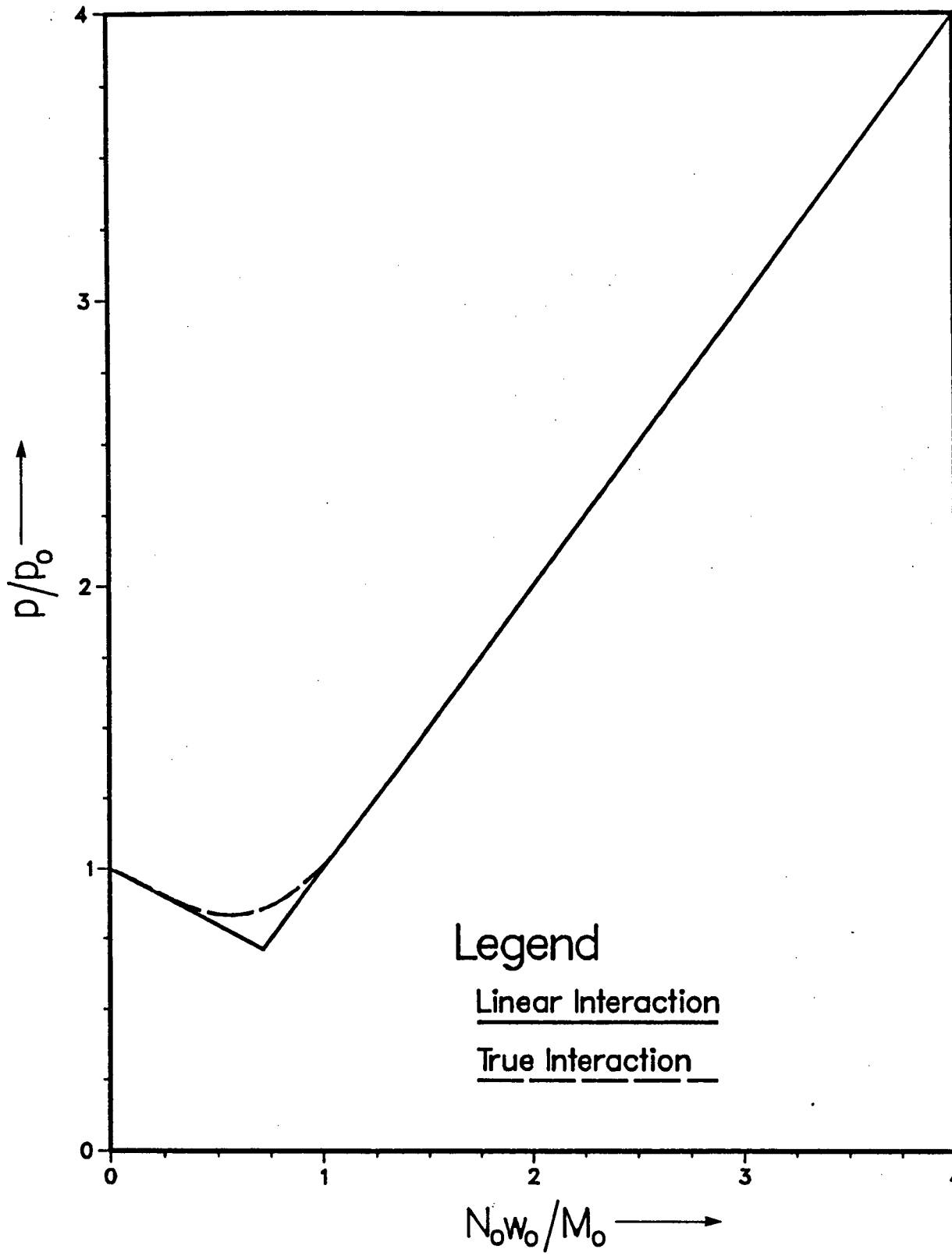

FIGURE 5.4 *Static load capacity of the T-beam.*

for small displacements, but instead includes a response phase of combined bending and axial load resistance.

5.3.1 COMBINED BENDING AND STRING RESPONSE

The linear yield curves of typical singly symmetric beam sections are shown in Figure 5.5. The initial response of the beam will be such that the bending moment in fully plastic sections will be equal to the ultimate moment M_o and the axial force will be equal to $\lambda^2 N_o$ where λ is a dimensionless measure of the symmetry (or non-symmetry) of the beam. Consideration of the flow rule shows that the above stress state exists for the range of values

$$1 - \lambda^2 \leq \frac{M_o \delta\psi}{N_o \delta\varepsilon} \leq \infty. \tag{5.3.1}$$

It is recalled that, if the beam deforms in the single midspan hinge or travelling hinge modes of Section 2.4.1, $\delta\varepsilon/\delta\psi = w_o$ for pinned beams and $\delta\varepsilon/\delta\psi = w_o/2$ for clamped beams. Hence, the small displacement phase during which the beam exhibits both bending and string resistance exists while

$$w_o \leq \frac{M_o}{N_o(1-\lambda^2)} \tag{5.3.2}$$

for pinned beams and

$$w_o \leq \frac{2M_o}{N_o(1-\lambda^2)} \tag{5.3.2a}$$

for clamped beams.

(a) Medium Loads ($p_o < p_m \leq 3p_o$)

When subjected to load pulses of medium intensity a pinned beam will be assumed to deform with a single midspan hinge as did the doubly symmetric beam. It is recalled from Sections 2.3 and 2.4 that for a virtual midspan displacement of δw_o there will be a corresponding virtual hinge rotation $\delta\theta = \delta w_o/l$ and a virtual extension $\delta\Delta = w_o\,\delta\theta$. The work dissipated in the plastic hinge through the virtual deformation is

$$\begin{aligned} \delta W_{int} &= M\delta\theta + N\delta\Delta \\ &= \left(M_o + \lambda^2 N_o w_o\right)\delta\theta. \end{aligned} \tag{5.3.3}$$

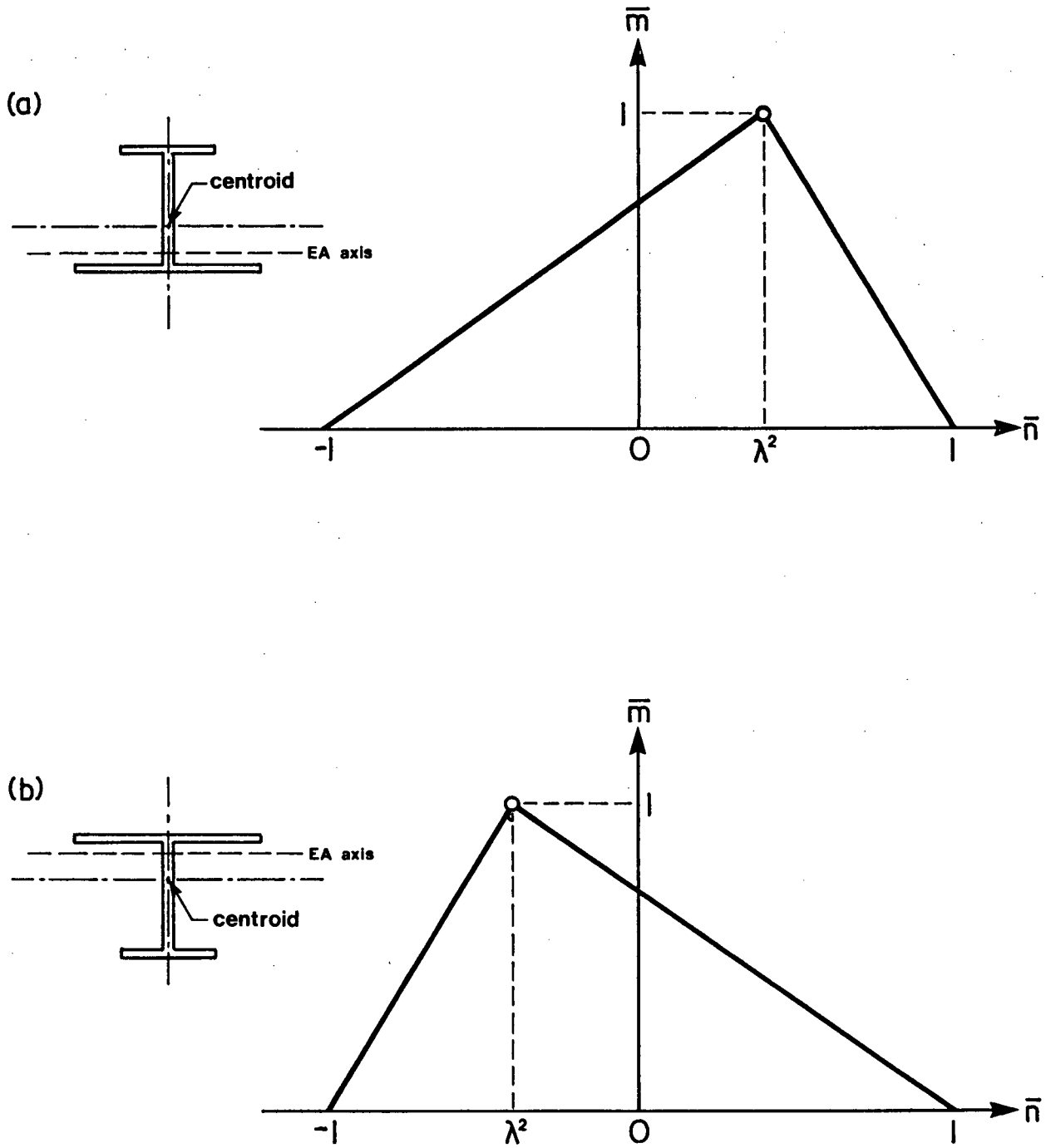

FIGURE 5.5 *Typical singly symmetric beam sections and their associated yield curves.*

Equation (2.4.5) will again give the external work done through the virtual deformation as

$$\delta W_{ext} = \left[\tfrac{1}{2}p(t)l^2 - \tfrac{1}{3}ml^2\ddot{w}_o\right]\delta\theta,$$

and equating the internal and external virtual work gives

$$\frac{3p(t)}{2m} - \ddot{w}_o = \frac{3}{ml^2}\left(M_o + \lambda^2 N_o w_o\right).$$

Making the substitution $M_o = \frac{1}{2}p_o l^2$ yields the differential equation of motion

$$\ddot{w}_o + \frac{3\lambda^2 N_o}{ml^2}w_o = \frac{3}{2m}\left[p(t) - p_o\right]. \tag{5.3.4}$$

In the case of a clamped beam, the internal virtual work is $\delta W_{int} = (2M_o + \lambda^2 N_o w_o)\,\delta\theta$ and $M_o = \frac{1}{4}p_o l^2$. It can be shown that the resulting differential equation of motion for a clamped beam is identical to that for a pinned beam.

If the beam is initially undeformed and at rest, the motion resulting from a blast-type pulse will be governed by the initial value problem comprised of Equation (5.3.4) and the initial conditions $w_o(0) = \dot{w}_o(0) = 0$. The solution of this initial value problem will be of the form

$$w_o(t) = A\cos\left(t\sqrt{\frac{3\lambda^2 N_o}{ml^2}}\right) + B\sin\left(t\sqrt{\frac{3\lambda^2 N_o}{ml^2}}\right) + w_{o_p}(t),$$

where A and B are constants to be determined by the initial conditions and $w_{o_p}(t)$ is the particular solution unique to the loading function $p(t) - p_o$. If, as in Figure 5.5(a), the section centroid lies above the section's equal area axis, the value of λ^2 is positive and the midspan displacement is given by

$$w_o(t) = A\cos\left(\frac{\lambda t}{l}\sqrt{\frac{3N_o}{m}}\right) + B\sin\left(\frac{\lambda t}{l}\sqrt{\frac{3N_o}{m}}\right) + w_{o_p}(t). \tag{5.3.5}$$

On the other hand, if the section centroid lies below the section's equal area axis as in Figure 5.5(b), the value of λ^2 is negative and the midspan displacement is given by

$$w_o(t) = A\cosh\left(t\sqrt{\frac{3N_o|\lambda^2|}{ml^2}}\right) + B\sinh\left(t\sqrt{\frac{3N_o|\lambda^2|}{ml^2}}\right) + w_{o_p}(t). \tag{5.3.6}$$

As was discussed in Section 2.3.1, the single midspan hinge deformation mode is not strictly correct when axial load is present in the beam. Although the assumed mechanism is kinematically admissible and equilibrium has been satisfied along the length of the beam, the presence of axial load causes the stress state at some point in the beam to lie outside of the yield curve, violating the plasticity condition. However, in Section 2.3 it was also shown that the load capacity of a beam does not vary greatly with differing (though kinematically admissible) deformation mechanisms. Response of the beam in this mode is then only an approximation of the true response of a rigid-plastic beam, but, in light of the approximations already made in the analysis, this does not seem unreasonable.

(b) High Loads ($p_m > 3p_o$)

When subjected to load pulses of high intensity, a beam will be assumed to deform with a flat midspan plastic segment bounded by two travelling hinges as did the doubly symmetric beam. This deformed configuration was shown in Figure 2.17, and kinematically admissible velocity and acceleration fields were given in Equations (2.4.8a,b).

On the flat midspan plastic segment ($0 \leq x \leq x_o$) the bending moment is constant and equal to M_o which requires the shear to be zero. The axial load $N = \lambda^2 N_o$ acts in a horizontal direction, and vertical equilibrium must be satisfied by $p(t) - m\ddot{w}_o(t) = 0$. Therefore, Equations (2.4.9) and (2.5.4a,b) again give the midspan response as

$$\ddot{w}_o(t) = \frac{p(t)}{m},$$
$$\dot{w}_o(t) = \int_0^t \frac{p(\tau)}{m}\, d\tau,$$
$$w_o(t) = \int_0^t \frac{p(\tau)}{m}(t-\tau)\, d\tau.$$

As was pointed out in Section 2.4, the rigid end segments of a beam under a high load are similar to the rigid halves of a beam under a medium load. Taking Equation (5.3.4) and replacing l with $(l - x_o)$ and $\ddot{w}_o$ with $\ddot{w}_o + \dot{x}_o\dot{w}_o/(l - x_o)$ yields

$$\ddot{w}_o + \frac{\dot{x}_o\dot{w}_o}{l - x_o} + \frac{3\lambda^2 N_o w_o}{m(l - x_o)^2} + \frac{3M_o}{m(l - x_o)^2} = \frac{3p(t)}{2m}. \tag{5.3.7}$$

Inserting the above expressions for w_o,$\dot{w}_o$ and $\ddot{w}_o$ into Equation (5.3.7) and rewriting M_o as $\frac{1}{2}p_o l^2$ results in a differential equation for the hinge position x_o:

$$-2(l-x_o)\dot{x}_o + \frac{p(t)(l-x_o)^2}{\int_0^t p(\tau)\,d\tau} = \frac{3p_o l^2}{\int_0^t p(\tau)\,d\tau} + \frac{6\lambda^2 N_o}{m}\cdot\frac{\int_0^t p(\tau)(t-\tau)\,d\tau}{\int_0^t p(\tau)\,d\tau}.$$

Making the substitution $\xi_o = l - x_o$, the differential equation reduces to

$$(\dot{\xi_o}^2) + \frac{p(t)}{\int_0^t p(\tau)\,d\tau}(\xi_o^2) = \frac{3p_o l^2}{\int_0^t p(\tau)\,d\tau} + \frac{6\lambda^2 N_o}{m}\cdot\frac{\int_0^t p(\tau)(t-\tau)\,d\tau}{\int_0^t p(\tau)\,d\tau},$$

for which the solution is

$$\xi_o^2 = \frac{3p_o l^2}{\int_0^t p(\tau)\,d\tau}\left[t + \frac{\lambda^2 N_o}{mM_o}\int_0^t p(\tau)(t-\tau)^2\,d\tau\right],$$

and, hence,

$$x_o(t) = l\left\{1 - \sqrt{\frac{3p_o}{\int_0^t p(\tau)\,d\tau}\left[t + \frac{\lambda^2 N_o}{mM_o}\int_0^t p(\tau)(t-\tau)^2\,d\tau\right]}\right\}. \tag{5.3.8}$$

For a clamped beam, equilibrium of a rigid end segment gives the equation

$$\ddot{w}_o + \frac{\dot{x}_o\dot{w}_o}{l-x_o} + \frac{3\lambda^2 N_o w_o}{m(l-x_o)^2} + \frac{6M_o}{m(l-x_o)^2} = \frac{3p(t)}{2m}. \tag{5.3.7a}$$

Because the midspan plastic segment is flat the midspan acceleration is again $\ddot{w}_o(t) = p(t)/m$. Recalling that for a clamped beam $M_o = \frac{1}{4}p_o l^2$, it is found that

$$x_o(t) = l\left\{1 - \sqrt{\frac{3p_o}{\int_0^t p(\tau)\,d\tau}\left[t + \frac{\lambda^2 N_o}{2mM_o}\int_0^t p(\tau)(t-\tau)^2\,d\tau\right]}\right\}. \tag{5.3.8a}$$

The hinges will meet at midspan at the time $t = t_2$ for which $x_o(t_2) = 0$. After this time the beam can be assumed to once again deform in the single midspan hinge mode according to Equation (5.3.4) and the initial conditions at time t_2. Midspan displacement can again be written in the form of Equation (5.3.5) or (5.3.6) but with t replaced by $t - t_2$.

As was the case for medium loads, the assumed mechanisms herein are incorrect when axial load is present — the plasticity condition is violated at some point in

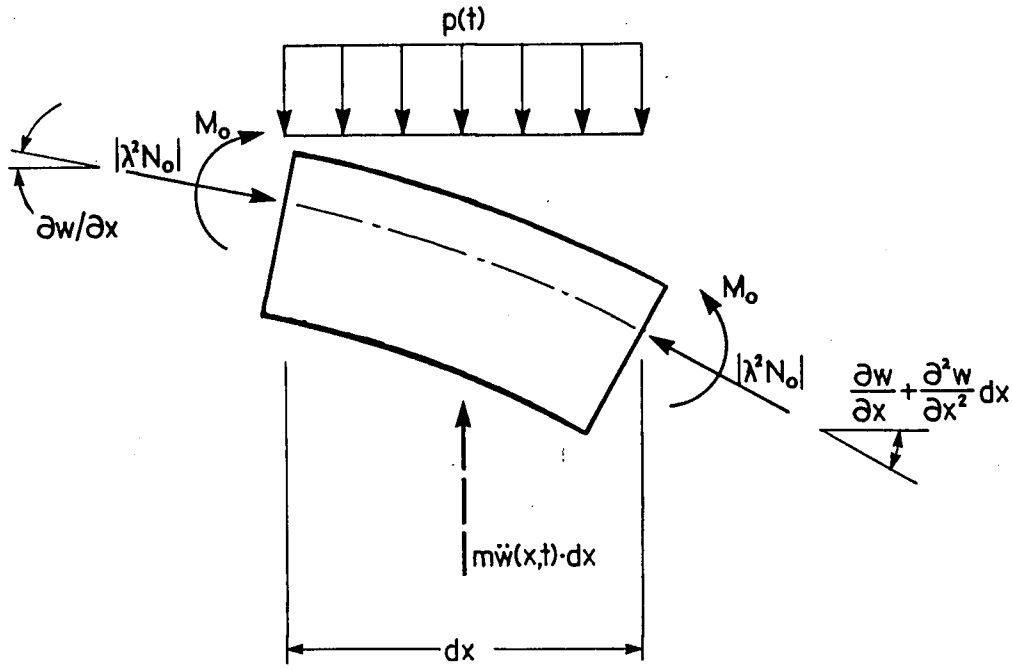

FIGURE 5.6 *Free body diagram of a curved plastic beam segment.*

the beam. However, as was discussed earlier, the assumed mechanisms should provide a very good estimate of the beam response.

There exists another flaw in the assumed deformation mode for high loads. It has been assumed that the midspan plastic segment is flat. But if $\lambda^2 < 0$ there is a possibility that the hinges will travel outward, even for a blast-type pulse. The midspan plastic segment would then have a curved shape near the hinges and would be flat only along $0 \leq x \leq x_o(0) = l(1 - \sqrt{3/\bar{p}})$. If, however, the free body diagram of a portion dx of the beam in the curved plastic segment is considered (Figure 5.6), vertical equilibrium of the beam increment gives

$$m\frac{\partial^2 w}{\partial t^2} + |\lambda^2 N_o|\frac{\partial^2 w}{\partial x^2} = p(t).$$

The beam will have negative curvature (*i.e.* $\partial^2 w/\partial x^2 < 0$) in the curved segment so that $\ddot{w}(t) > p(t)/m$. The displacements in the curved segment will catch up with those in

the flat segment, curvature will decrease in magnitude until it approaches zero, $\ddot{w}(t)$ will decrease until it approaches $p(t)/m$, and the plastic segment approaches a flat shape. The assumption of a completely flat plastic segment, though not always aesthetically satisfying, does seem to be a reasonable approximation to the true deflection profile, and will greatly simplify the analysis.

5.3.2 STRING RESPONSE

As the beam displacements become large, the stress state of the beam along its entire length becomes $(\overline{n}, \overline{m}) \equiv (1, 0)$, as was the case for doubly symmetric beams. The differential equation of string response of a singly symmetric beam is then identical to that of a doubly symmetric beam, and given by Equation (2.4.16). Hence the motion of the beam is governed by the initial value problem

$$\ddot{w}_o + \frac{N_o \pi^2}{4ml^2} w_o = \frac{4p(t)}{\pi m}$$

$$w_o(t_s) = \begin{cases} M_o/N_o(1-\lambda^2), & \text{for a pinned beam;} \\ 2M_o/N_o(1-\lambda^2), & \text{for a clamped beam,} \end{cases}$$

$$\dot{w}_o(t_s^+) = \begin{cases} \sqrt{2/3}\,\dot{w}_o(t_s^-), & \text{if } p_m \le 3p_o \text{ or } t_s \ge t_2; \\ \sqrt{\frac{2}{3}[1 + 2x_o(t_s)/l]}\,\dot{w}_o(t_s^-), & \text{if } p_m > 3p_o \text{ and } t_s < t_2. \end{cases}$$

The solution to this problem will again be of the form

$$w_o(t) = A\cos\left[\frac{\pi}{2}\sqrt{\frac{p_o N_o}{mM_o}}(t - t_s)\right] + B\sin\left[\frac{\pi}{2}\sqrt{\frac{p_o N_o}{mM_o}}(t - t_s)\right] + w_{o_p}(t)$$

where A and B are determined by the initial conditions at time t_s and $w_{o_p}(t)$ is the particular solution unique to the load function $p(t)$.

CHAPTER 6

CONCLUSION

6.1 SUMMARY OF RESULTS

The deformation response of symmetrically supported, axially restrained beams subjected to uniformly distributed pulse loads has been studied, leading to the development of an analytical procedure to predict the character and magnitude of such response. Beams to be analysed by this procedure must be at least singly symmetric and must be loaded through an axis of symmetry. The procedure is based upon the assumption that the beam material can be approximated as behaving in a rigid-perfectly plastic manner. The governing equations of motion have been derived from variational statements consisting of the principle of virtual work and d'Alembert's principle, and include the effects of finite geometry changes.

From the static analysis of axially restrained beams it has been found that the yield curve of a beam section may be replaced by a linear approximation thereof to obtain a good estimate of the beam's load capacity. Incorporating the linear yield curve approximation in a dynamic analysis of an axially restrained beam resulted in the uncoupling of the response into two distinct phases — an initial small deflection phase in which the beam retained bending resistance and deformed as a mechanism formed by

plastic hinges, and a subsequent large deflection phase in which the beam had no bending resistance and deformed as a plastic string. The results of such an analysis for a rectangular beam subjected to a rectangular load pulse compared well with the results of a previous solution by Vaziri [10] which used the true quadratic yield curve.

The linear yield curve approximation further resulted in linear differential equations of motion, and the response to load pulses of general load-time history could be solved in closed form. Blast-type pulses of triangular shape were found to induce significantly different permanent deflections in a beam than did a rectangular pulse. On the other hand, the effect of finite rise time of a triangular pulse's load intensity was found to be small if the rise time was less than about twenty to thirty percent of the pulse duration, suggesting that a considerably simpler blast-type pulse analysis would be adequate for such situations.

A procedure developed by C.K. Youngdahl [16] was used to convert a pulse of triangular shape to an "effective" rectangular pulse. The permanent deformation was then determined for this effective pulse and used as an estimate of the permanent deformation due to the triangular pulse. The results for the effective rectangular pulse were similar to those for the triangular pulse and were much more easily obtained. Evidently, the use of Youngdahl's procedure combined with the analysis of a rectangular pulse developed herein can provide a quick, simple solution to the permanent deformation of a dynamically loaded beam which is amenable to hand computation.

6.2 LIMITATIONS OF THE THEORY

It would seem that the problem of pulse loaded, axially restrained beams has been solved. While to some extent this is true, the analysis developed herein has its basis in a number of simplifying assumptions and omissions which limit its applicability and validity.

The beam material is modelled as obeying a rigid-perfectly plastic type of stress-strain relation. The effects of elasticity of the beam are ignored on the assumption that they are much smaller than the effects of plasticity. This assumption is correct when the energy absorbed by the beam in plastic deformation is much larger than the strain energy absorbed in elastic deformation and the duration of the load t_p is a fraction of the beam's fundamental period of elasic vibrations. If these conditions are not satisfied, the elastic response of the beam can become significant. While the analysis of the plastic response of the beam would still be essentially correct, the influence of elasticity may become very large and hence become the governing effect of the beam response. Load pulses of low intensity or long duration are likely to induce significant elastic response of the beam.

The yield stress of a material can increase with the amount of strain and the rate of strain imposed upon the material. These phenomena are known as strain hardening and strain rate sensitive behaviour, respectively, and structural steel exhibits both. The analytical procedure of this study takes neither phenomenon into account. Strain hardening of the beam material is generally regarded to have little effect on the permanent deformation response of the beam. Yield stress is usually increased by less than ten percent due to strain hardening, and only increased during the final stages of beam response after most of the deformation has occurred. The exclusion of strain hardening from the analysis should cause little concern. On the other hand, strain rate sensitive behaviour can have a large effect on the response of a steel beam. At high rates of strain (such as are encountered by impulsively loaded beams) hot rolled steel can exhibit yield stresses that are two or more times the static yield stress. Perrone [17] has suggested a simple, seemingly accurate means by which strain rate sensitive behaviour can be accounted for in a rigid-plastic analysis such as this.

This study does not take the effects of shear into account. Transverse shear forces seem to have a greater influence on the dynamic response of beams than on the

static response. Shear can interact with moment and axial load to cause a section to yield and can induce plastic deformations by way of shear sliding, as discussed by Symonds [18]. Although Symonds and others have shown that the effects of shear are usually unimportant for compact (*e.g.* rectangular) sections, shear can have a significant effect on the response of beams of non-compact section (*e.g.* I-beams, T-beams) which have relatively high ratios of moment capacity to shear capacity. As might be expected, the effects of shear diminish with increasing beam span.

Development of this study's solution for beam response has been facilitated by the use of linearized yield curves. The linearized yield curves inscribe the true yield curves. As a result, the overall section capacity has been reduced and the beam has been softened.

Most significantly, failure of the beam due to tensile tearing or shearing at the supports has not been considered. The beam material has been assumed to be infinitely ductile and, as noted previously, shear effects have been disregarded. Jones [19] derived critical velocities induced by impulsive loads which will lead to such failures in clamped rigid-plastic beams. His analysis might be used to provide rough estimates of such critical velocities for the presently considered dynamically loaded beams, or might be used as the basis for a more rigorous analysis.

Considering the neglected phenomena and simplifying assumptions mentioned above, it is impossible to assess the results of this study as conservative or non-conservative. Yet an analysis which retained all these phenomena would be unwieldy and perhaps unnecessary. Future investigation of their effects might best be done by numerical methods. If deemed appropriate the effects might then be incorporated to extend the solution herein. In the meantime, however, the results of this study should provide reasonably accurate estimates of the deflection response of dynamically loaded beams, and should be suitable for preliminary design of such beams.

REFERENCES

[1] Jones, N. "A Literature Review of the Dynamic Plastic Response of Structures," *Shock and Vibration Digest*, Vol. 7, No. 8, 1975, pp. 89–105.

[2] Jones, N. "Recent Progress in the Dynamic Plastic Behaviour of Structures, Parts I and II," *Shock and Vibration Digest*, Vol. 10, No. 10, 1978, pp. 13–19.

[3] Jones, N. "Recent Progress in the Dynamic Plastic Behaviour of Structures, Part III," *Shock and Vibration Digest*, Vol. 13, No. 10, 1981, pp. 3–16.

[4] Jones, N. "Recent Progress in the Dynamic Plastic Behaviour of Structures, Part IV," *Shock and Vibration Digest*, Vol. 17, No. 2, 1985, pp. 35–47.

[5] Ari-Gur, J., Anderson, D.L., and Olson, M.D. "Review of Air-Blast Response of Beams and Plates," 2nd Int. Conf. on Recent Advances in Structural Dynamics, U. of Southampton, Southampton, England, April 1984.

[6] Lee, E.H. and Symonds, P.S. "Large Plastic Deformations of Beams Under Transverse Impact," *ASME Journal of Applied Mechanics*, Vol. 19, No. 3, 1952, pp. 308–315.

[7] Symonds, P.S. "Dynamic Load Characteristics in Plastic Bending of Beams," *ASME Journal of Applied Mechanics*, Vol. 20, 1953, pp. 475–482.

[8] Symonds. P.S. "Large Plastic Deformations of Beams Under Blast Type Loading," Proc. of the 2nd U.S. National Congress of Applied Mechanics, ASME, 1954, pp. 505–515.

[9] Symonds, P.S. and Mentel, T.J. "Impulsive Loading of Plastic Beams with Axial Constraints," *Journal of the Mechanics and Physics of Solids*, Vol. 6, 1958, pp. 186–202.

[10] Vaziri, R., "Finite Deflection Dynamic Analysis of Rigid-Plastic Beams," *M.A.Sc. Thesis*, U.B.C., Vancouver, British Columbia, April 1985.

[11] Haythornwaite, R.M. "Beams With Full End Fixity," *Engineering*, Vol. 25, January 1957, pp. 110–112.

[12] Neal, B.G. *The Plastic Methods of Structural Analysis, 3rd ed.*, Chapman and Hall, London, 1977, p. 49.

[13] Gürkök, A. and Hopkins, H.G. "Plastic Beams at Finite Deflection Under Transverse Load with Variable End-Constraint," *Journal of the Mechanics and Physics of Solids*, Vol. 29, No. 5/6, 1981, pp. 447–476.

[14] Folz, B.R. "Numerical Simulation of the Non-Linear Transient Response of Slender Beams," *M.A.Sc. Thesis*, U.B.C., Vancouver, British Columbia, April 1986.

[15] Krajcinovic, D. "Dynamic Response of Rigid-Plastic Beams — General Case of Loading," *Journal of Structural Mechanics*, Vol. 3, 1975, pp. 439–457.

[16] Youngdahl, C.K. "Correlation Parameters for Eliminating the Effect of Pulse Shape on Dynamic Plastic Deformation," *ASME Journal of Applied Mechanics*, Vol. 37, No. 3, 1970, pp.744–752.

[17] Perrone, N. "On a Simplified Method of Solving Impulsive Loaded Structures of Rate-Sensitive Materials," *ASME Journal of Applied Mechanics*, Vol. 32, September 1965, pp. 489–492.

[18] Symonds, P.S. "Plastic Shear Deformations in Dynamic Load Problems," *Engineering Plasticity*, (ed.) Heyman, J. and Leckie, F.A., 1968, pp. 647–664.

[19] Jones, N. "Plastic Failure of Ductile Beams Loaded Dynamically," *ASME Journal of Engineering for Industry*, Feb. 1976, pp. 131–136.